

**GROUNDWATER AND SURFACE WATER INTERACTIONS  
IN THE WESTERN SANTA FE RIVER BASIN NEAR  
HIGH SPRINGS, FLORIDA**

By

Todd Richard Kincaid

A THESIS PRESENTED TO THE GRADUATE SCHOOL OF THE UNIVERSITY OF FLORIDA IN  
PARTIAL FULFILLMENT OF THE REQUIREMENTS FOR THE DEGREE OF MASTER OF SCIENCE

UNIVERSITY OF FLORIDA

1994

*COPYRIGHT TODD R. KINCAID 2006*

## **ACKNOWLEDGEMENTS**

Probably the most important but often least considered decision facing graduate students is the selection of a supervisory committee. In addition to being scientific mentors, they can greatly facilitate a graduate career by guiding students through the maze of bureaucratic red tape that constitutes the administration of large universities and departments. Dr. Katherine Ellins, the chairperson of my supervisory committee at the University of Florida, provided valuable insight to the data interpretation and helped me remain focused on graduation. The support and guidance from committee members Dr. Daniel Spangler and Dr. Milledge Murphey expedited my matriculation. Finally, Dr. Peter Huntoon, the chairman of my Ph.D. committee at the University of Wyoming has helped me refine the ideas gleaned from this work and provided invaluable support that has made publication of this material in various media possible.

Before this project could begin, all diving activities had to be painstakingly reviewed by the University of Florida Dive Board. In this regard, Dr. Milledge Murphey and Dr. Robert Millot were instrumental in obtaining the board's permission for the lengthy penetrations necessary to document the 222Rn profiles within the Devil's Ear cave system. Consequently, this project was the first endeavor at the University of Florida to collect scientific data at appreciable penetrations in a phreatic cave system.

I sincerely doubt that any significant contributions can be adequately attributed to individual effort. My friend and diving partner, Jarrod Jablonski, spent countless hours underwater collecting samples and observations from the Devil's Ear cave system. My friend Dr. Rich Hisert provided his expertise and assistance with the surface fieldwork as well as the analytical techniques. My friends Can Denizman, Todd Quillen, Kendall Fountain, Neil Johnson, Kris Saum, Charlotte Davison, Don Johnson, Pete Butt, and Rico Tennisman, as well as all the other volunteers helped collect samples during long and monotonous tracing experiments. Rhonda Johnson and Ginnie Springs Inc. extended great kindness and latitude by providing access to the springs and river that was necessary to conduct the field research. Finally, Wes and Terry Skiles of Karst Productions donated the beautiful pictures of the Santa Fe River and the Devil's Ear cave system contained in this work.

The National Science Foundation and the Departments of Sponsored Research and Geology at the University of Florida all provided partial financial sponsorship for this project.

At last and most important, I wish to acknowledge and thank my mother, Charlotte Poindexter for her love, support, and friendship and for always setting a shining example of the kind of person I would like to become.

*I have always viewed scientific research as a type of exploration into the unknown. In that light, I want to dedicate this book to all of the cave-diving explorers who continually risk their lives just to see what's around the next bend.*

## TABLE OF CONTENTS

<i>Acknowledgements</i> .....	<i>i</i>
<i>Table of Contents</i> .....	<i>ii</i>
<i>Abstract</i> .....	<i>viii</i>
CHAPTER 1 INTRODUCTION.....	1
Purpose and Scope .....	1
Study Area .....	4
Climate.....	4
Hypotheses.....	8
Significance.....	9
CHAPTER 2 HYDROGEOLOGICAL SETTING.....	11
Geology.....	11
Physiography .....	16
Hydrogeology.....	20
Topography and Drainage.....	24
The Devil's Ear Cave System .....	24
CHAPTER 3 BACKGROUND AND PREVIOUS RESEARCH.....	34
Tracers.....	34
Previous Hydrogeological Research .....	40
CHAPTER 4 METHODOLOGY.....	44
The River Experiments .....	44
Water Sampling .....	44
Discharge Measurements.....	45
SF <sub>6</sub> Injection .....	46
Gas Exchange .....	46
Groundwater Influx .....	48
Stream Flow Loss .....	50
Return Flow.....	50
The Cave Experiments .....	52
Cave Diving Techniques and Water Sampling.....	53
Surface Water Influx .....	55
Analytical Techniques.....	56
Radon-222 .....	56
Sulfur hexafluoride.....	57
CHAPTER 5 RESULTS.....	58
The River Experiments .....	58
Gas Exchange .....	63
Stream Flow Components.....	64
Error Calculation .....	79
The Cave Experiments .....	84
<sup>222</sup> Rn and % River Water Measurements.....	89
δ <sup>18</sup> O and Major Cations .....	93
CHAPTER 6 DISCUSSION.....	95
Groundwater - Surface Water Exchange.....	95
Return Flow.....	99
CHAPTER 7 SUMMARY AND CONCLUSIONS.....	100
References .....	102
Biographical Sketch (Updated 2006) .....	105

## LIST OF FIGURES

Figure 1. Pictures showing the mixing of groundwater and surface water at Devil's Ear spring which is the primary discharge point for the Devil's Ear cave system. A) Orange and red colors are natural and result from sunlight penetrating through the tannin-stained water. B) Tannin-stained river water mixing with groundwater over Devil's Ear spring. Pictures courtesy of Wes Skiles, Karst Productions Inc. ....	2
Figure 2. Location of the study area on the Santa Fe River between Rum Island and July spring, north-central Florida. ....	5
Figure 3. Aerial photographs of (a) the Santa Fe River near Devil's Ear spring and (b) Devil's Ear spring (bottom) and Devil's Eye spring (top), north-central Florida. Pictures courtesy of Wes Skiles, Karst Productions Inc. ....	6
Figure 4. Picture of July spring Looking Across the River from Devil's Ear spring. Picture courtesy of Wes Skiles, Karst Productions Inc. ....	8
Figure 6. Regional stratigraphy in western Alachua, southern Columbia, and northern Gilchrist counties. Adapted from Scott (1988 and 1991). ....	12
Figure 7. Regional cross-section from northwest to southeast across the Columbia limestone plain, High Springs Gap, and Northern Highlands physiographic provinces and the Santa Fe River. Adapted from Briel (1976). ....	14
Figure 7. Physiographic province map of north-central Florida showing the course of the Santa Fe River and its major tributaries. Adapted from White (1970) and Rupert (1988). ....	18
Figure 8. Hydrogeologic units of in the Santa Fe River basin, north-central Florida. Adapted from Hunn and Slack (1983). ....	22
Figure 9. Map of the potentiometric surface of the Floridan aquifer in north-central Florida showing the direction of groundwater flow and the course of the Santa Fe and Suwannee rivers. Adapted from Meadows (1991). ....	23
Figure 10. Section of the U.S.G.S. High Springs S.W. topographic quadrangle, 7.5 minute series, showing the drainage features and karst landscape in the field area between Rum Island and July spring on the Santa Fe River near High Springs, north-central Florida. ....	26
Figure 11. Map of the Devil's Ear cave system superimposed onto part of the U.S.G.S. High Springs S.W. topographic quadrangle showing the direction of groundwater flow through the conduits and the relative position of the overlying Santa Fe river, north-central Florida. ....	30
Figure 12. Pictures showing entrances to the Devil's Ear cave system from: a) Devil's Ear and b) Devil's Eye springs. The color variations in the water at Devil's Ear spring result from clear groundwater mixing with tannin stained river water. Photos courtesy of Wes Skiles, Karst Productions. ....	31
Figure 13. Pictures showing the size and structure of the main passage in the Devil's Ear cave system as well as sand dunes and ripple marks on the cave floor. Photos courtesy of Wes Skiles, Karst Productions Inc. ....	33
Figure 14. Location of Major Phosphate Districts in Florida. Adapted from Roessler et al. (1979). ....	36
Figure 15. Isopach map of sediments overlying the Floridan aquifer in the southern half of the Santa Fe river basin, north-central Florida. Adapted from Spangler and Silverman (1982). ....	37
Figure 16. Results of dye tracing experiments conducted at Ginnie Springs park, north-central Florida, showing groundwater flow directions and travel times. (Wilson and Skiles, 1988). ....	42
Figure 17. SF <sub>6</sub> recovery curves for a groundwater tracing experiment conducted in April, 1992 between an inactive pumping well and three springs on the Santa Fe River near High Springs, Florida, adapted from Kincaid and others (1992). Inset shows the predominant groundwater flow directions. ....	43
Figure 18. Method for calculating discharge at selected points in the Santa Fe River between Rum Island and July spring, north-central Florida. ....	45

Figure 19. The SF <sub>6</sub> river injection system.....	47
Figure 20. Picture Showing a Fully Equipped Cave Diver Riding a Scooter Through the Devil's Ear cave system. Photo Courtesy of Wes Skiles, Karst Productions Inc. ....	54
Figure 21. Picture showing the cave-diving team collecting a water sample to be measured for <sup>222</sup> Rn from a side conduit in the Devil's Ear cave system, north-central Florida. Photo courtesy of Bill Dooley.....	55
Figure 22. Comparison of measured stream discharge between Rum Island and Ginnie spring on the Santa Fe river, north-central Florida during the study period between September, 1991 and June, 1993. ....	58
Figure 23. Uncorrected <sup>222</sup> Rn and SF <sub>6</sub> data and measured discharge in the Santa Fe River of north-central Florida between Rum Island and Ginnie spring for the (A) September, 1991, (B) February 1992, and (C) June 1993 sampling periods.....	62
Figure 24. (a) Corrected <sup>222</sup> Rn and SF <sub>6</sub> concentrations vs. transect distance and (b) measured and calculated discharge vs. transect distance measured during the September, 1991 sampling of the Santa Fe River between Rum Island and Ginnie spring, north-central Florida. Peaks in <sup>222</sup> Rn concentrations correspond to ground water influx to the river. Peaks in SF <sub>6</sub> concentrations indicate the return of river water that had been diverted underground up-stream.....	70
Figure 25. (a) Corrected <sup>222</sup> Rn and SF <sub>6</sub> concentrations vs. transect distance and (b) measured and calculated discharge vs. transect distance measured during the February, 1992 sampling of the Santa Fe River between Rum Island and July spring, north-central Florida. Peaks in <sup>222</sup> Rn concentrations correspond to ground water influx to the river. Peaks in SF <sub>6</sub> concentrations indicate the return of river water that had been diverted underground up-stream.....	71
Figure 26. (a) Corrected <sup>222</sup> Rn and SF <sub>6</sub> concentrations vs. transect distance and (b) measured and calculated discharge vs. transect distance measured during the June, 1993 sampling of the Santa Fe River between Rum Island and July spring, north-central Florida. Peaks in <sup>222</sup> Rn concentrations correspond to ground water influx to the river. Peaks in SF <sub>6</sub> concentrations indicate the return of river water that had been diverted underground up-stream.....	73
Figure 27. Variations in calculated stream discharge and flow components determined at high and low values of the gas transfer velocity for the reach of the Santa Fe River between Rum Island and Ginnie spring. Position of the vertical bars indicates flow component magnitude. Length of the vertical bars indicates variation with gas transfer velocity. ....	75
Figure 28. Variation in flow components with gas transfer velocity on the reach of the Santa Fe River between Rum Island and Ginnie spring, north-central Florida for the sampling periods between September, 1991 and June, 1993. ....	77
Figure 29. Variations in flow components with overall river discharge for the reach of the Santa Fe River between Rum Island and Ginnie spring, north-central Florida for the sampling periods between September, 1991 and June, 1993. ....	78
Figure 30. Map of the Devil's Ear cave system on the Santa Fe river, north-central Florida showing the sampling locations and the relative position of the overlying Santa Fe river. ....	86
Figure 31. <sup>222</sup> Rn concentrations and the corresponding percentage of river water in the conduit flow measured across transects (A) A-A' and (B) B-A' through the Devil's Ear cave system on the Santa Fe river, north-central Florida.....	91
Figure 32. Contour maps showing the distribution of intruded river water in the Devil's Ear cave system on the Santa Fe river, north-central Florida during the (A) February, 1992 and (B) June, 1993 cave sampling experiments. Darker regions are the areas of greatest river water intrusion to the aquifer.....	92
Figure 33. δ18O values and major cation concentrations measured in the Devil's Ear cave system on the Santa Fe river, north-central Florida during the (A) February, 1992 and (B) June, 1993 cave experiments. More negative δ18O values correspond to purer ground water. ....	94
Figure 34. Comparison of water levels in the Floridan aquifer near the Devil's Ear cave system and rainfall in the Northern Highlands and lowland physiographic provinces, north-central Florida. Notice that there was more rainfall in the highlands than in the lowlands during the February,	

1992 sampling period when there was more river water intrusion to the Devil's Ear cave system but the flow stage of the Santa Fe River was at its lowest point. Data are from the Suwannee River and St. Johns River water management districts. .... 96

Figure 35. Groundwater - surface water exchange between the Santa Fe River and the extremely permeable conduits in the Floridan aquifer across a 30 m thick section of Ocala Limestone which is a leaky confining layer. (A) The stage of the river is above the potentiometric surface of the aquifer forcing downward leakage from the river to the aquifer. (B) The potentiometric surface of the aquifer is above the stage of the river forcing upward leakage from the aquifer to the river. .... 97

## LIST OF TABLES

Table 1. Comparison of Schmidt Numbers for $^{222}\text{Rn}$ , $\text{SF}_6$ , and $\text{O}_2$ at Selected Temperatures.....	48
Table 3. $^{222}\text{Rn}$ and $\text{SF}_6$ concentrations and measured stream parameters from the sampled transect of the Santa Fe River between Rum Island and Ginnie spring, north-central Florida for each of the sampling periods between September, 1991 and June, 1993.....	60
Table 4. Calculation of the gas transfer velocity ( $k$ ) for the Santa Fe River between Rum Island and Ginnie spring during the sampling periods between September, 1991 and June, 1993. ....	63
Table 5. $^{222}\text{Rn}$ concentrations measured in various wells and springs between September, 1991 and June, 1993 near the Santa Fe River between Rum Island and Ginnie spring, north-central Florida.....	64
Table 6. Corrected $^{222}\text{Rn}$ and $\text{SF}_6$ concentrations, stream flow components, and calculated discharge for the reach of the Santa Fe River between Rum Island and Ginnie spring, north-central Florida during the September, 1991 sampling period. ....	66
Table 7. Corrected $^{222}\text{Rn}$ and $\text{SF}_6$ concentrations, stream flow components, and calculated discharge for the reach of the Santa Fe River between Rum Island and July spring, north-central Florida during the February, 1992 sampling period. ....	67
Table 8. Corrected $^{222}\text{Rn}$ and $\text{SF}_6$ concentrations, stream flow components, and calculated discharge for the reach of the Santa Fe River between Rum Island and July spring, north-central Florida during the June, 1993 sampling period. ....	68
Table 9. Comparison of calculated and published spring discharges for select springs along the reach of the Santa Fe River between Rum Island and Ginnie spring, north-central Florida for the sampling periods between September, 1991 and June, 1993.....	79
Table 10. Errors associated with ground water influx and return flow calculations for the reach of the Santa Fe River between Rum Island and Ginnie spring, north-central Florida for the September, 1991 sampling period. ....	81
Table 11. Errors associated with ground water influx and return flow calculations for the reach of the Santa Fe River between Rum Island and July spring, north-central Florida for the February, 1992 sampling period. ....	82
Table 12. Errors associated with ground water influx and return flow calculations for the reach of the Santa Fe River between Rum Island and July spring, north-central Florida for the June, 1993 sampling period. ....	83
Table 13 Dive logs and agendas for the 1992 and 1993 research dives conducted in the Devil's Ear cave system on the Santa Fe river, north-central Florida. ....	85
Table 14. $^{222}\text{Rn}$ , $\delta^{18}\text{O}$ , and major cation concentrations measured in the Devil's Ear cave system on the Santa Fe river, north-central Florida and local wells and springs for the February, 1992 and June, 1993 cave experiments. ....	88

## **ABSTRACT**

The Devil's Ear cave system is an extensive network of phreatic karst conduits that are directly overlain by the 1.5 km reach of the Santa Fe River between Rum Island and July springs. The cave and the river are situated on a karst limestone plain where the Ocala Limestone is exposed at the surface leaving the Floridan aquifer unconfined. Fluctuations in the stage of the Santa Fe River and the hydraulic head in the Floridan aquifer drive dynamic interactions between the surface water in the river and groundwater in the cave. Natural tracers Radon-222 ( $^{222}\text{Rn}$ ) and  $\delta^{18}\text{O}$  and the artificial tracer Sulfur-hexafluoride ( $\text{SF}_6$ ) were used to quantify these interactions and describe their hydrogeological implications.

A  $\text{SF}_6$  injection system was designed to introduce gas saturated water into the Santa Fe River upstream of the study area. The gas transfer velocity of the river surface was determined by sampling the reduction in  $\text{SF}_6$  concentration in the downstream segment of the river. The gas transfer velocity was then used in conjunction with  $^{222}\text{Rn}$  sampling transects to quantify groundwater influxes and stream flow losses. Several undocumented groundwater springs and seeps were reflected by  $^{222}\text{Rn}$  peaks. Stream flow losses were recorded along discrete sections of the river when the measured downstream discharge was less than the upstream value plus the calculated groundwater inputs that occurred in between. A *return flow* component was also measured which constitutes water that briefly flows through the extensively dissolved limestone under the stream bed before reentering the river. The results of three such river experiments demonstrate that the magnitude of the flow components are proportional to the river discharge. Calculated discharges from the major springs in the study area were comparable to published values.

$^{222}\text{Rn}$  concentrations measured in 50 water samples taken from as far as 1.2 km into the Devil's Ear cave system revealed three distinct zones where river water is rapidly intruded into the Floridan aquifer. A two-component mixing model was used to quantify the intruded river water which was found to account for as much as 62 percent of the discharge at Devil's Ear spring. Observations of diminished water clarity in the cave system following large precipitation events in the highland provinces of the Santa Fe River basin indicate that river water intrusion to the aquifer can occur in as little as one day. The results of this investigation imply that, in regions such as the western Santa Fe River basin, intruded river water provides a significant vehicle for contamination of the unconfined Floridan aquifer. A conceptual model is provided to describe the mechanisms controlling the exchange of water between the river and the cave.

# **CHAPTER 1**

## **INTRODUCTION**

### *Purpose and Scope*

The reach of the Santa Fe River between Rum Island and Ginnie spring is located on the border between Columbia and Gilchrist counties in northern peninsular Florida. The river flows over and lies on top of exposed Ocala Limestone leaving the Floridan aquifer unconfined. The interactions between groundwater and surface water in this area represent a dynamic and complicated system in which there is significant groundwater influx to the river as well as surface water intrusion to the Floridan aquifer. The pictures in Figure 1 show the mixing of groundwater and surface water over Devil's Ear spring, the main discharge point for the Devil's Ear cave system which lies underneath part of the river channel. The dark brown and red colors result from the tannin surface water mixing with clear groundwater.

Considering these interactions, surface drainage to the river may present a serious source of contamination to the Floridan aquifer, which is the primary source of fresh drinking water in the area. The purpose of this investigation was to study these interactions and develop a conceptual model of the flow mechanics between the river and the aquifer in this region.

A multi-phase study of the Santa Fe River and the Devil's Ear cave system was implemented to achieve four specific objectives. In order of importance they were:

- 1) study the interactions between groundwater and surface water in an environmentally sensitive area,
- 2) further develop the use of  $^{222}\text{Rn}$  and  $\text{SF}_6$  as geochemical tracers in the study of groundwater/surface water interactions in large rivers,
- 3) conduct experiments and observations in an underwater cave system, and
- 4) develop a diving research plan that will serve as a precedent for further research in underwater speleology at the University of Florida.

The water flow components in both the Santa Fe River and the Devil's Ear cave system were simultaneously studied to achieve these objectives.



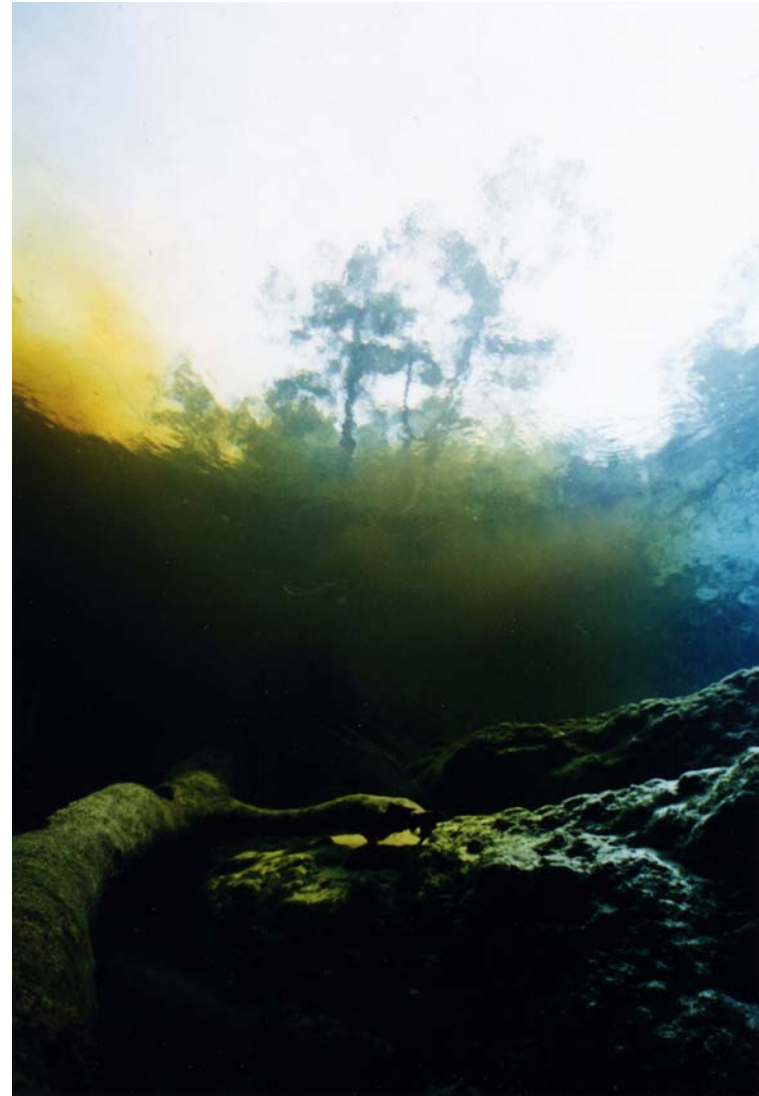
**A****B**

Figure 1. Pictures showing the mixing of groundwater and surface water at Devil's Ear spring which is the primary discharge point for the Devil's Ear cave system. A) Orange and red colors are natural and result from sunlight penetrating through the tannin-stained water. B) Tannin-stained river water mixing with groundwater over Devil's Ear spring. Pictures courtesy of Wes Skiles, Karst Productions Inc.

## Study Area

Figure 2, shows the location of the field area relative to the state of Florida. The area under investigation consists of a two-kilometer reach of the Santa Fe River between Rum Island and Ginnie spring which makes the border between Gilchrist and Columbia counties in north central Florida. This reach was chosen because of the extensive Devil's Ear cave system which underlies part of the river discharging water at Devil's Ear, Devil's Eye, and July springs.

The best access to the study area is provided by canoe along the river from either Rum Island or Ginnie springs. County roads 340 and 138 from High springs, Florida provide access to Ginnie springs Park and Rum Island park respectively. Figure 3a shows an aerial view of the Santa Fe River near Devil's Ear spring. Figure 3b shows an aerial view of Devil's Ear spring in the river channel and Devil's Eye spring at the top of the picture. Figure 4 is a view of July spring located across the river from Devil's Ear spring.

## Climate

North Florida is characterized by a humid and subtropical climate. The summer season in this region is long and warm with regular afternoon temperatures ranging between 32 and 38°C. Winters are generally mild in which temperatures drop below 0°C less than 30 times throughout an average winter (Biddlecomb, 1993).

The mean annual precipitation in this region is 135 cm with about 52 percent falling between June and September (Winsberg, 1990). Summer rainfall, usually associated with afternoon thunderstorms, occurs with greater intensity over a shorter duration than winter rainfall. Warm dry air rises from the land during the day and converges with cooler moisture-laden air from the Gulf of Mexico and the Atlantic Ocean producing thunderstorms (Winsberg, 1990). Winter rainfall, associated with frontal activity from the interior of the continent, is usually more uniform and of longer duration (Winsberg, 1990).

Droughts occur in Florida with a frequency of less than ten years (Winsberg, 1990). North-central Florida just recently emerged from drought conditions in late 1991. Rainfall in the region in 1990 was 25 percent lower than average significantly lowering groundwater levels in the Floridan aquifer setting record lows in some areas (Biddlecomb, 1993).

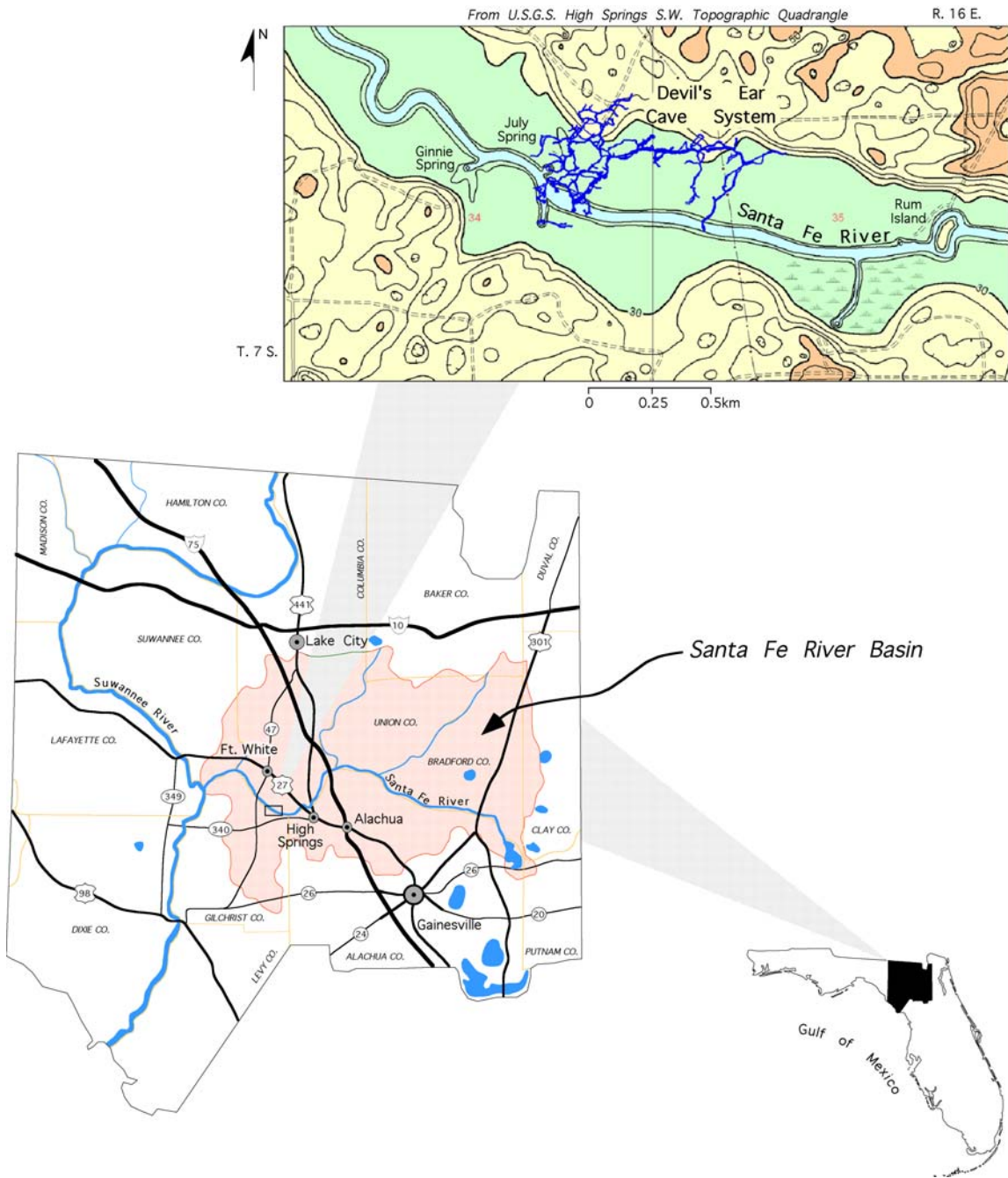


Figure 2. Location of the study area on the Santa Fe River between Rum Island and July Spring, north-central Florida.

**A**



**B**



*Figure 3. Aerial photographs of (a) the Santa Fe River near Devil's Ear spring and (b) Devil's Ear spring (bottom) and Devil's Eye spring (top), north-central Florida. Pictures courtesy of Wes Skiles, Karst Productions Inc.*



Figure 4. Picture of July spring Looking Across the River from Devil's Ear spring. Picture courtesy of Wes Skiles, Karst Productions Inc.

### Hypotheses

The following hypotheses were developed to investigate the relationship between the river water and groundwater in this region.

- 1) The Santa Fe River is a major source of the water circulating through the Devil's Ear cave system.
- 2) A major portion of the spring discharge to the Santa Fe River is resurgent surface water not pure groundwater from the Floridan aquifer.
- 3) The Santa Fe River is both a gaining and losing stream in this region depending on the stage of the river.

$^{222}\text{Rn}$  and  $\text{SF}_6$  were employed as tracers to test these hypotheses. Water samples were collected both from the river and the cave system and measured for their dissolved  $^{222}\text{Rn}$  concentrations to determine the groundwater component of the water at the sampling point.  $\text{SF}_6$  was deliberately injected into the river and sampled both in the river and the cave system. Samples collected from the river were used to calculate the gas transfer velocity between the river and the atmosphere. Any  $\text{SF}_6$  measured in the cave system would unequivocally prove a hydraulic connection between the cave system and the river.

## Significance

Groundwater is a vital natural resource in Florida. According to Fernald and Patton (1984), groundwater provides 87% of Florida's public water supply and 94% of the dispersed private supply. Fernald and Patton further report that of all the groundwater consumed in Florida, over 44% comes from the Floridan aquifer. Because of the increasing demand for potable groundwater, groundwater protection has become a primary concern for state and local government officials as well as water resource managers in Florida.

Suburban development near Gainesville, growth of mining and industry in the area, and the development of the recreation areas along the Santa Fe River indicate that the Santa Fe River basin is likely to experience significant population growth (Hunn and Slack, 1983). The growing dairy industry in north-central Florida and the proliferation of chicken farming have caused increased concern for the protection of the water quality in local springs, rivers, and the Floridan aquifer from organic pollution. In 1981, approximately 81 dairy farms operated in north Florida with approximately 37,000 dairy cows. Where these dairy cows are kept in high density feed lots, groundwater and surface water commonly contain large quantities of nitrate, ammonia and soluble organic nitrogen species that are susceptible to nitrification to nitrates (Andrews, 1992). A compilation of water quality studies at nine dairy farms in north Florida conducted by Andrews (1992) indicated that where unconfined, the Floridan aquifer is vulnerable to contamination from wastes applied to the land surface due to high recharge rates through thin or non-existent overlying material. Andrews further shows that surface water bodies near dairy farms receive large quantities of nutrient-rich runoff that could cause eutrophication and threaten biotic communities.

State regulatory agencies have segregated groundwater and surface water as to the regulations for permissible levels of contaminants. These regulations often allow higher levels of certain contaminants such as nitrate to be discharged to a river or stream than would be permissible in an aquifer designated as a potable water source such as the Floridan aquifer.

This research demonstrates that in regions such as the western Santa Fe River basin where the Floridan aquifer is unconfined, there is a much higher degree of exchange between groundwater and surface water than has been previously acknowledged. The results of this research will aid water resource managers to develop policies and regulations that will prevent future industrial and agricultural pollution of groundwater resources by reevaluating the permissible contaminant levels in surface water bodies such as the Santa Fe river. Furthermore, this research may aid state and local regulators to make more educated decisions regarding zoning and land use permits in environmentally sensitive areas.

In addition to the broader environmental significance, this research may serve as a basis for future scientific studies in the application of natural and artificial tracers for the investigation of groundwater/surface water interactions in karstic regions. A modified SF<sub>6</sub> river injection system and method for the preparation of SF<sub>6</sub> standards were designed for this project. These new systems may serve as a methodological basis for future researchers.

Another significant aspect of this project involves the first hand investigations conducted within the Devil's Ear cave system. In the past, researchers have had limited ability to conduct studies in phreatic karst systems due to the technical difficulties of accessing underwater caves. However, recent advancements in cave diving equipment and the increased availability of quality dive training are enabling scientific investigations to be conducted at even extreme penetrations into underwater cave systems. This project is a landmark investigation because safe cave diving practices have been used as a research tool to make on site observations and collect field data from an environment new to the scientific community.

Overseen by the Dive Board at the University of Florida, a panel of professors and scientists from a broad spectrum of backgrounds, this study was the first large scale, underwater speleological project to be supported by the University of Florida. The cave diving methodologies utilized in this project will provide the standard at the University of Florida for future research in underwater cave systems.

## **CHAPTER 2**

### **HYDROGEOLOGICAL SETTING**

#### Geology

The geology of the field area primarily consists of the Eocene Ocala Limestone which is either exposed at the surface or sporadically covered by a thin veneer of Holocene siliclastic sediments. However, the phosphatic sands and clays of the Hawthorne and Alachua Formations are present in neighboring geomorphic zones and play an important role as source regions for  $^{222}\text{Rn}$  used as a natural tracer in this investigation. Figure 5 is a general stratigraphic column of the geologic formations present in the regions surrounding the field area. Figure 6 shows a general cross-section of the region from northwest to southeast across the field area.

The Ocala Limestone, formerly the Ocala Group which was subdivided into the Crystal River, Williston, and Inglis formations (Puri, 1957; Scott, 1991) is the most prevalent geologic formation in the field area. The Ocala Limestone is a very fossiliferous, occasionally recrystallized and dolomitic, marine limestone of late Eocene age (Rupert, 1988; Scott, 1991). The thickness of the Ocala Limestone in this region ranges between 60 and 90 meters (Chen, 1965). The structural surface of the Ocala Limestone is essentially 0 NGVD throughout the field area and the depth from land surface to the top of the unit ranges from 0 to 60 meters (Miller, 1986). Foraminifera, mollusks, bryozoans, and echinoids are the most abundant fossil types occurring in the Ocala Limestone. Typically, the lithology of the unit grades upward from alternating hard to soft white to gray to tan fossiliferous and sometimes recrystallized limestones of the former Inglis and lower Williston Formations into white to cream, abundantly fossiliferous and chalky limestones of the former upper Williston and Crystal River Formations. The limestones outcropping in the specific area of investigation most closely resemble those of the former Crystal River Formation.

In the field area, the Ocala Limestone is either exposed at land surface or covered by a thin veneer of sands and occurs as an irregular, heavily eroded and karstic plain. This irregular surface, seen in open quarries and in sinkholes, is similar in structure and appearance to the epikarstic "Stone Forest" of south China described by Huntoon (1992a;b).



ERA	EPOCH	FORMATION	CHARACTERISTICS
CENOZOIC	Recent to Pleistocene & Pliocene		sinkhole fill, fluvial terraces, and thin surficial sand; fine to medium grain sands with minor organics and heavy minerals
	Pleistocene to Miocene	Alachua Fm.	* <i>Source of <math>^{222}\text{Rn}</math></i> gray to blue-gray clayey sand that weathers red-brown; sinkhole fill and residuum from post Eocene deposits with limestone boulders and phosphate
	Middle to Lower Miocene		* <i>Source of <math>^{222}\text{Rn}</math></i>
		Hawthorn Fm.	phosphatic clayey sand to sandy-clay with varying amounts of Fullers Earth and carbonate
	Oligocene	Suwannee Limestone	pale yellow, moderately indurated, porous fossiliferous calcarenite; <i>Rhyncholampus gouldii</i> fossils common
Eocene	Ocala Limestone	* <i>Formation containing the Devil's Ear cave system</i> white to cream, soft and granular, massive, fossiliferous limestone; well indurated; <i>Lepidocyclus</i> fossils common	

© Todd R. Kincaid

Figure 6. Regional stratigraphy in western Alachua, southern Columbia, and northern Gilchrist counties. Adapted from Scott (1988 and 1991).

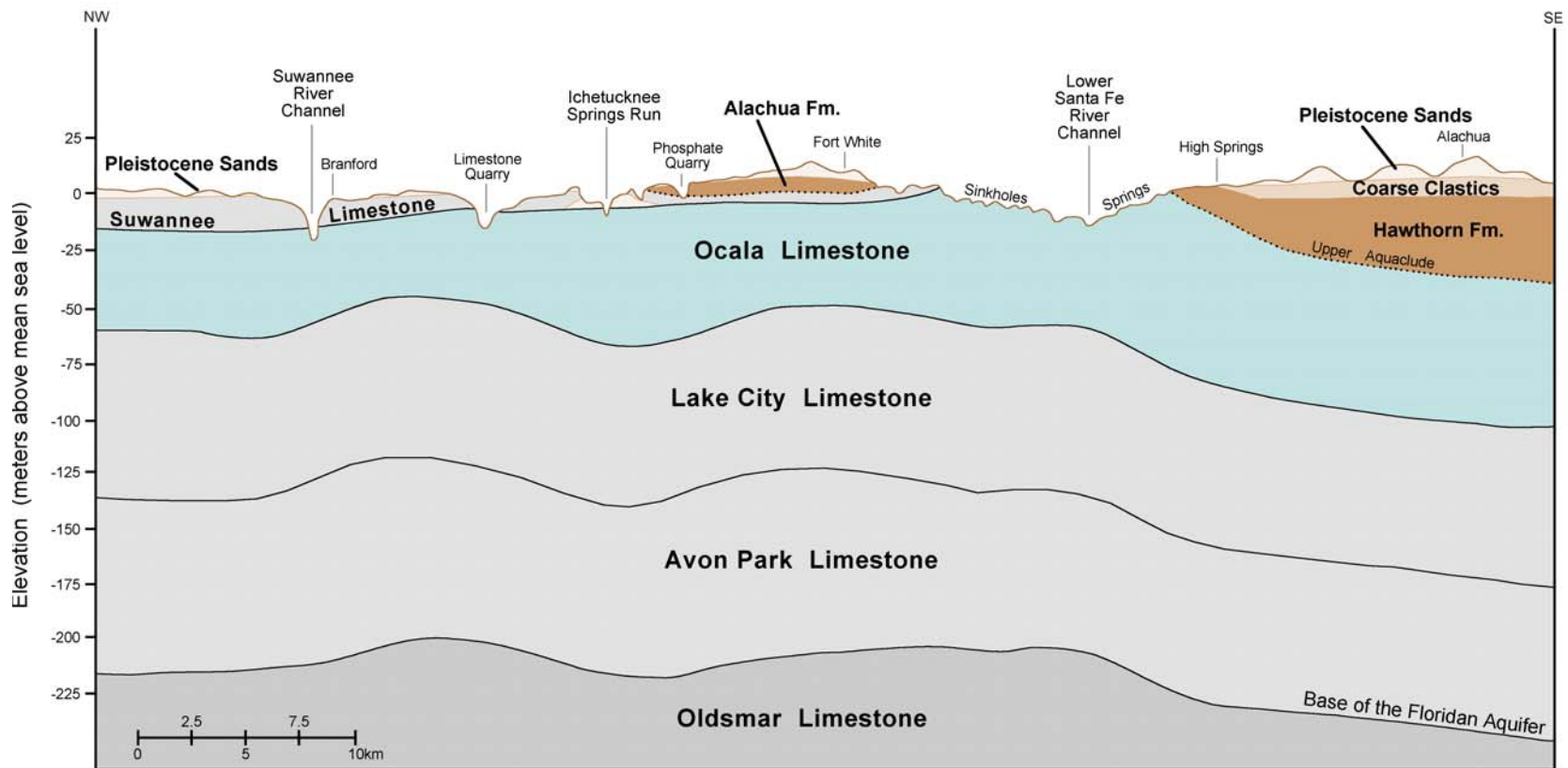


Figure 7. Regional cross-section from northwest to southeast across the Columbia limestone plain, High Springs Gap, and Northern Highlands physiographic provinces and the Santa Fe River. Adapted from Briel (1976).

The Lower Oligocene Suwannee Limestone has a very limited distribution in the area of investigation (Scott, 1991). Though isolated occurrences of the Suwannee Limestone have been reported at or near the Santa Fe river, overall the unit has been removed by erosion and dissolution from most of north-central Florida. At its occurrences, the Suwannee Limestone consists of variably vuggy and muddy limestone containing frequent highly recrystallized beds (Scott, 1991).

The Hawthorne Formation is considered to be Early to Middle Miocene Age (Williams et al., 1977). The formation is characterized by a high degree of lithologic variability where units pinch out, interfinger or intergrade laterally and vertically (Williams et al., 1977). In general, two lithologic types are described as typically Hawthorne. The first is a phosphatic sandy and sometimes dolomitic limestone and the second is that of a gray to bluish-gray phosphatic sandy clay or clayey sand (Scott, 1988). The clayey units in this formation act as an aquiclude and cause the Floridan aquifer to be under confined conditions in the areas of Hawthorne occurrence (Meyer, 1962). The Hawthorne Formation has been removed from all of the lowland provinces in the field area effectively leaving the Floridan aquifer unconfined except where overlain by the sporadic occurrences of the Alachua Formation. The primary occurrence of the Hawthorne Formation is in the topographically higher provinces surrounding the field area where it may reach thickness of as much as 30 meters (Miller, 1986).

The Alachua Formation described by Meyer (1962), Puri and others (1967), Williams and others (1977), and Rupert (1988) is presently thought to consist primarily of weathered and reworked Hawthorne materials (Scott, 1988). The lithology of the formation consists of a complicated mixture of discontinuous interbedded clay, sand, and sandy clay including commercially important phosphatic sand and gravel deposits (Rupert, 1988). The formation has been further reported to contain water-worn chert, erratic limestone boulders, silicified limestone, light blue and green montmorillonite clay lenses, pebbles and boulders or phosphatic rock conglomerate, colloidal phosphate, and vertebrate fossils (Puri et al., 1967). The Alachua Formation was deposited on the eroded surface of the Ocala Limestone, consequently its thickness varies considerably over short distances. In the area of investigation, the Alachua Formation occurs as a thick sequence (25 to 35 meters) in the structural low areas and as a discontinuous 3 to 8 meter thick cover overlying parts of some of the higher provinces.

### Physiography

The physiography of the region consists of three major zones, the Northern Highlands, the Central Highlands, and the Gulf Coastal Lowlands (White, 1970). The Central Highlands and the Gulf Coastal Lowlands have been further subdivided based on topography (Puri et al., 1967; Rupert, 1988). The Central Highlands contains three geomorphic subdivisions in this region, the Brooksville Ridge, the Western Valley, and the High Springs Gap. The Gulf Coastal Lowlands contains the Wacasassa Flats, the Bell Ridge, the Chiefland Limestone Plain, and the Santa Fe and Suwannee River Valley Lowlands. Wilson and Skiles (1988) also describe the Columbia Limestone Plain as a subdivision of the Gulf Coastal lowlands in southern Columbia county bordering the field area on the north side of the Santa Fe

river. The most prominent geomorphic feature in the region is the Cody Scarp which makes the border with the Northern Highlands physiographic province. Interested readers are referred to the works of Puri and others (1967), Rupert (1988), White (1970), and Williams and others (1977) for more detailed descriptions of the physiography and geomorphology of the region. Figure 7 shows the major physiographic features in the area of investigation.

The Northern Highlands Plateau is a high flat area of low relief and an average elevation of 45 meters NGVD which is a continuous highland extending north and east from Gainesville into Georgia (Williams et al., 1977). The Ocala Limestone dips gently to the east and northeast in the region and lies at a depth usually greater than 30 to 45 meters below land surface (Williams et al., 1977). The Hawthorne Formation overlies the Ocala Limestone and acts as an aquaclude creating artesian conditions in the Floridan aquifer and supporting a higher secondary aquifer under water-table conditions (Williams et al., 1977). A thin veneer of sands and clayey sands between 0 and 10 meters thick caps the Hawthorne Formation at the land surface.

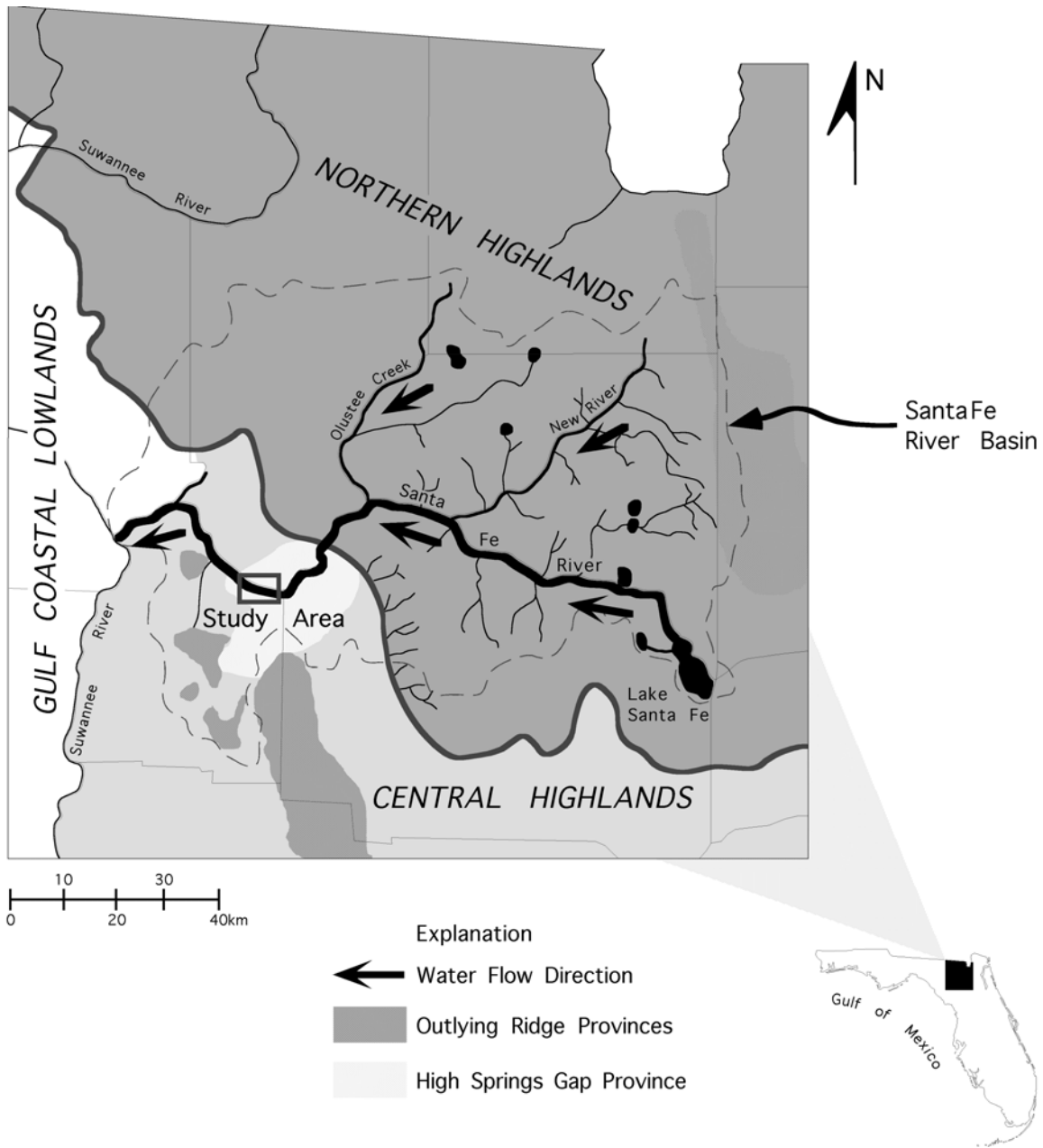


Figure 7. Physiographic province map of north-central Florida showing the course of the Santa Fe River and its major tributaries. Adapted from White (1970) and Rupert (1988)

The most prominent features in this province are cypress hammocks and poorly drained swamps (Williams et al., 1977). Drainage in the region is generally to the north into the Santa Fe River.

The Central Highlands province lies to the southwest of the Northern Highlands in this region. This geomorphic province includes a series of localized ridges and valleys, which generally parallel the coasts down the central peninsula of Florida (Rupert, 1988). The High Springs Gap, Brooksville Ridge, and Western Valley are subdivisions of the Central Highlands zone in this region.

The High Springs Gap is a geomorphic lowland situated in northeastern Gilchrist and northwestern Alachua counties and directly borders the Northern Highlands to the southwest. The Ocala Limestone is covered by a thin veneer of sands or exposed at the surface in this province causing the formation of many karstic features such as sinkholes and disappearing streams. In fact, the entire Santa Fe River disappears underground at Oleno Sink in this province and reemerges over 5 km to the southwest.

The Brooksville Ridge is a topographic highland trending northwest-southeast and extending for over 175 km between Gilchrist county in the north and Pasco county in the south (Rupert, 1988). The phosphatic Alachua Formation and a thick sequence of Pleistocene sands overlies the uneven and solution riddled surface of the Ocala Limestone (Williams et al., 1977).

The Western Valley is a lowland limestone plain composed of the Ocala Limestone overlain by a thin soil cover (Williams et al., 1977). In this region, the Western Valley predominantly lies in Alachua county and borders the Brooksville Ridge on the east and the Northern Highlands on the south. The essentially level surface of this limestone plain is formed by the eroded surface of the Ocala Limestone (Williams et al., 1977). Numerous sinkholes and caves have been documented in this province.

The Gulf Coastal Lowlands province generally parallels the present Gulf Coast of Florida from Fort Myers north and west to the Alabama state line. In the vicinity of the field area, this province extends inland from the present Gulf of Mexico shoreline to western edges of the Brooksville Ridge and High Springs Gap physiographic provinces. The Gulf Coastal Lowlands province is characterized by broad, flat marine plains underlain by Eocene limestones and covered by a thin layer of Pleistocene sands (Rupert, 1988). This province is subdivided into the Bell Ridge, Chiefland Limestone Plain, Columbia Limestone Plain, Santa Fe and Suwannee River Valley Lowlands, and the Wacasassa Flats.

The Bell Ridge is a 30 km long series of sand ridges believed to be outliers of the Brooksville Ridge (Rupert, 1988). The sand hills of the Bell Ridge comprise phosphatic sands and clays from the Alachua Formation which directly overlie the karstic surface of the Eocene Ocala Limestone.

The Chiefland Limestone Plain is described by Rupert (1988) as an eroded and highly karstic limestone plain, comprised of the Ocala Limestone, covered by a thin veneer of sands. The province is bordered on the west by the Suwannee River Valley Lowlands and the east by the Bell Ridge and

Wacasassa Flats. The Columbia Limestone Plain described by Wilson and Skiles (1988) is similar to the Chiefland Limestone Plain but lies on the north side of the Santa Fe River in southern Columbia county.

The river valley lowlands of the Santa Fe and Suwannee Rivers are thin, broad valleys created by river erosion. The valleys are underlain by the eroded surface of the Ocala Limestone and covered by thin sequence of Holocene siliclastic sediments (Rupert, 1988). As with the other limestone plains described in this region, the eroded surface of the Ocala Limestone is similar to the epikarstic regions described by Huntoon (1992a;b) in South China.

The Wacasassa Flats comprises the low, swampy area about 8 km wide and 40 km long trending north-south through central Gilchrist county and borders the Chiefland Limestone Plain to the west and the High Springs Gap and Brooksville Ridge on the east. The Wacasassa Flats are a structural low filled with Miocene and Pleistocene siliclastic sediments which retard downward infiltration of groundwater resulting in the generally swampy conditions (Rupert, 1988).

The Cody Scarp or the Northern Highlands Marginal Zone (Williams et al., 1977) is the prominent geomorphic feature creating the boundary between the Northern Highlands and the Gulf Coastal Lowlands and Central Highlands. This feature is characterized by a dramatic drop in elevation. The elevation changes from nearly 60 meters in the Northern Highlands to 20-30 meters in the topographically lower provinces (Williams et al., 1977). Drainage from the upland province has created an extensively karstified transition zone between the Northern Highlands where the Floridan aquifer is confined and the limestone plains of the Gulf Coastal Lowlands where the Floridan aquifer is unconfined (Scott, 1991).

Though the Hawthorne and Alachua Formations are absent in the karst plain regions encompassing the specific vicinity of the field area, their presence underlying the Northern Highlands, Brooksville Ridge, Bell Ridge, and Wacasassa Flats provinces are significant to the scope of this research. The phosphatic deposits characteristic to both these formations are the probable source of the  $^{222}\text{Rn}$  dissolved in the groundwater that was used as the primary tracer in this study.

### Hydrogeology

The Santa Fe River basin occupies over 3,500 square kilometers in north-central Florida and is a major tributary basin of the Suwannee river. The basin has large supplies of high quality surface water and groundwater. The principal streams in the basin include the Santa Fe and New rivers and Olustee creek in the east and the Santa Fe and Ichetucknee rivers in the west. The principal source of groundwater is the Floridan aquifer which consists of a thick sequence of limestone beds, the upper 100 - 250 meters of which yield potable water. The eastern portion of the basin lies within the Northern Highlands province and is underlain by the Hawthorne Formation creating confined conditions in the Floridan aquifer. The western portion of the basin is a karst plain where sediments overlying the Ocala Limestone, if any, are not effective in confining the Floridan aquifer. The western part of the basin has the largest surface water supplies and the greatest potential for high yield groundwater wells (Hunn and

Slack, 1983). The area of investigation in this study lies within the western part of the Santa Fe River basin.

The Floridan aquifer is unconfined along the western half of the Santa Fe River and throughout most of the rest of the western part of the Santa Fe River basin. A confining layer is present in the outlying areas and a surficial aquifer is present only in the upland areas of the Northern Highlands province. Figure 8 shows the hydrogeologic units of the Santa Fe River basin.

The confining layer in the western Santa Fe River basin is comprised of limestone, sands and clays from the Alachua Formation (Hunn and Slack, 1983). This layer has some local water yielding zones primarily composed of limestone but also shell beds and sands. The primary discharge from these zones occurs as leakage to the underlying Floridan aquifer (Hunn and Slack, 1983).

Hunn and Slack (1983) indicate that in the western part of the basin, the Floridan aquifer is directly recharged by rainfall at an estimated rate of 46 cm per year. They further report that transmissivities in the upper 60 meters of the aquifer range from 3,000 to 50,000 meters squared per day permitting well yields of between 7500 to 20,000 liters per minute depending on the well construction.

The equipotentials of the potentiometric surface cross the Santa Fe River indicating that the river is a gaining stream receiving water from the Floridan aquifer. According to the potentiometric surface map adapted from Meadows (1991), shown in Figure 9, this is especially true in the western Santa Fe River basin where groundwater flow converges on the river from three directions. In fact, there are many springs along the western portion of the river that directly discharge water from the Floridan aquifer to the river.

However, the potentiometric surface map fails to show that in many places along the river in the western Santa Fe basin, stream flow is lost to the aquifer. In fact the entire river is diverted underground at Oleno Sink in Oleno State Park near High Springs and emerges again 5 km downstream. Changes in water chemistry and an increase in stream discharge at the resurgence point indicate that the stream flow is augmented with groundwater at some point along the underground flow path. There are three other points along the western section of the river where large siphons, visible at the surface, indicate that stream water is being diverted underground. At one location near Columbia spring personal communication with local residents revealed that primitive tracer studies had been conducted which proved a direct connection between a siphon on the north bank of the river and Columbia spring. The results of this investigation further document these complicated groundwater / surface water interactions and the inability of standard potentiometric surface maps to record them.



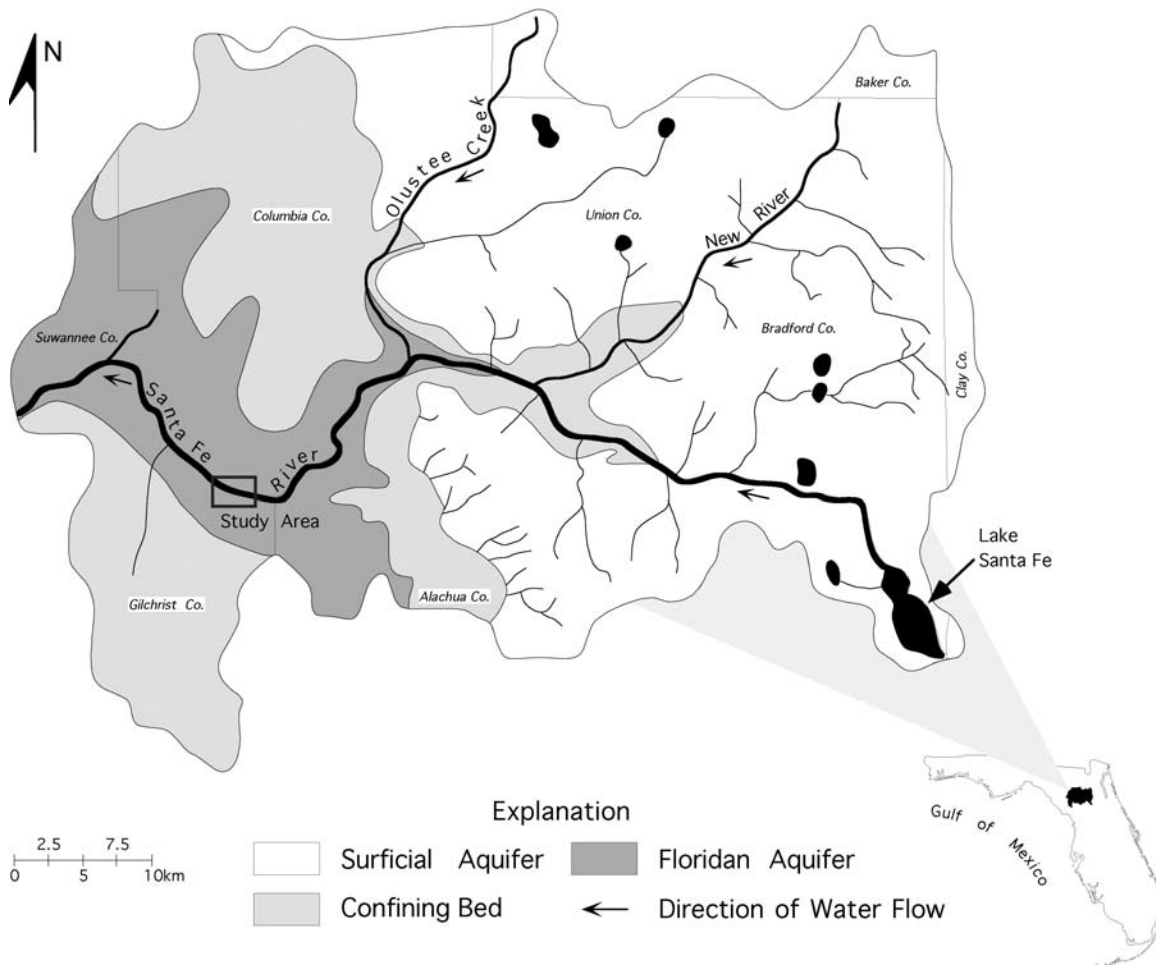


Figure 8. Hydrogeologic units of in the Santa Fe River basin, north-central Florida. Adapted from Hunn and Slack (1983).

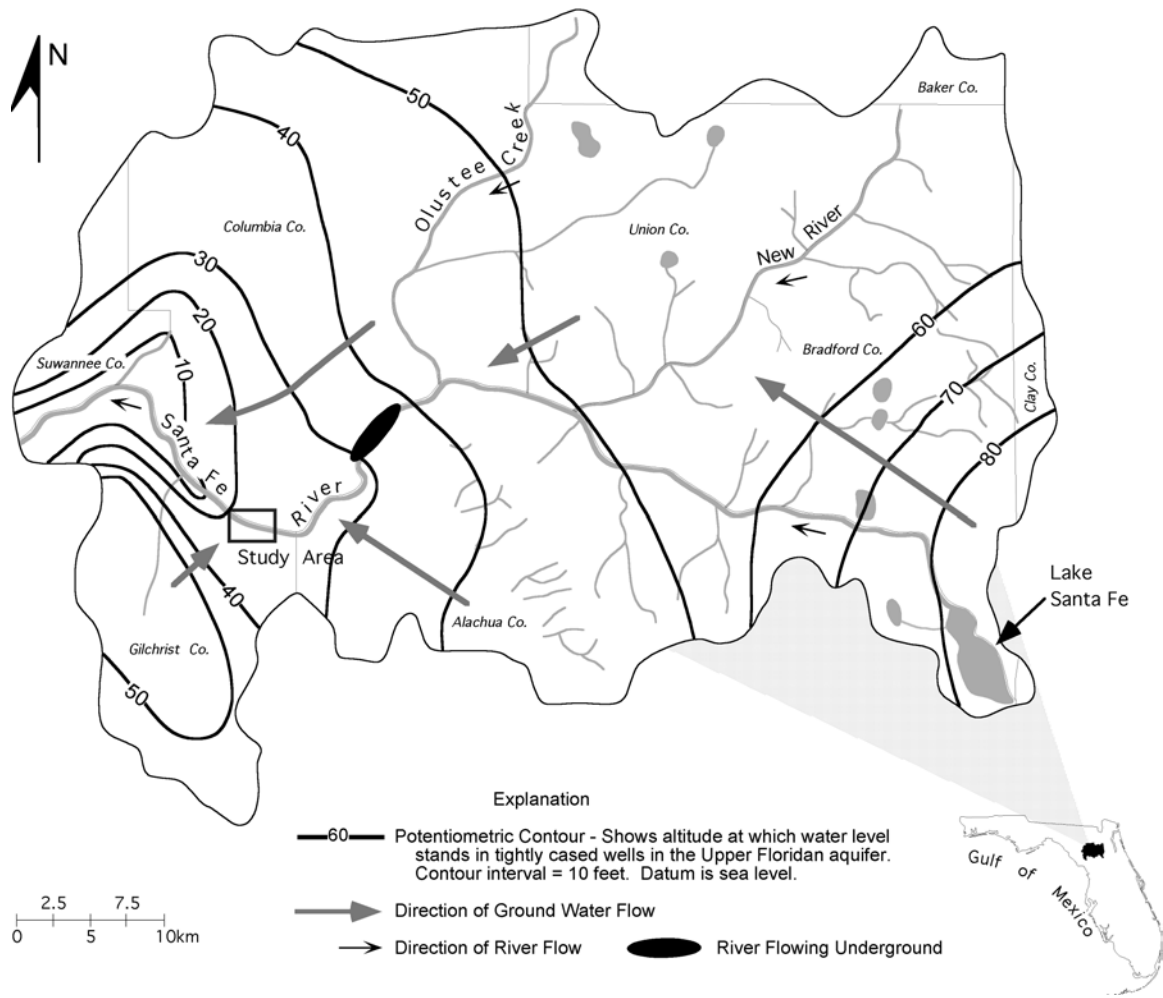


Figure 9. Map of the potentiometric surface of the Floridan aquifer in north-central Florida showing the direction of groundwater flow and the course of the Santa Fe and Suwannee rivers. Adapted from Meadows (1991).

### Topography and Drainage

Figure 10 is adapted from a portion of the USGS High Springs SW. Florida topographic quadrangle showing the specific field area and an expanded view of the Santa Fe River basin in the state of Florida. Land surface elevation in the Santa Fe River basin ranges from approximately 3 meters NGVD at the confluence with the Suwannee River to about 76 meters NGVD on the eastern boundary in west Clay county. The elevation around the study area ranges between 9 and 15 meters NGVD and the gradient of the Santa Fe River in this area is essentially zero. The predominant surface drainage to the river basin occurs in the Northern Highlands physiographic province incorporating New river and Olustee creek. The western third of the basin including parts of Alachua, Columbia, Gilchrist, and Suwannee counties, lacks surface drainage except for the Santa Fe and Ichetucknee rivers, thus all the water that would otherwise drain to surface streams percolates down to the Floridan aquifer and travels through the aquifer to points of discharge (Hunn and Slack, 1983).

### The Devil's Ear Cave System

The Devil's Ear cave system is comprised of the network of underwater cave passages that proceed upstream from Devil's Ear spring. Devil's Ear spring is, in itself, a second magnitude spring that has gone mostly unnoticed in the scientific community because it is located in the Santa Fe River channel and is not visible from the surface throughout much of the year. Devil's Ear spring is physically connected to two other springs, Devil's Eye and July where the combined discharge raises the group to first order status. All three springs are located on the Santa Fe River and are considered part of the Ginnie springs group (Wilson and Skiles, 1988). Descriptions of the cave system are based on the observations conducted as part of this investigation.

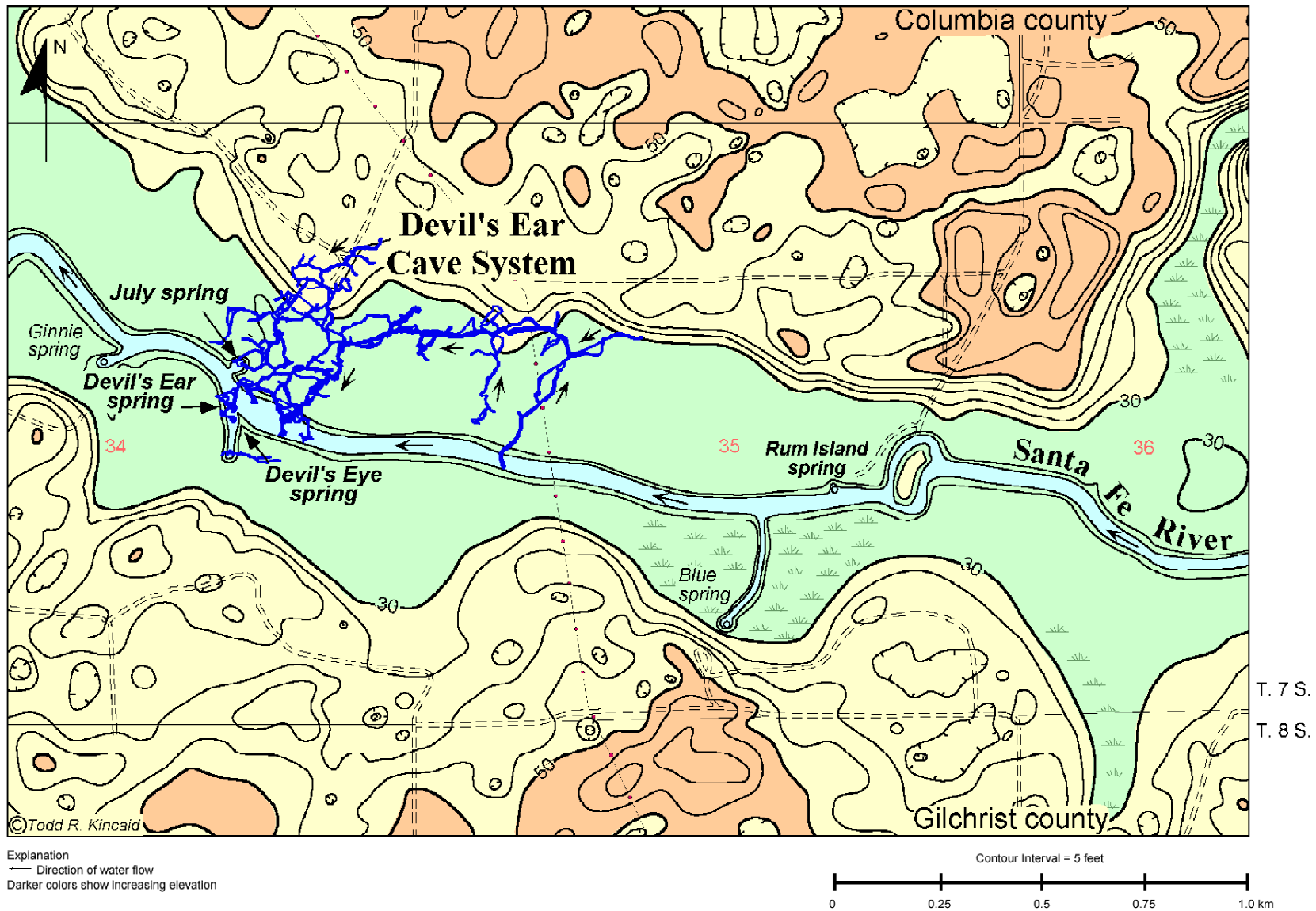


Figure 10. Section of the U.S.G.S. High Springs S.W. topographic quadrangle, 7.5 minute series, showing the drainage features and karst landscape in the field area between Rum Island and July spring on the Santa Fe River near High Springs, north-central Florida.

The Devil's Ear cave system is an extensive underwater network of passages that have developed in the Ocala Limestone. Conduit diameters range from two to twenty meters. The main passage in the cave system begins at Devil's Ear spring and proceeds for over 1,500 meters upstream in an easterly direction where it continues through conduits too small for a diver to negotiate.

Based on the classification scheme described by White (1988) the Devil's Ear cave system is a maze-type cave with an anastomotic pattern. The side passages in the cave system typically deviate in two general directions from the main passage, however most eventually intersect the large, main tunnel. Some branch off on the north side of the main passage and others on the south toward the overlying Santa Fe river. Figure 11 is a copy of the most accurate map of the cave system available (Burman, Unpublished Map). The conduits were surveyed with a compass and marked line and the dimensions of the passages in the first half of the system were measured with a small sonar gun. Figures 12a and 12b are pictures of the entrance to the cave system at Devil's Ear and Devil's Eye springs.

The cave passages trend at a depth of between 0 and 35 meters below land surface. Bedding in the limestone seems to be the dominant structural control on the formation of the passages as the cave system consistently trends at 33 meters below land surface except at the discharge points where the main conduits rise to the level of the river at the three springs. Underneath the Santa Fe river, several passages proceed vertically toward the surface exploiting joints in the limestone. The maze-type layout of the cave passages reflects the fact that the aquifer in this region receives direct recharge through a karst surface (White, 1988). The cave passages become smaller and more dendritic farther from the discharge points.

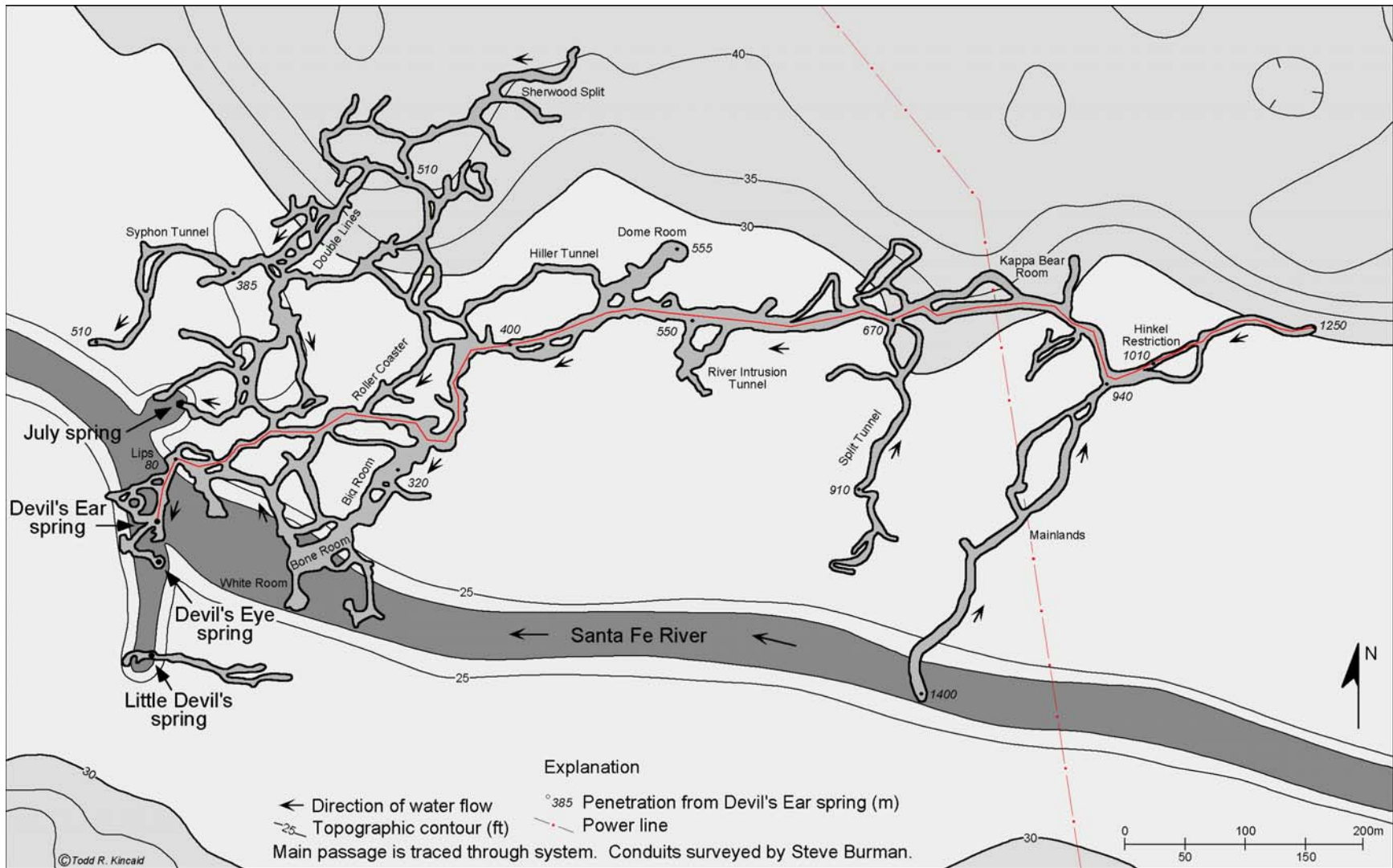


Figure 11. Map of the Devil's Ear cave system superimposed onto part of the U.S.G.S. High Springs S.W. topographic quadrangle showing the direction of groundwater flow through the conduits and the relative position of the overlying Santa Fe river, north-central Florida.

**A**



**B**



*Figure 12. Pictures showing entrances to the Devil's Ear cave system from: a) Devil's Ear and b) Devil's Eye springs. The color variations in the water at Devil's Ear spring result from clear groundwater mixing with tannin stained river water. Photos courtesy of Wes Skiles, Karst Productions.*

The cave system is formed entirely within the Ocala Limestone however the conduits contain much clay, sand, and silt probably delivered to the system from the overlying sediments and fill material in the river and sinkholes in the recharge area. Clay and silt deposits are frequently encountered in the smaller side passages and may be over one meter thick in places. Large quantities of both loose and consolidated fine to coarse sand occur frequently in the cave. Unconsolidated deposits can be over three meters thick and in some places well consolidated sandstone extends laterally across the cave floor. In some of these locations, the sandstone has broken away revealing a lower level of the cave system almost completely filled with sediment.

Many sedimentary structures are visible in the cave system. Sand dunes reaching as high as three meters from the cave floor have formed in the main passage at junctions with side tunnels. In some places scallop marks are visible in the limestone walls and ripple marks in the sand deposits on the floor. Goethite occurs as a speleothem type formation on the walls and ceiling throughout much of the cave system. In some places these deposits seem to grow out of cracks or fractures in the wall and appear to droop downward toward the floor. Finally, in a small isolated room near the back of the system, interesting nodules of calcite cemented sand, clay, and organic material form either singularly or connected in a lattice structure. Figure 13 shows the size and structure of the main passage in the cave system as well as sand dunes and ripple marks on the cave floor.

Many of the springs in Florida experience reverse flow conditions when the associated river rises sufficiently to reverse the hydraulic gradient. During these periods, spring discharge ceases and river water flows into the cave through the spring opening. Reverse flow has never been reported at Devil's Ear or Devil's Eye springs. In fact, when the Santa Fe River rises the discharge from the springs increases. However, a rising river stage is reflected by the clarity of the water discharging from the springs.

Water clarity in the Devil's Ear cave system is typically clear but is greatly reduced during higher stages of the Santa Fe river. During periods of high river flow, several of the passages on the south (river) side of the cave system deliver dark, tea-colored water to the main passage. This, brown water can be seen seeping into the tunnel through small cracks and openings in the rock. Even during these periods of turbid discharge at the springs, the water clarity in the cave system clears upstream of the dark water tunnels.



A



B



Figure 13. Pictures showing the size and structure of the main passage in the Devil's Ear cave system as well as sand dunes and ripple marks on the cave floor. Photos courtesy of Wes Skiles, Karst Productions Inc.

## **CHAPTER 3**

### **BACKGROUND AND PREVIOUS RESEARCH**

#### Tracers

##### Radon

Radon, atomic number 86 and atomic mass 222, is the heaviest known gas. It is essentially inert occupying the last place in the noble gas group of the periodic table. Of the twenty six known isotopes, there are three predominant radioactive alpha emitters, Radon-222, 220, and 219. Radon-222 ( $^{222}\text{Rn}$ ) has a half-life of 3.823 days and is naturally derived from radium-226. Radon-220 (thoron), half-life of 55.6 seconds, emanates from thorium. And, radon-219 (actinon), half-life of 3.96 seconds, emanates from actinium.  $^{222}\text{Rn}$  is the only natural radioactive gas occurring in appreciable amounts (Rogers, 1958). The naturally occurring, measurable quantities  $^{222}\text{Rn}$  make it the isotope of interest in this study. Broecker and Peng (1982) compare some of the physical properties of  $^{222}\text{Rn}$  with other common gasses and a complete list of the physical properties of radon is contained in the Handbook of Chemistry and Physics (1992).

$^{222}\text{Rn}$  is the decay product of  $^{226}\text{Ra}$ , which has a half-life of 1600 years. In a closed system, 99 percent equilibrium between  $^{226}\text{Ra}$  and  $^{222}\text{Rn}$  concentrations will be established within approximately 25 days (Rogers, 1958) and (Otton, 1992). Both  $^{226}\text{Ra}$  and  $^{222}\text{Rn}$  are part of the uranium-238 decay series. Uranium-238 and  $^{226}\text{Ra}$  are common constituents in continental sedimentary rocks and sediments (Key, 1981) and (Ellins et al., 1989; 1990).  $^{222}\text{Rn}$  is highly soluble in water and a volatile gas which is quickly absorbed in the atmosphere where it exists in low concentrations (Rogers, 1958) and (Elsinger and Moore, 1983). Three physical properties:

- 1) the short duration required to establish equilibrium between  $^{222}\text{Rn}$  and its  $^{226}\text{Ra}$ ,
- 2) the ubiquity of  $^{226}\text{Ra}$  in continental sedimentary material, and
- 3) the volatility of naturally occurring gaseous  $^{222}\text{Rn}$  make  $^{222}\text{Rn}$  a commonly used natural tracer with many applications.

Rogers (1958) was the first to use  $^{222}\text{Rn}$  to investigate the relationship between groundwater and surface water. Rogers examined  $^{222}\text{Rn}$  concentrations in streams of the Wasatch Mountains near Salt Lake City, Utah. He demonstrated that  $^{222}\text{Rn}$  concentrations in a flowing stream will be low due to the volatility of the gas and the slow decay rate of the radium source that may be contained in rock and sediment exposed in the stream channel. Furthermore, he demonstrated that  $^{222}\text{Rn}$  concentrations in groundwater were much higher than those in surface water and the groundwater from springs was the source of  $^{222}\text{Rn}$  in the streams. Thus, Rogers showed that increases in  $^{222}\text{Rn}$  concentrations measured in the streams were indicative of groundwater inputs.

Following the work of Rogers (1958), Ellins and others (1989; 1990; 1991) have done extensive research on ground-water / surface-water interactions in larger rivers including the Rio Grande de Manati in Puerto Rico and the Santa Fe River in north-central Florida. Ellins and others (1990) report that the primary mechanism for  $^{222}\text{Rn}$  accumulation in groundwater is the radioactive decay of  $^{226}\text{Ra}$  on or near the grain boundaries of the aquifer material. Furthermore, Ellins reports that to a lesser extent  $^{222}\text{Rn}$  concentrations in groundwater may be augmented by the dissolution of aquifer material which supplies soluble  $^{226}\text{Ra}$  to the groundwater. Since the groundwater is not exposed to the atmosphere,  $^{222}\text{Rn}$  concentrations will not decrease in the aquifer due to volatilization. Also, because of the noble gas configuration of radon, it is chemically inert and will not react with aquifer material or dissolved substances.

The National Council on Radiation Protection and Measurements reports atmospheric levels of  $^{222}\text{Rn}$  to be 0.222 alpha particle disintegrations per minute per liter of water (dpm/L) over continents, 0.022 dpm/L in coastal areas and islands and as low as 0.002 over oceans and arctic areas. They go on to report that  $^{222}\text{Rn}$  levels in groundwater are much greater and vary considerably; 11,000 dpm/L on average and as high as 440,000 dpm/L in the granitic areas of Maine. Because the  $^{222}\text{Rn}$  levels in the atmosphere are very low,  $^{222}\text{Rn}$  dissolved in streams is rapidly lost due to gas exchange across the air/water interface. The work of Rogers (1958) and Ellins and others (1989; 1990; 1991) clearly demonstrates that groundwater discharge to a surface stream is marked by an immediate increase in  $^{222}\text{Rn}$  concentrations in the stream water. There is no other naturally occurring constituent in water for which the ratio of groundwater compared to surface water is so high (Ellins et. al., 1990). The subsequent interpretations of the groundwater/surface flow interactions in the Santa Fe River between the Rum Island and July Spring are directly based on this principal.

#### Source of $^{222}\text{Rn}$ In Groundwater

There are two major sources of dissolved  $^{226}\text{Ra}$  and consequently  $^{222}\text{Rn}$  in the groundwater in Florida: 1) phosphatic sediments and formations and monzonite sands and 2) crystalline basement rocks (Kaufmann and Bliss, 1978). Kaufmann and Bliss (1978) report that exchanges between U and Th with Ca in the phosphate structure concentrate these elements in phosphate minerals especially apatite. Consequently the radioactive decay of U and Th gives rise to  $^{226}\text{Ra}$  and  $^{222}\text{Rn}$  in phosphatic deposits. Furthermore, they report that a major source of these constituents to groundwater in the upper Floridan aquifer is the Hawthorn Formation. Kaufmann and Bliss go on to show that elevated  $^{226}\text{Ra}$  levels in the lower Floridan aquifer are derived from crystalline basement rocks and the increased solubility of radium in groundwater enriched with chloride. Kaufmann and Bliss (1978) and Simpson and Others, (1985) report that  $^{226}\text{Ra}$  levels increase with salinity.

Florida rivers are 1-to-2 orders of magnitude more enriched in  $^{226}\text{Ra}$  compared to the rest of the world's rivers (Fanning et al., Unpublished Manuscript). Fanning and others report that the probable

reason for the enrichment is that most of Florida's major rivers drain phosphate mining districts. Furthermore, they report that the delivery of dissolved  $^{226}\text{Ra}$  to the Gulf of Mexico from Florida's major rivers is 33% of that from the Mississippi River despite the fact that the Mississippi discharges 14 times more water than the cumulative discharge of Florida rivers.

Figure 14 shows the location of the major phosphate mining districts in Florida. The north Florida district covers the area of investigation and is predominantly centered in the Northern Highlands, Brooksville Ridge, and Bell Ridge physiographic provinces. Within these provinces, the Hawthorn and Alachua Formations are commercially important phosphatic sand and gravel deposits.

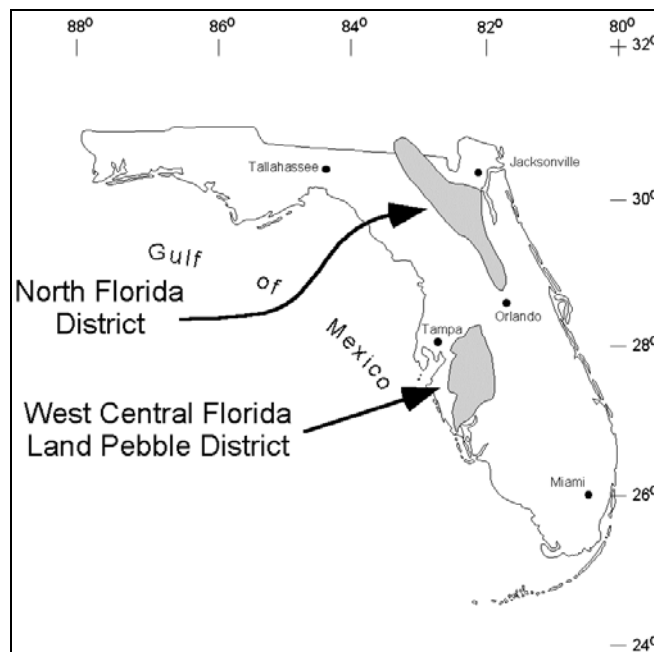


Figure 14. Location of Major Phosphate Districts in Florida. Adapted from Roessler et al. (1979).

Figure 15 is an isopach map of the sediments overlying the Floridan aquifer in the vicinity of the field area. Figure 15 shows two areas of thick sediments, the Northern Highlands region to the east and the Bell Ridge to the south. The map also indicates a thin veneer of sediments covering most of the rest of the area. All of the overlying sediments shown in Figure 15 contain large quantities of phosphatic minerals. The Hawthorn Formation is exposed to the east in the Northern Highlands physiographic province and the Alachua Formation is exposed to the south in the Bell Ridge and also in the thin veneer of sediment cover in parts of the High Springs Gap. The phosphatic minerals contained in these formations are the primary source of dissolved  $^{226}\text{Ra}$  and consequently  $^{222}\text{Rn}$  in the groundwater in the field area. Another source may be up welling of deep groundwater from the Lower Floridan aquifer.

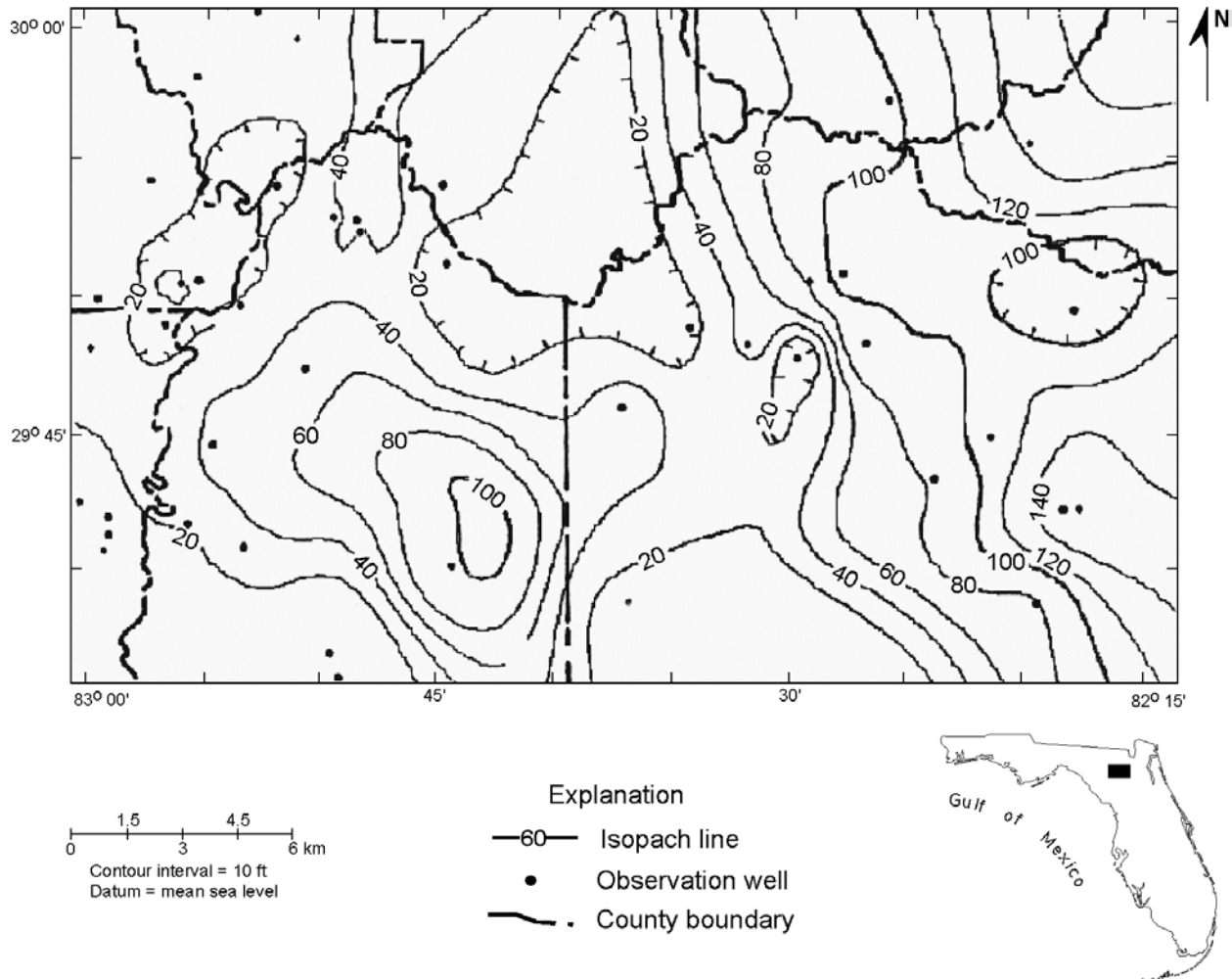


Figure 15. Isopach map of sediments overlying the Floridan aquifer in the southern half of the Santa Fe river basin, north-central Florida. Adapted from Spangler and Silverman (1982).

Though the phosphatic deposits in the Hawthorn and Alachua Formations may be a considerable source of  $^{226}\text{Ra}$ , the dissolution of solid  $^{226}\text{Ra}$  from the outlying sediments is insufficient to support the large quantity of  $^{222}\text{Rn}$  found in the groundwater. Rama and Moore, (1984) conducted studies of the micro-porosity of  $^{226}\text{Ra}$  rich sediments in South Carolina which indicated that  $^{222}\text{Rn}$  was being released from within the grains. They concluded that  $^{222}\text{Rn}$  and other isotopes in the U-Th decay series are released to the micropore waters by alpha recoil from the pore walls. Finally, the  $^{222}\text{Rn}$  is able to diffuse out into the surrounding water. This process elevates the  $^{222}\text{Rn}$  concentration in the groundwater above levels expected due solely to radioactive decay of  $^{226}\text{Ra}$  exposed to the groundwater on the pore walls.

### Sulfur hexafluoride

Sulfur hexafluoride (SF<sub>6</sub>) is a non-toxic, artificial gas that is non-biodegradable and chemically inert (Ellins et al., 1991). The molecular weight of SF<sub>6</sub> is 146.05 g. The gas has a vapor pressure at 21 °C of 22.8 atm and has an extremely low solubility in water at 5.4 cm<sup>3</sup> SF<sub>6</sub>/kg (Wanninkhof, 1986).

Wanninkhof, (1986) employed SF<sub>6</sub> as a gaseous tracer to study the gas exchange rates across the air/water boundary in three lakes of different sizes: Rockland Lake, New York, surface area of 1 km<sup>2</sup>; Crowley Lake, California, surface area of 20 km<sup>2</sup>; and Mono Lake, California with a surface area of 190 km<sup>2</sup>. As a part of his study, he included an in depth discussion of the physical properties of the gas and its analysis. The following is a summary of this discussion and is included here to provide background information about the gas pertinent to this investigation.

Since the development of the electron capture detector (ECD) for gas chromatography, it has been possible to measure very low backgrounds of halogenated gaseous compounds such as SF<sub>6</sub>. Wanninkhof reports that the current atmospheric background of SF<sub>6</sub> is believed to be 1.6 ppt. Furthermore, he reported that since SF<sub>6</sub> is highly electronegative, quantities as low as 5x10<sup>-17</sup> moles can be detected using a gas chromatograph equipped with an ECD. SF<sub>6</sub> has a low solubility in water which means that very small quantities of the gas are required to saturate the water at a concentration well above the atmospheric background. The low atmospheric background, low detection limits, and low solubility in water make SF<sub>6</sub> both economical and practical to use as a gaseous tracer for reaeration experiments.

Since Wanninkhof's work in 1986, SF<sub>6</sub> has been employed as a gaseous tracer to study gas exchange and reaeration in rivers (Ellins et al., 1991), as a groundwater tracer to delineate underground flow paths (Hisert and Ellins, 1991), and as a soluble tracer to study mixing variations in stream flow (Hisert et al., 1991).

Ellins and others, (1991) have shown that once plateau concentrations of SF<sub>6</sub> are reached in the surface discharge of a stream, the decline of SF<sub>6</sub> concentration downstream can be related to the gas exchange across the air/water boundary. The gas exchange coefficient, or gas transfer velocity, can then be related to the reaeration coefficient of the river. Several successful gas exchange experiments were conducted on various reaches of the Santa Fe river, Florida. In addition to the calculation of gas exchange, Ellins and others, (1991) have shown that, during plateau concentrations, anomalous peaks in the SF<sub>6</sub> concentrations downstream can be related to stream water that has been diverted underground and returned to the main stream channel.

Hisert and Ellins, (1991) were the first to use SF<sub>6</sub> as a groundwater tracer to delineate the underground flow path of the Santa Fe River through a karstic terrain near High Springs, Florida. In three

separate experiments, SF<sub>6</sub> was injected into Oleno Sink where the Santa Fe is diverted underground and two additional karst windows, Sweetwater Lake and Jim's Sink. Each time the gas was successfully detected at seven intervening karst windows and once at the river's resurgence.

Finally, Hisert and others (1991) used SF<sub>6</sub> to determine the stream mixing characteristics in the Santa Fe river. In that study, SF<sub>6</sub> was injected to the river and several points downstream were sampled in a grid-like manner to determine how the tracer disperses vertically and laterally in stream flow. Hisert reports that the Santa Fe River became well mixed with respect to width of stream after one kilometer but vertical mixing took place after only a few hundred meters. In addition, he reported that the optimum sampling depth is approximately the upper third of the water column.

In this investigation, SF<sub>6</sub> was used both to calculate gas exchange and as a groundwater tracer. First, following the methodology described by Ellins and others, (1991), SF<sub>6</sub> was used to calculate the gas transfer velocity for the reach of the Santa Fe River under investigation. And second, after a 48 hour continuous injection of SF<sub>6</sub> to the Santa Fe River upstream of the Devil's Ear cave system, cave divers collected water samples from specific locations in the cave that were thought to be hydrologically connected to the river.

#### Oxygen - 18

Oxygen-18 (<sup>18</sup>O) is one of the three isotopes of oxygen. Variations in the <sup>18</sup>O/<sup>16</sup>O ratios ( $\delta^{18}\text{O}$ ) in natural waters result from isotopic fractionation primarily due to evaporation and condensation (Ellins, 1992). Oxygen isotope ratios are expressed in parts per mil (‰) using the delta notation ( $\delta^{18}\text{O}$ ). The fractionation process between <sup>18</sup>O and <sup>16</sup>O leads to different isotopic ratios permitting the distinction of different waters on the basis of their  $\delta^{18}\text{O}$  signature. Consequently,  $\delta^{18}\text{O}$  has been widely used as a natural tracer to study groundwater properties including type, origin, and age. Refer to the following works for a thorough description and discussion on the use of  $\delta^{18}\text{O}$  and other stable isotopic fractionation systems as primary tracers in groundwater hydrology: (Ellins, 1992), (Simpson et al., 1985), and (Gonfiantini and Simonot, 1987).

In this study, variations in  $\delta^{18}\text{O}$  values measured at select locations in the Devil's Ear cave system were used as a check on the <sup>222</sup>Rn data collected in the cave. The measured values were compared to  $\delta^{18}\text{O}$  values for surface waters and groundwaters. Hisert (1994) reports average  $\delta^{18}\text{O}$  values in various surface water bodies in Oleno State Park, near High Springs, Florida of approximately -1.5 ‰. Measured  $\delta^{18}\text{O}$  values in springs and wells in the immediate vicinity of the Devil's Ear cave system and the Santa Fe River ranged between -3.7 and -4.0 ‰. These measured and reported  $\delta^{18}\text{O}$  values show that there is a significant difference between surface water and groundwater with respect to oxygen isotopic fractionation. Surface water has a more enriched  $\delta^{18}\text{O}$  signature due to the selective

evaporation of  $^{16}\text{O}$  that occurs at the surface. Therefore, samples taken from points in the cave system that are suspected of being source areas for surface water influx to the cave will have a more positive  $\delta^{18}\text{O}$  signature.

### Previous Hydrogeological Research

Briel (1976) used the uranium disequilibrium in the springs and surface waters of the Santa Fe River basin to characterize the sources of river discharge components. Two previous investigations were conducted in the vicinity of the Devil's Ear system to determine the recharge area for the nearby springs and potential groundwater flow characteristics in the region. Wilson and Skiles (1988) conducted a dye tracing experiment using rhodamine-wt at four groundwater wells on the south side of the Santa Fe River near Ginnie Spring. Kincaid and others (1992) implemented a groundwater tracing experiment using SF<sub>6</sub> to investigate the karst plain region north of the Santa Fe River and its potential as a source of recharge to the Devil's Ear cave system.

Briel, (1976) investigated the disequilibrium between  $^{234}\text{U}$  and  $^{238}\text{U}$  in different parts of the river as well as various springs in the Santa Fe River basin as a mechanism for the differentiation of the water sources. Essentially, he discovered three primary sources contributing water to the river discharge, surface water and two different groundwater sources. He concluded that the types of groundwater in the Santa Fe springs probably originated from widely separated recharge areas. Furthermore, he found that the stage of the river exerts a delicate hydraulic control on the aquifer. Briel reported that the surface water signature increases in Devil's Eye and July springs during flood stages of the Santa Fe river. Finally, Briel indicated that water from local swamps and water filled sinkholes recharges several of the Santa Fe River springs.

Wilson and Skiles (1988) conducted a set of four dye tracing experiments using rhodamine-wt to establish the hydrologic relationship between the nine springs that make up Ginnie Springs Park. The study was commissioned by the Ginnie Springs Water Bottling Company to assess the feasibility of operating a high yield pumping well for the bottling and sale of "spring water". In each experiment, the dye tracer was injected into one of four wells drilled into cavernous zones of the Floridan aquifer. Figure 16 taken from their report shows the results of each of these experiments. Their results clearly showed a consistent dispersion of the dye to more than one spring. The repeated dispersion indicated the absence of effective groundwater drainage divides within a few hundred meters of the spring discharge points. They further report that the dispersion indicates the presence of an extensive network of three dimensional braided conduits in the aquifer. The most significant aspect of the Wilson and Skiles study pertaining to the Devil's Ear investigation is that in none of the four tracing experiments was any dye recovered in the any of the spring outlets from the Devil's Ear cave system (Devil's Ear, Devil's Eye, and July springs). They conclude that Ginnie, Dogwood, and Little Devil's springs are hydrologically related and that the springs are connected by a pervasive network of braided conduits.



Kincaid and others (1992) conducted a tracing experiment to investigate the potential recharge area for the Devil's Ear cave system and to further establish SF<sub>6</sub> as a viable groundwater tracer in karstic regions. In that study, SF<sub>6</sub> was injected to a groundwater well and a water filled sinkhole on the north side of the Santa Fe river. Water samples were collected from three springs, Rum Island, July, and Little Devil's springs over a 55 hour period following the tracer injection. The tracer was detected in all three springs which indicated that all three are hydraulically connected to the karst plain region on the north side of the Santa Fe river. Figure 17 shows the SF<sub>6</sub> recovery curves for the three springs with an inset describing the groundwater flow pathways. The peak separation at Rum Island spring indicates the existence of a small braided conduit system connecting it to the northern recharge area where the three independent peaks reflect different conduit pathways. Peak separations between the three sampling points indicates that the overall groundwater flow path proceeds from the northern recharge area to Rum Island where it intersects the Devil's Ear cave system and subsequently connects the other two springs.

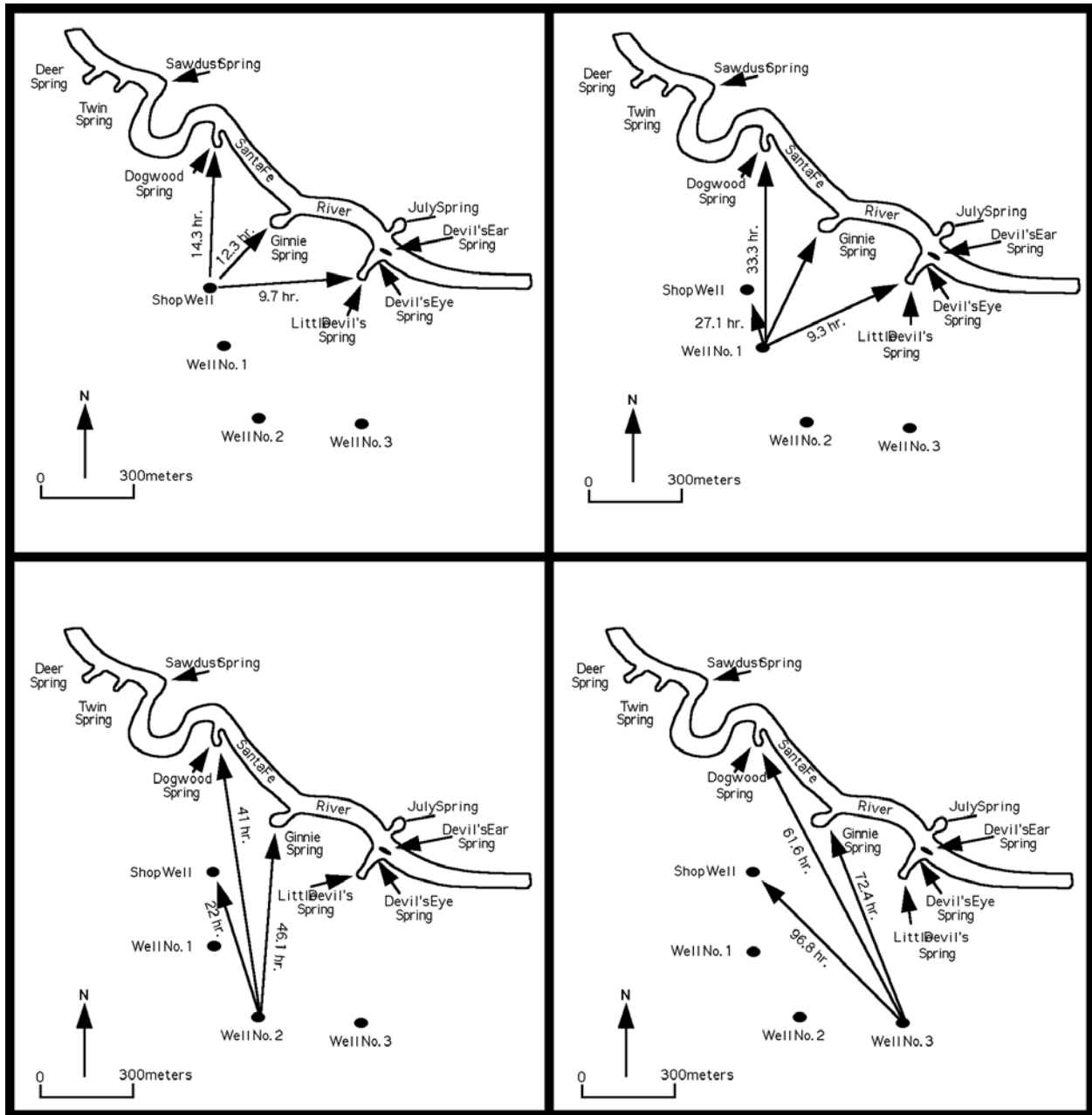


Figure 16. Results of dye tracing experiments conducted at Ginnie Springs park, north-central Florida, showing groundwater flow directions and travel times. (Wilson and Skiles, 1988).

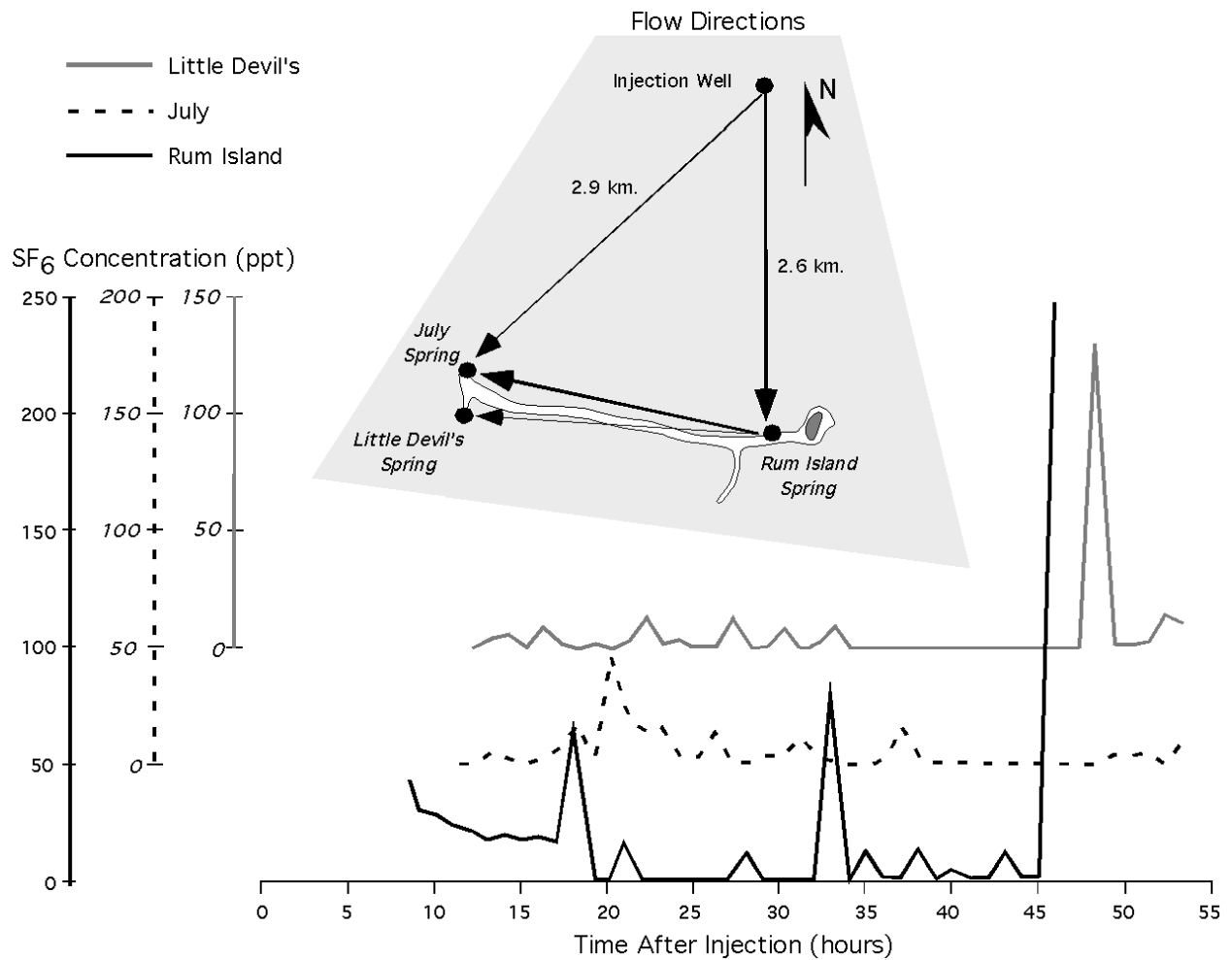


Figure 17.  $SF_6$  recovery curves for a groundwater tracing experiment conducted in April, 1992 between an inactive pumping well and three springs on the Santa Fe River near High Springs, Florida, adapted from Kincaid and others (1992). Inset shows the predominant groundwater flow directions.

## **CHAPTER 4**

### **METHODOLOGY**

#### *The River Experiments*

Three river transects were conducted on Sept. 17, 1991, Feb. 19, 1992, and June 5, 1993. The transects were conducted at high, low, and medium flow stages of the Santa Fe river, respectively. The object of each transect was to measure discharge,  $^{222}\text{Rn}$ , and  $\text{SF}_6$  concentrations over a 2 km. reach of the Santa Fe River downstream of the injection point at Rum Island. The results of these transects enabled the calculation of an average gas transfer velocity for this reach of the river. In turn, groundwater inputs to the river and stream flow losses to the underlying Devil's Ear cave system were determined based on  $^{222}\text{Rn}$  and  $\text{SF}_6$  fluctuations in the stream.

#### *Water Sampling*

All the river water samples were obtained from a canoe paddled downstream to each of the sampling locations and collected at regular intervals in the river. The water sampling bottles for  $^{222}\text{Rn}$  analyses consisted of evacuated 250 ml plastic graduated cylinders, each having one fill tube and two extraction tubes connected into the bottle through a rubber stopper at the top. By opening the sample tube and releasing the vacuum, the bottles were filled with river water to approximately 180 ml leaving sufficient head space for the accumulation of  $^{222}\text{Rn}$  gas. The samples were collected from the upper half meter of the water column. To obtain a true representation of the river at the sampling location, the water samples were integrated with respect to width of stream. To accomplish this, the sample tube was connected to a pole hung over the side of the canoe and the sample bottle was filled slowly as the canoe was paddled across the river.

Water samples for  $\text{SF}_6$  analysis were collected in small glass biological oxygen demand (BOD) type bottles, glass syringes, or typical 80 ml glass bottles with viton septums. These bottles were filled from the upper half meter of the water column by simply holding the bottle underwater and opening and replacing the cap. Because of the volatility of  $\text{SF}_6$ , the samples were filled with no head space remaining in the bottle.

Because of the simple method of filling the B.O.D. and 80 ml bottles, it was impossible to obtain an integrated sample from the river with these containers. For this reason,  $\text{SF}_6$  samples were collected in three locations across the river channel at each sampling location, 1/3, middle, and 2/3 of the stream width. Later, the measured  $\text{SF}_6$  concentrations in the three bottles were averaged to produce a representative sample of the river at each sampling location.

## Discharge Measurements

The width, depth, and velocity of the river were recorded at select locations on the transect reach during each of the experiments. As with the water samples, all these measurements were made from a canoe. The width of the river was measured by stretching a line, knotted every 3 meters across the river. The approximate width of the river was then calculated by counting the knots. The river depth and velocity were then measured at each knot, every three meters across the stream. Depth was measured by dropping a measured line with an attached two pound weight to the bottom. The stream velocity was measured with a Weathertronics velocity meter in 1991 and a Ocean Dynamics velocity meter in 1992 and 1993. Velocity measurements were made from the upper 1/3 of the stream depth.

The overall width of the river was broken down into three meter sections forming either triangles or rectangles or both. Following the standard USGS discharge calculation method, component flow values were calculated for each section. This was done by multiplying the measured velocity recorded in the section by the area of that section (width of section x depth of section). The component flow values were then added to produce the total discharge at the selected point in the river. Figure 18 shows the method for the calculation of discharge at the selected points in the river.

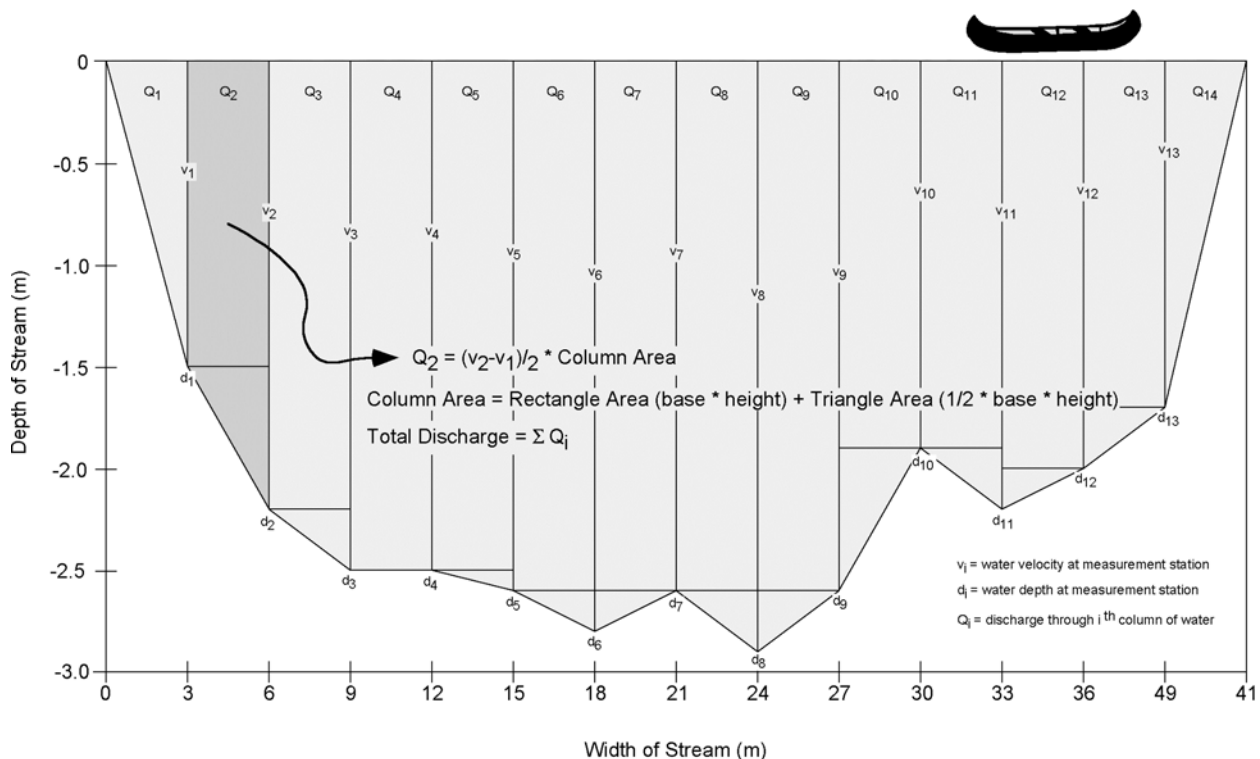


Figure 18. Method for calculating discharge at selected points in the Santa Fe River between Rum Island and July spring, north-central Florida.

### SF<sub>6</sub> Injection

Personal communications with other researchers using SF<sub>6</sub> as a gas tracer in reaeration studies indicated that the direct injection of gaseous SF<sub>6</sub> to a stream is problematic. Because of the need to achieve well mixed conditions in the stream with respect to vertical and horizontal mixing and longitudinal dispersion, an injection system was modified to allow SF<sub>6</sub> saturated water to be introduced to the river at one or two points across the width of the channel. The injection system consisted of:

- 1) a cylinder of pure SF<sub>6</sub> gas,
- 2) a 250 liter plastic barrel with two small openings at the top,
- 3) a two stage Matheson gas regulator,
- 4) a two channel peristaltic pump, and
- 5) tygon and rubber tubing.

The 250 liter barrel was filled with river water at the site of injection. SF<sub>6</sub>, regulated through the two stage regulator, was delivered to the barrel by a small section of rubber tubing and bubbled through the water from a small diffusion stone placed at the bottom of the barrel. For approximately five minutes the SF<sub>6</sub> was vigorously injected to the barrel water by setting the back pressure on the regulator to ten pounds per square inch (psi). Afterwards the pressure was reduced to one or two psi and continued throughout the injection. In this way, the water in the barrel was insured to remain saturated with SF<sub>6</sub>. At this point, the saturated water was pumped out of the barrel and delivered to the river with the peristaltic pump. Two injections points in the river, 1/3 and 2/3 stream width, were used and the total flow rate from the barrel was approximately 800 ml per minute. The injection began two hours before each experiment and continued throughout the sampling interval. Figure 19 shows the injection system with the components labeled.

### Gas Exchange

The primary mechanism for radon removal from a turbulent river such as the Santa Fe is gas exchange across the air/water interface (Ellins et al., 1990). In order to calculate the groundwater contribution to the river and the stream flow loss, an accurate estimate of the gas transfer rate for <sup>222</sup>Rn from the river water surface to the atmosphere must be determined. The stagnant film model (Broecker and Peng, 1982; Elsinger and Moore, 1983) serves as the basis for the calculation of the gas transfer velocity (k). According to Broecker and Peng (1982), this method requires the following assumptions.

1. The upper few meters of the water column must have uniform concentrations of the gas, i.e. the river water column must be well mixed.
2. The column of air above the water surface must also have uniform concentrations of the gas.
3. These two well-mixed reservoirs are separated by a stagnant film of water.
4. Gasses cross this boundary only by molecular diffusion.

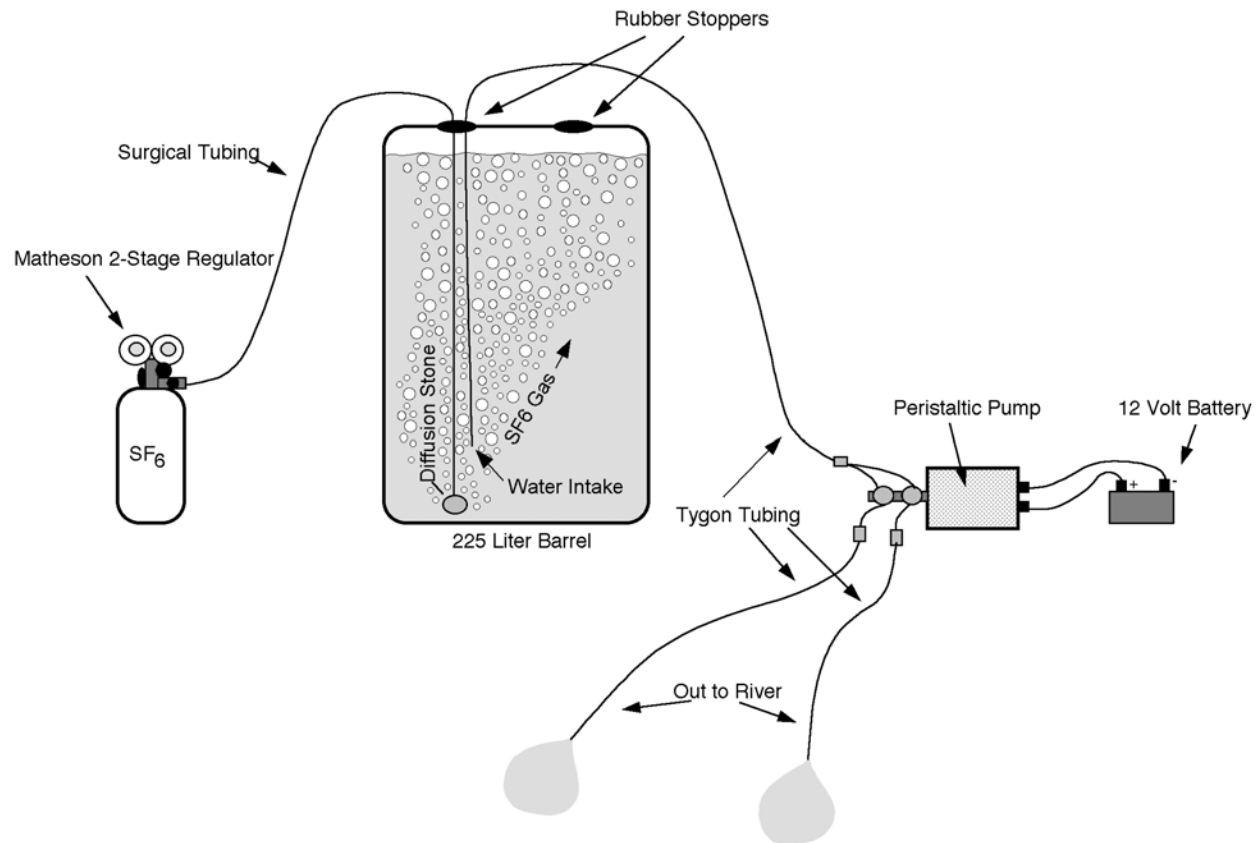


Figure 19. The SF<sub>6</sub> river injection system.

Gas transfer coefficients are strongly dependent on temperature. Higher temperatures yield faster gas exchange (Ellins et al., 1990). The gas transfer coefficient is often determined from the measurement of another gas and sometimes at different temperatures. In this case, the coefficient must be corrected for the difference in temperature and diffusivity. Ledwell, (1982) and Wanninkhof, (1986) demonstrated that a dimensionless ratio known as the Schmidt number can be used to correlate the exchange coefficients of different gasses. The Schmidt number is defined as the kinematic viscosity of water ( $\nu$ ) divided by the molecular diffusivity of the gas ( $D$ ). Both  $\nu$  and  $D$  are temperature dependent values, thus the Schmidt number serves as an excellent correlation factor over a given temperature range. The correction of the gas exchange coefficient, as reported by Wanninkhof (1986), is based on:

$$k = Sc^n; \quad (1)$$

where:

$Sc$  = Schmidt number =  $\nu/D$ ;

$n$  = exponent, the magnitude of which depends on the turbulence of the interface.

The correction from one gas to another is:

$$k_a = ((Sc_a)^n)/((Sc_b)^n) * k_b; \quad (2)$$

where: a and b refer to gases a and b.

Ellins and others (1990) reported that the magnitude of the exponent (n) for a turbulent stream without bubble entrainment such as the Santa Fe River is -0.5. Table 1 (Ellins et al., 1990) is a list of Schmidt numbers for  $^{222}\text{Rn}$ ,  $\text{SF}_6$ , and  $\text{O}_2$  for temperatures ranging from 15° to 30° Celsius.

TABLE 1. Comparison of Schmidt Numbers for  $^{222}\text{Rn}$ ,  $\text{SF}_6$ , and  $\text{O}_2$  at Selected Temperatures.

Temp. °C	$^{222}\text{Rn}$	$\text{SF}_6$	$\text{O}_2$
15	1288	1089	689
20	950	839	531
21	741	678	418
22	683	607	378
23	953	833	523
24	903	793	498
25	853	754	472
27	802	714	446
30	501	477	291

Because of the complicated interactions between groundwater and surface flow in the Santa Fe river, the gas transfer velocity of  $^{222}\text{Rn}$  could not be measured directly. Frequent groundwater inputs to the stream prevent the measurement of a decrease in  $^{222}\text{Rn}$  concentrations in the river due solely to gas exchange. For this reason,  $\text{SF}_6$ , a deliberate, conservative, gaseous tracer with similar physical properties to  $^{222}\text{Rn}$  was used to calculate k. The following equation (Ellins et al., 1990) was used to calculate the apparent gas transfer velocity for  $\text{SF}_6$  along this reach of the river:

$$k = h \cdot (v/x) \cdot \ln((\text{SF}_6\text{up} \cdot \text{Qup}) / (\text{SF}_6\text{down} \cdot \text{Qdown})); \quad (3)$$

where:

k = gas transfer velocity (m/day),

h = mean depth of stream along the reach (m),

v = mean stream velocity along the reach (m/day),

x = reach distance (m),

$\text{SF}_6\text{up}$  =  $\text{SF}_6$  concentration upstream,

$\text{SF}_6\text{down}$  =  $\text{SF}_6$  concentration downstream,

Qup = stream discharge upstream, and

Qdown = stream discharge downstream.

### Groundwater Influx

Groundwater contributions increase the background  $^{222}\text{Rn}$  concentration in a stream. After groundwater influx to the stream has occurred,  $^{222}\text{Rn}$  concentrations in the stream should decrease due to gas exchange at the air/water interface. Calculation of groundwater influx over a specific stream reach



is based on a measured increase in the  $^{222}\text{Rn}$  concentration over the expected, background concentration due solely to gas exchange. The following equation from Elsinger and Moore (1983) is used to calculate the background  $^{222}\text{Rn}$  concentration at a sampling point:

$$R_b = R_{S(\text{up})} * e^{-\{D/(zhv)\} * x}; \quad (5)$$

where:

$R_b$  = the background  $^{222}\text{Rn}$  concentration due to gas exchange,

$R_{S(\text{up})}$  = the  $^{222}\text{Rn}$  concentration at the prior upstream sampling location,

$D$  = the molecular diffusivity of the gas ( $\text{m}^2/\text{s}$ ),

$z$  = the thickness of the stagnant film =  $D/k$  (m),

$h$  = the average stream depth(m),

$v$  = the average stream velocity (m/s), and

$x$  = the sampling interval (m).

By substituting  $D/k$  for  $z$  in equation 5, the background calculation can be simplified to the following form:

$$R_b = R_{S(\text{up})} * e^{-\{k/(hv)\} * x}; \quad (6)$$

where:  $k$  = the gas transfer velocity derived from  $\text{SF}_6$  measurements (m/s).

For points in the stream where the measured  $^{222}\text{Rn}$  concentration exceeds the background level, the added groundwater component of the stream flow at that point can be calculated based on the following mass balance equation (Ellins et al., 1990):

$$R_S(Q_S) = R_{Gw}(Q_{Gw}) + R_b(Q_S - Q_{Gw}); \quad (7)$$

where:

$R_S$  = the  $^{222}\text{Rn}$  concentration in the stream,

$R_{Gw}$  = the measured  $^{222}\text{Rn}$  concentration in the groundwater,

$R_b$  = the background  $^{222}\text{Rn}$  concentration due to gas exchange,

$Q_S$  = the measured discharge of the stream, and

$Q_{Gw}$  = the groundwater component of stream flow.

Solving for  $Q_{Gw}$  yields the following equation:

$$Q_{Gw} = Q_S * \{(R_b - R_S)/(R_b - R_{Gw})\} \quad (8)$$

Error calculations are described in Chapter 5 which indicate a plus or minus 20% error margin involved in this method. Potential sources of error include:

- 1) sampling and analytical techniques,
- 2) discharge measurement, and
- 3) calculation of the gas exchange coefficient.

### Stream Flow Loss

Since there is no surface drainage from the river, measured stream flow losses along the Rum Island to Devil's Ear reach of the Santa Fe River are presumed to be due to infiltration to the underlying aquifer. Swirling siphons have been observed at the surface of the river at points farther upstream of the field area. The size and frequency of these features vary with the stage of the river.

Stream flow losses are physically measured in the river when downstream discharge plus the calculated groundwater influx component is measured to be less than at an upstream point. The following, simple equation was employed to determine the magnitude of such losses:

$$(Q_{\text{down}} + Q_{\text{gw}}) - Q_{\text{up}} = Q_{\text{loss}}; \quad (9)$$

where:

$Q_{\text{down}}$  = measured discharge at the downstream location,

$Q_{\text{gw}}$  = calculated groundwater components of flow between measuring locations,

$Q_{\text{up}}$  = measured discharge at the upstream location, and

$Q_{\text{loss}}$  = stream flow loss between measuring points.

*Note: stream flow loss will be a negative value.*

Sources of error involved in the calculation of stream flow loss components in the stream include:

- 1) discharge measurement and
- 2) calculation of the groundwater influx components.

### Return Flow

Ellins and others (1991) postulated the existence of a return flow component to the stream discharge based on observed peaks in SF<sub>6</sub> concentrations along a stream transect. The concept suggests that elevated SF<sub>6</sub> concentrations in the stream are due to stream water that has been diverted underground, thus preventing loss of SF<sub>6</sub> to the atmosphere, and then returning to the surface at a point downstream elevating the SF<sub>6</sub> concentration in the stream above the expected background level. With the same reasoning used to calculate groundwater influx, equations were developed in this study to attempt to characterize the return flow component of stream discharge. First, the background SF<sub>6</sub> concentration in the river was calculated based on the model proposed by Elsinger and Moore, (1983):

$$S_{\text{bge}} = S_{\text{S(up)}} * e^{-\{k/(hv)\} * x}; \quad (10)$$

where:

$S_{\text{bge}}$  = the background SF<sub>6</sub> concentration due to gas exchange,

$S_{\text{S(up)}}$  = the SF<sub>6</sub> concentration at the prior upstream sampling location,

$h$  = the average stream depth,

$v$  = the average stream velocity,

$k$  = the gas transfer velocity derived from SF<sub>6</sub> measurements, and

$x$  = the sampling interval.

Groundwater inputs to the stream complicate the measurement of return flow components since a groundwater contribution will dilute the SF<sub>6</sub> concentration in the stream. To account for this dilution, the following correction is applied to the background SF<sub>6</sub> value:

$$S_b = S_{bge} * \{(Q_s - Q_{gw})/Q_s\}; \quad (11)$$

where:

$S_b$  = the SF<sub>6</sub> background in the stream due to gas exchange and dilution from groundwater influx,

$S_{bge}$  = the background SF<sub>6</sub> concentration due to gas exchange,

$Q_s$  = the discharge of the stream, and

$Q_{gw}$  = the groundwater component of stream discharge.

With the adjusted background value, equation 7 can be modified to describe the return flow component in the stream. The new flow component balance is described by:

$$S_s(Q_s) = S_{rf}(Q_{rf}) + S_{bge}(Q_s - Q_{rf}); \quad (12)$$

where:

$S_s$  = the SF<sub>6</sub> concentration in the stream,

$S_{rf}$  = the measured SF<sub>6</sub> concentration at the upper most sampling location,

$S_{bge}$  = the background SF<sub>6</sub> concentration due to gas exchange,

$Q_s$  = the measured discharge of the stream, and

$Q_{rf}$  = the return flow component of stream flow.

Solving for  $Q_{rf}$  yields the following equation:

$$Q_{rf} = Q_s * \{(S_{bge} - S_s)/(S_{bge} - S_{rf})\} \quad (13)$$

The term  $S_{rf}$  must be assumed to be the SF<sub>6</sub> concentration at the upper most sampling location since there is no way to localize the location of the lost flow.

Error calculations for this method are described in Chapter 5 which indicate a plus or minus 30% error margin for this method. Sources of error include:

- 1) sampling and analytical techniques,
- 2) discharge measurement,
- 3) calculation of the gas exchange coefficient, and
- 4) locating the point of stream flow loss.

### The Cave Experiments

In order to better understand the interactions between the Santa Fe River and the Devil's Ear cave system, it was necessary to conduct first hand investigations within the cave itself. Using  $^{222}\text{Rn}$  as a natural tracer and the same principles discussed for the river experiments, surface water intrusion to the cave system was isolated and its behavior studied. In order to accomplish this, a complicated sampling strategy was employed in which over 50 water samples were collected, during two experiments, from various points covering most of the substantial conduits. Advanced cave diving equipment and techniques were employed to allow two researchers to penetrate as far as 1500 meters into the cave system on over 25 separate dives. The researchers made observations about the cave morphology and collected water samples that would be measured for  $^{222}\text{Rn}$ , major cation, and  $\delta^{18}\text{O}$  concentrations.

The University of Florida had never before sponsored an underwater speleological investigation such as the magnitude of this project. The university mandated that all the diving related activities meet the close scrutiny of the Dive Board, a panel of researchers primarily involved in openwater diving safety and research. The Devil's Ear study was only the second underwater speleological project to be proposed to the board. Bill Streever conducted an earlier investigation of endemic crayfish at Peacock spring but only focused on the first few hundred feet of the cave entrance. The overall unfamiliarity of many of the Dive Board members with cave diving techniques and the magnitude of the dives involved in the project caused a considerable obstacle in the commencement of the diving plan.

In the final form passed by the Dive Board, the diving research plan constituted two separate investigations conducted during two different stages of the Santa Fe river. Approximately 50 dives in the system were proposed to collect water samples and make morphologic observations. The  $^{222}\text{Rn}$  sampling strategy entailed the collection of discrete water samples from five major areas in the cave system:

- 1) 1200 meters of the main upstream passage between the basin and the Hinkel Restriction which is upstream of the major feeder tunnels,
- 2) the right line area that includes the Big Room and underlies the Santa Fe river,
- 3) the River Intrusion tunnel, a 300 meter side tunnel that has been observed to contribute tea colored water to the system,
- 4) the Split Tunnel, an 800 meter side passage containing vertical fissures that underlies the Santa Fe River and has also been observed to contribute tea colored water to the cave system , and
- 5) the Mainlands, a distant region of the system that feeds water to the main passage from the area beneath the river that is also tea colored during certain periods.

In addition to the  $^{222}\text{Rn}$  sampling events, a sampling plan was proposed to sample two specific locations in the cave, the River Intrusion Tunnel and the Split Tunnel, for  $\text{SF}_6$  after an injection was performed in the river two days prior. Refer to Figure 11 to locate the sampled regions in the cave system.

The Dive Board mandated that they maintain close involvement throughout the entire diving program. The dive plan proposed two divers to accomplish the research goals. A dive master, Jarrod Jablonski, was assigned to ensure the safety of the dives and the efficiency of the dive plan and a scientific coordinator, Todd Kincaid, to ensure the integrity of the sampling strategy. A specific dive plan was required to be filed with the board one week in advance of every dive. In turn, the specifics of every dive were closely scrutinized by the Diving Safety Officer.

After seven months of persistence, the Dive Board passed the final proposal. Even in the reduced stage this proposal was the most ambitious underwater speleological study to ever be attempted at the University of Florida.

### Cave Diving Techniques and Water Sampling

The cave diving techniques employed during the research dives followed the standards prescribed by the National Speleological Society-Cave Diving Section and the National Association for Cave Diving. First, both research divers were fully trained cave divers with over 5 years of experience in Florida caves including more than 300 dives. Double 104 ft<sup>3</sup> (3000 L) tanks with fully redundant regulator systems were used to supply an ample air for the dives. A continuous guide line was followed at all times that led out of the cave to direct surface access. Lighting was provided by a 50 watt canister light with 2.5 hours of burn time with three additional smaller backup lights kept in reserve. Thermal protection against the long underwater exposures to 21°C groundwater was provided by neoprene dry suits with thin undergarments. Diver propulsion vehicles (scooters) were used to propel the divers back to the sampling locations. Over 3/4 of each divers air supply was saved in case of a scooter failure which would have required a diver to swim or be towed out of the cave. Finally, oxygen was used in the water for all decompression commitments. British decompression tables were used to determine the necessary decompression commitments required for each dive. Figure 20 shows a cave diver riding a scooter through the Devil's Ear cave system. The research dives were conducted in much the same manner.

Water samples for <sup>222</sup>Rn measurements were collected in 250 ml plastic bottles. The bottles were evacuated prior to the dive so that approximately 180 ml could be filled leaving sufficient head space for <sup>222</sup>Rn accumulation. As many as 15 bottles were carried into the cave on each dive contained in a net bag attached to one of the divers' chests. At each sampling location, a sample bottle was removed from the net bag, filled, and placed into another bag reserved for full bottles. While the sample was being taken the other diver recorded the sample number, time and sample location. At the most distant or difficult to reach locations, duplicate samples were taken in case one was lost. Figure 21 shows the cave-diving team collecting a water sample for <sup>222</sup>Rn from a side conduit in the Devil's Ear cave system.

Other water samples were collected for  $\delta^{18}\text{O}$  and major cation analyses. These samples were collected in small glass vials that were filled with distilled water prior to the dive. At the sampling location,

the vial was drained by injecting air into the bottle with a small air nozzle attached to the divers tanks. Once drained, the bottle was refilled with ambient water; the process was repeated several times to insure a representative sample.



*Figure 20. Picture Showing a Fully Equipped Cave Diver Riding a Scooter Through the Devil's Ear cave system. Photo Courtesy of Wes Skiles, Karst Productions Inc.*



Figure 21. Picture showing the cave-diving team collecting a water sample to be measured for  $^{222}\text{Rn}$  from a side conduit in the Devil's Ear cave system, north-central Florida. Photo courtesy of Bill Dooley.

### Surface Water Influx

Based on the same theory described in the preceding discussion of the river experiments,  $^{222}\text{Rn}$  measurements were used to estimate the groundwater component of conduit flow within the Devil's Ear cave system. Sample transects were run in the main conduits on two occasions in conjunction with the 1992 and 1993 river experiments.

The quantity of intruded river water in the samples taken from the Devil's Ear cave system was determined using the following equation:

$$R_s = R_{riv} * Riv + R_{aq} * (1 - Riv) \quad (14)$$

where:

$R_s$  = the  $^{222}\text{Rn}$  concentration in the sample,

$R_{riv}$  = the background  $^{222}\text{Rn}$  concentration in the river,

$Riv$  = the decimal fraction of river water in the sample, and

$R_{aq}$  = the background  $^{222}\text{Rn}$  concentration in the aquifer.

Solving the equation for the percentage of river water in a given sample produces

$$\%Riv = \left( \frac{Rs - Raq}{Rriv - Raq} \right) * 100.$$

Background  $^{222}\text{Rn}$  concentrations in the aquifer were measured by sampling five wells near the field area but more than 1 km from the river. *Raq* was determined to be 780 dpm/L in February 1992 and 852 dpm/L in June 1993 by averaging the values obtained from the five wells. Measuring *Rriv* in the field area revealed values ranging between 252 and 540 dpm/L. These values were not considered accurate estimations of the background  $^{222}\text{Rn}$  concentration in the river because of large groundwater inputs from several springs. Instead, *Rriv* was determined by averaging several measurements collected by Ellins and others (1991) and Hisert (1994) that were taken just upstream of the field area where there is less groundwater input. Averaging these reported  $^{222}\text{Rn}$  concentrations produced a value for *Rriv* of 60 dpm/L. The model only assumes fixed end-member concentrations for the mixing waters. Note that a greater value for *Rriv* would result in an increased value for *%Riv*.

Variations in  $\delta^{18}\text{O}$  provided a qualitative check on the  $^{222}\text{Rn}$  mixing results. Water samples, collected in the 1993 sampling period, were analyzed for  $\delta^{18}\text{O}$  to qualitatively check the results obtained from the  $^{222}\text{Rn}$  mixing model. Greater  $\delta^{18}\text{O}$  values were expected to correspond to sampling locations with small  $^{222}\text{Rn}$  concentrations and thus confirm regions of river water intrusion to the cave system.

### Analytical Techniques

#### Radon-222

After the  $^{222}\text{Rn}$  samples were returned to the laboratory, the sample containers were attached to portable extraction systems designed at Lamont Doherty Research Institute. The extraction system delivers the gas from the sample head space to Lucas-type counting cells. The cells were left for two hours so that the  $^{222}\text{Rn}$  in the cell could equilibrate with its daughter products. At that point, the counting cells were put into alpha-scintillation counters where light photons emitted by the alpha disintegrations of  $^{222}\text{Rn}$  and its daughters were counted by a photomultiplier and recorded as counts per minute. Each cell was counted three times and allowed to accumulate at least 1000 counts for statistical reliability. The results of the counting process were entered into a simple computer program that calculated the  $^{222}\text{Rn}$  activity in the cell in decintegrations per minute per liter (dpm/L). A thorough description of the methodology involved in the  $^{222}\text{Rn}$  analysis is discussed by Key (1981) and Ellins and others (1990).



### Sulfur hexafluoride

The first step in the process of using SF<sub>6</sub> as a tracer was to develop a set of standards for use as a basis of comparison in the SF<sub>6</sub> analysis. A new method of SF<sub>6</sub> standard preparation was designed and implemented in this investigation. Basically, a purchased 1 ppm reference standard was diluted in small portable scuba cylinders with ultra high purity nitrogen.

Using the carefully prepared SF<sub>6</sub> standards as reference concentrations, the SF<sub>6</sub> samples were analyzed by gas chromatography using a Shimadzu Gas Chromatograph GC-8A equipped with an electron capture detector (ECD) following the procedures described by Wanninkhof (1986). The water samples were first transferred to 50 ml glass syringes. The syringes were filled with 20 ml of the water sample and then 30 ml of ultra high purity nitrogen, vigorously shaken for two minutes and then injected to the sample loop of a multiport injection system. Next, the sample was injected to the GC through a two meter column filled with Porapac-Q maintained at 80°C. The gas peaks were separated in the column packing and recorded as peaks on a Chromjet integrator.

## CHAPTER 5

### RESULTS

#### The River Experiments

Three river transect experiments were carried out on the 2 km. reach of the Santa Fe River between Rum Island and Ginnie spring on September 17, 1991, February 19, 1992, and June 5, 1993. The transects were carried out at three different flow stages of the Santa Fe river. The 1991 transect reflects the highest flow stage where the average discharge across the transect was 28 m<sup>3</sup>/s. The lowest flow stage occurred in 1992, when the average discharge was 19 m<sup>3</sup>/s. The 1993 transect reflects the intermediate flow stage with an average discharge of 21 m<sup>3</sup>/s. On each occasion, detailed discharge measurements were carried out at various points along the reach to characterize fluctuations in stream discharge. Figure 22 shows the fluctuation in stream discharge over the duration of the study period. Discharge measurements combined with the data received from SF<sub>6</sub> and <sup>222</sup>Rn sampling were used to determine the:

- (1) gas transfer velocity for SF<sub>6</sub> and <sup>222</sup>Rn in the stream,
  - (2) ground water influx to the stream, and
- stream flow losses to the aquifer.

Tabulated results for the 1991, 1992, and 1993 transects are presented in Table 3. Measured SF<sub>6</sub> and <sup>222</sup>Rn concentrations are compared to stream discharge and depicted in Figure 23.

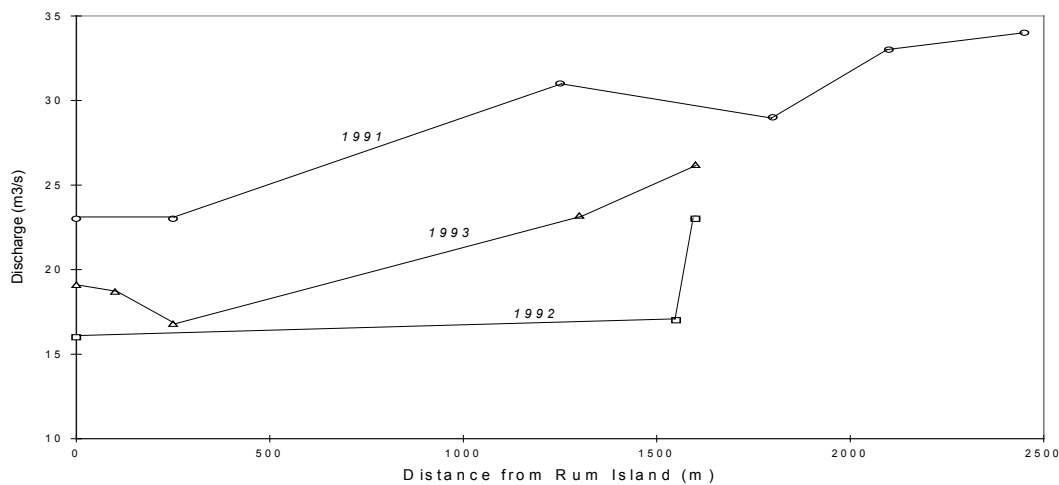


Figure 22. Comparison of measured stream discharge between Rum Island and Ginnie spring on the Santa Fe river, north-central Florida during the study period between September, 1991 and June, 1993.

Table 3.  $^{222}\text{Rn}$  and  $\text{SF}_6$  concentrations and measured stream parameters from the sampled transect of the Santa Fe River between Rum Island and Ginnie spring, north-central Florida for each of the sampling periods between September, 1991 and June, 1993.

Location	Dis. from Rum Is. (m)	Sep. 1991 Transect					Feb. - 1992 Transect					Jun. - 1993 Transect				
		$^{222}\text{Rn}$ (dpm/L)	$\text{SF}_6$ (pmol/kg)	Depth (m)	Velocity (m/s)	Discharge ( $\text{m}^3/\text{s}$ )	$^{222}\text{Rn}$ (dpm/L)	$\text{SF}_6$ (pmol/kg)	Depth (m)	Velocity (m/s)	Discharge ( $\text{m}^3/\text{s}$ )	$^{222}\text{Rn}$ (dpm/L)	$\text{SF}_6$ (pmol/kg)	Depth (m)	Velocity (m/s)	Discharge ( $\text{m}^3/\text{s}$ )
Rum Is.	0	227		1.7	0.26	23	405		1.9	0.25	16	293		2.3	0.18	19.1
Rum Is. spg.	100											448		1.9	0.23	18.7
Blue spg.	250	294	1062	1.5	0.28	23	323	2623				343	1529	1.7	0.20	16.8
	400											348	1159			
	500	280	596				391	1185				542	881			
	600											266	915			
	700											185	900			
	750	287	801				268	1534								
	800											212	1069			
	900											236	896			
	1000	320	836				320	1116				267				
	1100											343	786			
	1200											224	1120			
	1250	299		1.7	0.34	31	336	1123								
	1300	302	781				250	1178				221	1159	2.1	0.19	23.2
	1350	303	815				325	1130								
	1400	287	836				261	1171				285	852			
	1450	330	836				376	1253								
Devil's Ear spg.	1500	380	842				257	1548				304	771			
	1550	267	582				316	1589	1.0	0.40	17					
July spg.	1600	295	719	0.7	0.46	23	356	808	2.5	0.19	23	310	751	3.0	0.17	26.2
	1650	297	733				356	856								
	1700	495	438													
	1750	430	555													
	1800	310	562	2.0	0.30	29										
	1850	316	356													
	2000	281	315													

Location	Dis. from Rum Is. (m)	Sep. 1991 Transect					Feb. - 1992 Transect					Jun. - 1993 Transect				
		<sup>222</sup> Rn (dpm/L)	SF <sub>6</sub> (pmol/kg)	Depth (m)	Velocity (m/s)	Discharge (m <sup>3</sup> /s)	<sup>222</sup> Rn (dpm/L)	SF <sub>6</sub> (pmol/kg)	Depth (m)	Velocity (m/s)	Discharge (m <sup>3</sup> /s)	<sup>222</sup> Rn (dpm/L)	SF <sub>6</sub> (pmol/kg)	Depth (m)	Velocity (m/s)	Discharge (m <sup>3</sup> /s)
Ginnie spg.	2050	405	418													
	2100	284		2.4	0.24	33										
	2150	410	671													
	2200	406	678													
	2450	431	278	2.6	0.25	34										
Average		Value:		1.8	0.3	28			1.8	0.28	19			2.2	0.19	20.8

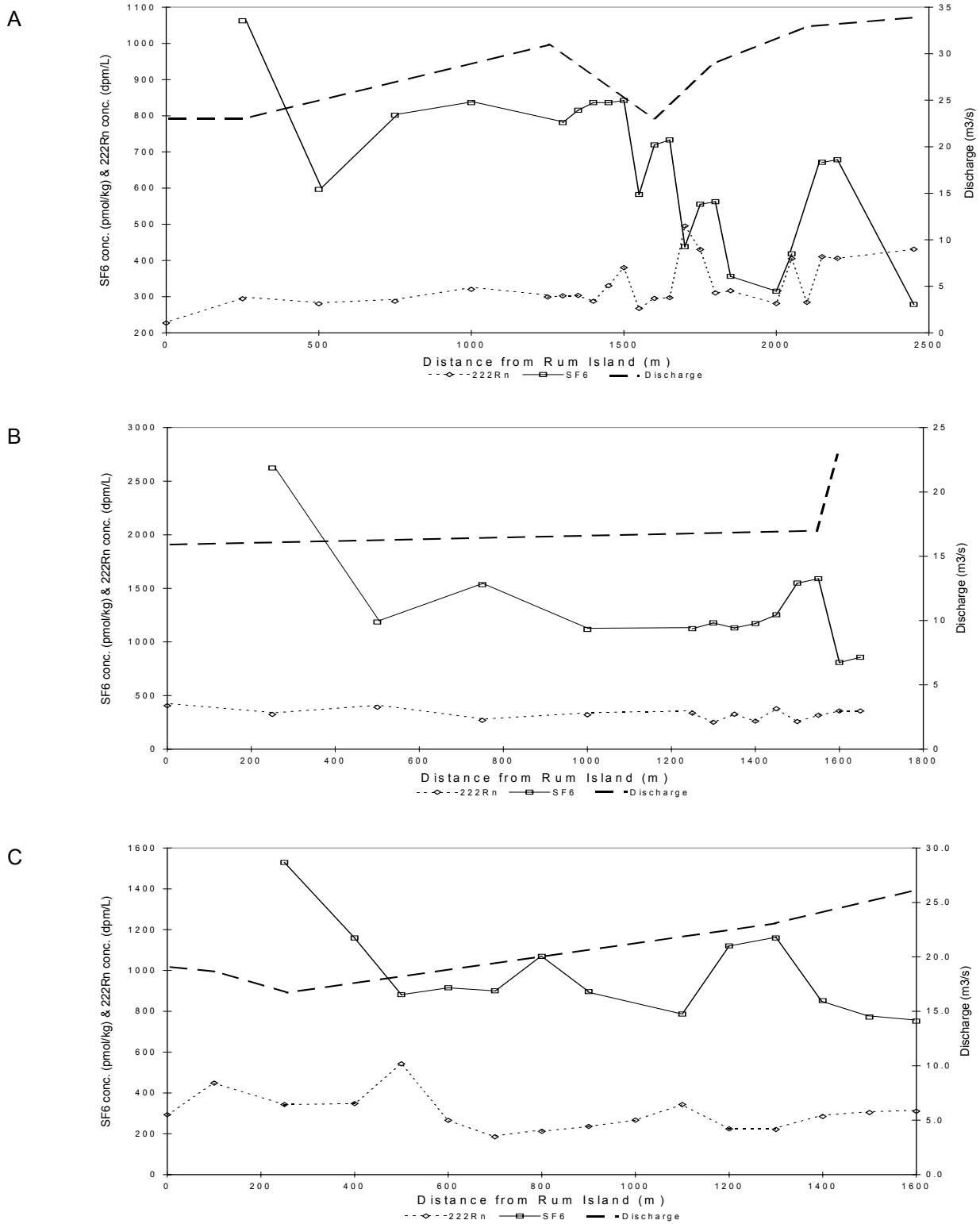


Figure 23. Uncorrected  $^{222}\text{Rn}$  and  $\text{SF}_6$  data and measured discharge in the Santa Fe River of north-central Florida between Rum Island and Ginnie spring for the (A) September, 1991, (B) February 1992, and (C) June 1993 sampling periods.

Due to vertical mixing considerations, SF<sub>6</sub> sampling began 250 m from the injection point at Rum Island. Figure 23 demonstrates that the SF<sub>6</sub> concentration in the stream was highest during the low flow stage and lowest during the high flow stage. This dilution in tracer concentration results from increased discharge.

The <sup>222</sup>Rn peaks depicted in Figure 23 are indicative of ground water inputs to the stream. Although the peaks are more conspicuous during the lower discharge periods, the results of the three experiments indicate that the ground water influx, stream flow loss, and return flow components increase with increasing stream discharge.

### Gas Exchange

The gas transfer velocity for SF<sub>6</sub> was experimentally determined on each of the three transect dates using the method described in chapter 4. Values for k were calculated using equation 3. The <sup>222</sup>Rn gas transfer velocity was then derived by applying the correction factor listed in equation 2 to the k value obtained from the measured SF<sub>6</sub> concentrations in the river. To account for the variability in the calculation, high and low end member gas transfer coefficients were used in the subsequent techniques for calculating ground water influx and stream flow loss. The gas transfer velocity for SF<sub>6</sub> ranged from 1.86 to 12.82 m/day and 1.98 to 13.63 m/day for <sup>222</sup>Rn. Though only slightly, the gas transfer velocity for SF<sub>6</sub> was consistently lower than that calculated for <sup>222</sup>Rn. Consequently, the <sup>222</sup>Rn values were used in the calculation of the ground water influx components and the SF<sub>6</sub> values were used in the calculation of return flow components. Table 4 shows a list of stream parameters, SF<sub>6</sub> concentrations up and down-stream, and calculated k values for SF<sub>6</sub> and <sup>222</sup>Rn for each of the three river experiments.

*Table 4. Calculation of the gas transfer velocity (k) for the Santa Fe River between Rum Island and Ginnie spring during the sampling periods between September, 1991 and June, 1993.*

Date	Ave. Depth m	Ave. Vel. m/s	Reach Distance m	SF <sub>6</sub> up pmol/kg	SF <sub>6</sub> down pmol/kg	Q up m <sup>3</sup> /s	Q down m <sup>3</sup> /s	k SF <sub>6</sub> m/day	Derived k <sup>222</sup> Rn m/day
9/17/91	1.8	0.30	2200	1062	678	23	33	1.86	1.98
2/19/92	1.8	0.28	1650	2000	856	16	23	12.82	13.63
6/5/93	2.2	0.19	1600	1529	751	17	26	6.02	6.40

	SF <sub>6</sub>	<sup>222</sup> Rn
High k value:	12.82	13.63
Low k value:	1.86	1.98
Average k value:	6.90	7.34

### Stream Flow Components

Ground water influx, stream flow loss, and return flow components of the stream discharge between Rum Island and July spring were calculated after each of the three river transects using the equations described in chapter 4, the experimentally determined high and low values for  $k$ , and the measured  $^{222}\text{Rn}$  signature of the local ground water. Background  $^{222}\text{Rn}$  concentrations in the local ground water were determined by sampling various wells and spring boils in the immediate vicinity of the river reach. The average  $^{222}\text{Rn}$  concentration from the ground water samples taken during each sampling period was used in the flow component calculations for both the river and cave experiments. Table 5 shows the  $^{222}\text{Rn}$  values for samples taken from various wells and springs during each transect period. The average  $^{222}\text{Rn}$  concentrations in the local ground water were 784 dpm/L in 1991, 780 dpm/L in 1992, and 850 dpm/L in 1993.

*Table 5.  $^{222}\text{Rn}$  concentrations measured in various wells and springs between September, 1991 and June, 1993 near the Santa Fe River between Rum Island and Ginnie spring, north-central Florida.*

Location	1991 $^{222}\text{Rn}$ Conc. dpm/L	1992 $^{222}\text{Rn}$ Conc. dpm/L	1993 $^{222}\text{Rn}$ Conc. dpm/L
Little Devils spring	*	793	850
Ginnie spring	757	765	870
Ginnie Well	810	800	830
Ground water Well	*	780	850

*note: \* indicates that no sample was taken*

$^{222}\text{Rn}$  and  $\text{SF}_6$  values measured in the stream on each transect were corrected for the 10% error associated with the sampling and analytical techniques. The first step in the application of the correction process was to eliminate all data points that fell within 10% of the immediate up-stream value. Background concentrations were then calculated for both  $^{222}\text{Rn}$  and  $\text{SF}_6$ . Next, the data set was reanalysed and the data points that fell within 10% of the corresponding calculated background value were again eliminated. Finally, the background concentrations were recalculated based only on the corrected  $^{222}\text{Rn}$  and  $\text{SF}_6$  values. The application of this correction process is necessary because it eliminates spurious fluctuations in the  $^{222}\text{Rn}$  and  $\text{SF}_6$  transect graphs due to sampling and analytical error. Uncorrected data will yield misleading background concentrations and false estimates of the stream flow components. All calculations used to determine stream flow components were based on these corrected values. Table 3 contains the original data. Tables 6, 7, and 8 show the corrected values for  $^{222}\text{Rn}$  and  $\text{SF}_6$  concentrations measured in the stream, the calculated background  $^{222}\text{Rn}$  and  $\text{SF}_6$

concentrations at each sampling location, as well as the calculated ground water influx, stream flow loss, and return flow components for each sampling period and k value. Finally, each table shows the calculated discharge (measured stream flow + ground water inputs) at each sampling location. Figures 24, 25, and 26 show corrected  $^{222}\text{Rn}$  and  $\text{SF}_6$  concentrations and the measured and calculated stream discharge vs. transect distance for each sampling period.

In Figure 24a, the most prominent features are  $^{222}\text{Rn}$  peaks #1 and #2 and  $\text{SF}_6$  peak #4. The initial rise in  $^{222}\text{Rn}$  concentration at the beginning of the transect coincides with the ground water contribution from Rum Island and Blue springs. Peak #1 indicates the presence of a ground water spring or seep in the river up-stream of Devil's Ear spring. Peak #2 reflects the ground water contribution from the Devil's group of springs.

The initial linear drop in  $\text{SF}_6$  concentration is an artifact of the correction process. Samples collected from that part of the river reach contained similar  $\text{SF}_6$  concentrations. Many of those data points were eliminated because their variation fell within the range of sampling and analytical error. The dramatic increase depicted in  $\text{SF}_6$  peak #4 reflects the contribution of return flow up-stream of Ginnie spring.

Figure 24b compares the measured discharge with the discharge calculated from the ground water inputs. The most prominent deviations occur in the vicinity of the major spring groups along the transect. The dramatic stream flow loss reflected at 1600 meters on the transect is indicative of the total loss occurring over the 400 meter stretch immediately up-stream.



Table 6. Corrected  $^{222}\text{Rn}$  and  $\text{SF}_6$  concentrations, stream flow components, and calculated discharge for the reach of the Santa Fe River between Rum Island and Ginnie spring, north-central Florida during the September, 1991 sampling period.

Location	Dis. from Rum Is. (m)	Cor. $^{222}\text{Rn}$ (dpm/L)	Cor. $\text{SF}_6$ (pmol/kg)	Meas. Dis. ( $\text{m}^3/\text{s}$ )	Backgrd. $^{222}\text{Rn}$ k= 1.98	Backgrd. $\text{SF}_6$ k= 1.86	G.W. Influx ( $\text{m}^3/\text{s}$ )	Stream Loss ( $\text{m}^3/\text{s}$ )	Return Flow ( $\text{m}^3/\text{s}$ )	Calc. Dis. ( $\text{m}^3/\text{s}$ )	Backgrd. $^{222}\text{Rn}$ k= 13.63	Backgrd. $\text{SF}_6$ k= 12.82	G.W. Influx ( $\text{m}^3/\text{s}$ )	Stream Loss ( $\text{m}^3/\text{s}$ )	Return Flow ( $\text{m}^3/\text{s}$ )	Calc. Dis. ( $\text{m}^3/\text{s}$ )
Rum Is.	0	227		23						23.0						23.0
Blue spg.	250	295	1062	23	225					23.0	211					23.0
	500				222	930	3.0			26.0	196	845	3.9			26.9
	750				292	920				26.0	274	786				26.9
	1000	320			289	863	1.4			27.4	255	661	2.8			29.7
	1250			31	317	872				31.0	297	622				31.0
	1300				316	871				31.0	293	613				31.0
	1350				315	869				31.0	289	604				31.0
	1400	287			315	867				31.0	285	592	0.1			31.1
	1450	330			286	795	2.7			33.7	283	534	2.9			34.1
	1500	380			329	720	3.5			37.2	325	474	3.7			37.8
Devil's Ear spg.	1550	267			379	718		-15.5		37.2	374	467		-16.2		37.8
July spg.	1600	295		23	266	717	1.3			23.0	263	253	1.4			23.0
	1650				294	484				23.0	291	249				23.0
	1700	495	438		294	343	9.4		4.3	32.4	287	173	9.6		9.7	32.6
	1750	430	555		494	310		-3.4	10.6	32.4	488	304		-3.6	10.8	32.6
	1800	310		29	429	554				29.0	424	547				29.0
	1850		356		309	553				29.0	306	539				29.0
	2000		315		307	354				29.0	292	341				29.0
	2050	405	418		307	261	6.0	-2.0	6.9	35.0	288	251	6.8	-2.8	7.4	35.8
	2100			33	404	342				33.0	399	327				33.0
	2150		671		403	341			15.1	33.0	393	322			15.6	33.0
Ginnie spg.	2200				402	670				33.0	388	661				33.0
	2450	431	281	34	398	606	2.9	-1.9		34.0	360	512	5.7	-4.7		34.0
				Total	Flow	Comps.:	30.2	-22.8	36.9				36.9	-27.3	43.5	

Table 7. Corrected  $^{222}\text{Rn}$  and  $\text{SF}_6$  concentrations, stream flow components, and calculated discharge for the reach of the Santa Fe River between Rum Island and July spring, north-central Florida during the February, 1992 sampling period.

Location	Dis. from Rum Is. (m)	Cor. $^{222}\text{Rn}$ (dpm/L)	Cor. $\text{SF}_6$ (pmol/kg)	Meas. Dis. ( $\text{m}^3/\text{s}$ )	Backgrd. $^{222}\text{Rn}$ k= 1.98	Backgrd. $\text{SF}_6$ k= 1.86	G.W. Influx ( $\text{m}^3/\text{s}$ )	Stream Loss ( $\text{m}^3/\text{s}$ )	Return Flow ( $\text{m}^3/\text{s}$ )	Calc. Dis. ( $\text{m}^3/\text{s}$ )	Backgrd. $^{222}\text{Rn}$ k= 13.63	Backgrd. $\text{SF}_6$ k= 12.82	G.W. Influx ( $\text{m}^3/\text{s}$ )	Stream Loss ( $\text{m}^3/\text{s}$ )	Return Flow ( $\text{m}^3/\text{s}$ )	Calc. Dis. ( $\text{m}^3/\text{s}$ )	
Rum Is.	0	405		16						16.0						16.0	
Blue spg.	250	323	2623		400					16.0	375					16.0	
	500	391	1185		319	2285	2.2			18.3	299	2076	2.7			18.7	
	750	268	1534		387	1032			5.8	18.3	362	938			6.6	18.7	
	1000	320			265	1400	1.5			19.7	248	1286	1.9			20.6	
	1250				316	1384				19.7	296	1189				20.6	
	1300	250			316	1381				19.7	291	1171				20.6	
	1350	325	1144		249	1249	2.0			21.7	246	1046	2.1		1.4	22.7	
	1400	261			324	1035				21.7	320	1022				22.7	
	1450	376			260	902	3.2			24.9	257	881	3.2			26.0	
	1500	257	1253		375	900			5.1	24.9	370	867			5.7	26.0	
Devil's Ear spg.	1550	316	1548	17	256	1124	1.7	-7.9	4.8	17.0	253	1103	1.8	-10.8	5.0	17.0	
July spg.	1600				315	1403				18.8	311	1380				19.1	
	1650	356	856	23	315	1306	1.8			23.0	306	1244	2.1			23.0	
				Total	Flow	Comps.:	12.4	-7.9	15.7				13.8	-10.8	18.7		

Table 8. Corrected <sup>222</sup>Rn and SF<sub>6</sub> concentrations, stream flow components, and calculated discharge for the reach of the Santa Fe River between Rum Island and July spring, north-central Florida during the June, 1993 sampling period.

Location	Dis. from Rum Is. (m)	Cor. <sup>222</sup> Rn (dpm/L)	Cor. SF <sub>6</sub> (pmol/kg)	Meas. Dis. (m <sup>3</sup> /s)	Backgrd. <sup>222</sup> Rn k= 1.98	Backgrd. SF <sub>6</sub> k= 1.86	G.W. Influx (m <sup>3</sup> /s)	Stream Loss (m <sup>3</sup> /s)	Return Flow (m <sup>3</sup> /s)	Calc. Dis. (m <sup>3</sup> /s)	Backgrd. <sup>222</sup> Rn k= 13.63	Backgrd. SF <sub>6</sub> k= 12.82	G.W. Influx (m <sup>3</sup> /s)	Stream Loss (m <sup>3</sup> /s)	Return Flow (m <sup>3</sup> /s)	Calc. Dis. (m <sup>3</sup> /s)	
Rum Is.	0	293		19						19.0						19.0	
Rum Is. spg.	100	448		19	291		5.2	-5.2		19.0	280		5.4	-5.4		19.0	
Blue spg.	250	343	1529	17	444			-2.0		17.0	418			-2.0		17.0	
	400		1159		340	1055			3.7	17.0	320	994			5.2	17.0	
	500	542			337	832	6.5			23.5	306	792	7.1			24.1	
	600	266			538	826				23.5	518	767				24.1	
	700	185			264	821				23.5	254	744				24.1	
	800	212	1069		184	792	0.7		9.1	24.2	177	696	0.9		11.2	25.0	
	900	236	896		211	1004	0.7			24.9	202	967	0.9			25.8	
	1000	267			234	837	0.9			25.8	225	805	1.1			26.9	
	1100	343			265	767	2.2			28.0	255	716	2.4			29.4	
	1200	224	1120		341	762			13.1	28.0	328	694			15.0	29.4	
	1300			23	223	1113		-5.0		23.0	214	1085		-6.4		23.0	
	1400	285	852		221	1006	2.3			25.3	204	938	2.8			25.8	
Devil's Ear spg.	1500				283	770				25.3	272	736				25.8	
July spg.	1600	310		26	281	726	1.3	-0.5		26.0	260	649	2.1	-0.2		26.0	
				Total	Flow	Comps.:	19.8	-12.7	25.9				22.7	-14.0	31.4		

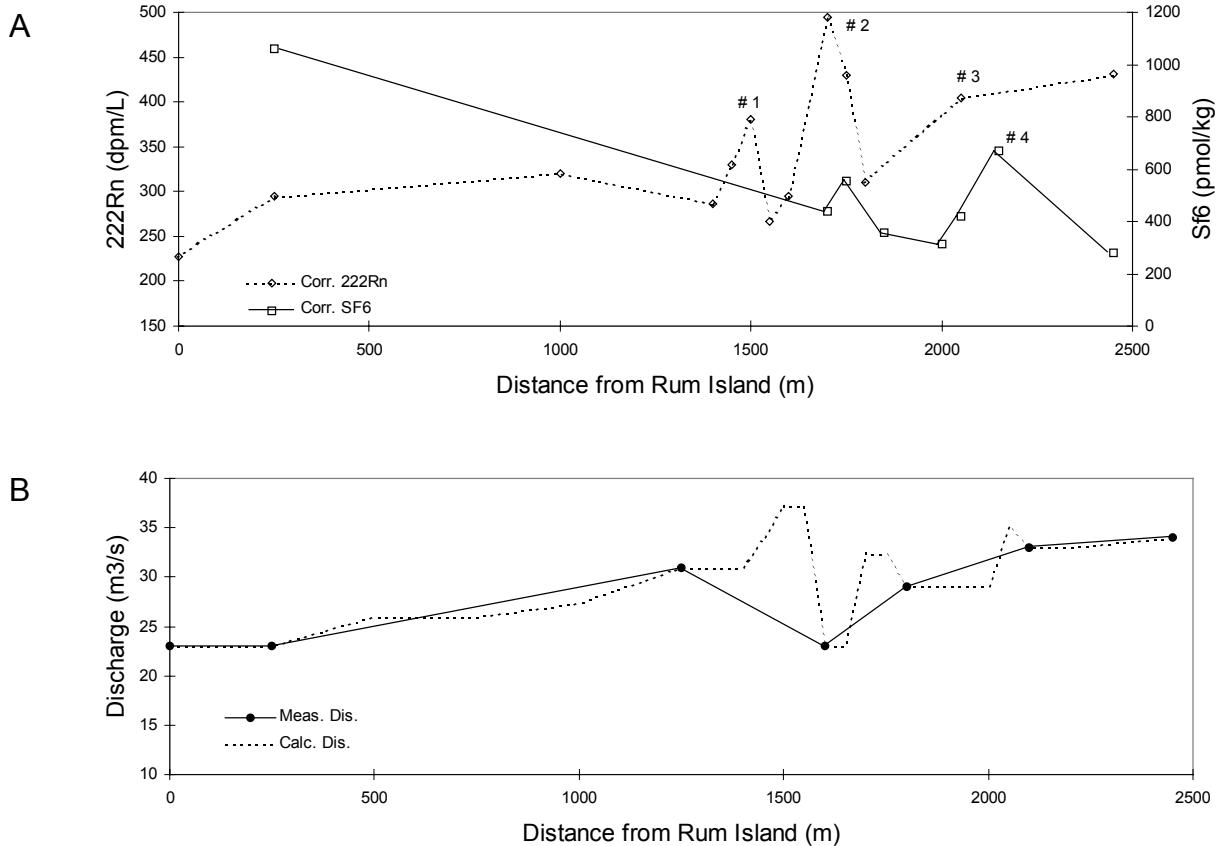


Figure 24. (a) Corrected  $^{222}\text{Rn}$  and  $\text{SF}_6$  concentrations vs. transect distance and (b) measured and calculated discharge vs. transect distance measured during the September, 1991 sampling of the Santa Fe River between Rum Island and Ginnie spring, north-central Florida. Peaks in  $^{222}\text{Rn}$  concentrations correspond to ground water influx to the river. Peaks in  $\text{SF}_6$  concentrations indicate the return of river water that had been diverted underground up-stream.

The February 17, 1992 transect was conducted at the lowest measured flow stage during the study period. The transect presented in Figure 25a indicates that the ground water/stream flow interactions are more prominent during the lower flow stage of the river. The apparent shift in  $^{222}\text{Rn}$  peaks down-stream of their source is probably caused by longitudinal dispersion.

$^{222}\text{Rn}$  peak #1, located at 450 meters on the transect, shows the ground water contribution from Blue spring located up-stream at 250 meters.  $^{222}\text{Rn}$  peaks #2, #3, and #4 reflect the ground water contribution from the Devil's group and July springs. The condensed fluctuations in  $^{222}\text{Rn}$  concentrations between 300 and 400 dpm/L associated with peaks 2, 3, and 4 between 1300 and 1600 meters are attributed to mixing and longitudinal dispersion in the stream associated with the ground water influx.

The initial dip in the SF<sub>6</sub> plot corresponds to the <sup>222</sup>Rn peak near Blue spring where ground water influx has diluted the SF<sub>6</sub> concentration in the river. SF<sub>6</sub> peaks #5 and #6 reflect subsequent increases in the SF<sub>6</sub> concentration in the river. These increases reflect a combination of lateral and longitudinal mixing variations in the stream and points of return flow to the river.

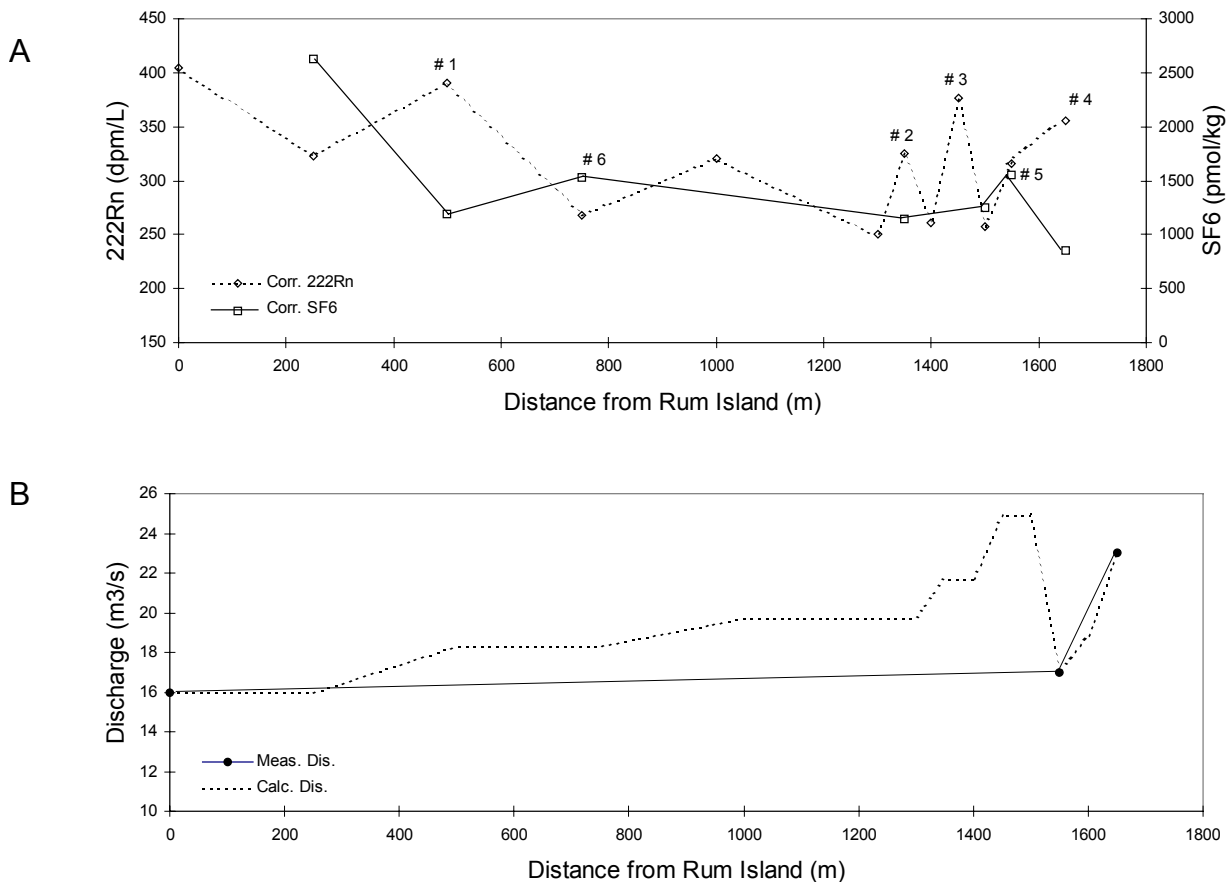


Figure 25. (a) Corrected <sup>222</sup>Rn and SF<sub>6</sub> concentrations vs. transect distance and (b) measured and calculated discharge vs. transect distance measured during the February, 1992 sampling of the Santa Fe River between Rum Island and July spring, north-central Florida. Peaks in <sup>222</sup>Rn concentrations correspond to ground water influx to the river. Peaks in SF<sub>6</sub> concentrations indicate the return of river water that had been diverted underground up-stream.

Figure 25b compares the measured discharge to the discharge calculated from ground water inputs. As in the 1991 plot, the largest calculated flow increases are located near the major spring groups on the transect. Also following the 1991 example, the stream flow loss indicated at 1500 meters is the culmination of losses occurring over the entire length of the transect.

Longitudinal dispersion is again a factor in the distribution of the  $^{222}\text{Rn}$  peaks in the 1993 experiment.  $^{222}\text{Rn}$  peak #1 and #2 in Figure 26a reflect the ground water contributions from Rum Island and Blue springs.  $^{222}\text{Rn}$  peak #3 reflects a spring vent in the river channel up-stream of Devil's Ear spring. Though the position of the peak shifts, a spring or seep up-stream of Devil's Ear spring is reflected in each of the three transects.  $^{222}\text{Rn}$  peak #4 is a gradual rise in  $^{222}\text{Rn}$  concentration that reflects the ground water contribution from the Devil's group and July springs.  $\text{SF}_6$  peaks #5 and #6 indicate two significant return flow contributions along the transect. The dip in  $\text{SF}_6$  concentration at 1100 meters on the transect corresponds to  $^{222}\text{Rn}$  peak #3. The  $\text{SF}_6$  dip reflects both ground water dilution and accompanying fluctuations in  $\text{SF}_6$  concentrations in the river due to lateral mixing and longitudinal dispersion.

Figure 26b compares the measured discharge to the calculated discharge during the June 6, 1993 sampling period. The majority of the calculated increase in discharge can be attributed to the ground water contribution from Blue spring. As in the previous transects, the stream flow loss depicted at 1300 meters is a reflection of losses occurring over the entire transect.

In order to relate the  $^{222}\text{Rn}$  plots of the three transect dates, the flow stage of the river must be considered. By comparison, the three transects reveal more frequent  $^{222}\text{Rn}$  peak fluctuations, especially in the vicinity of Devil's Ear and July springs, as the flow stage of the river drops.

At the highest flow stage, the 1991 transect (Figure 24a), shows the three most substantial  $^{222}\text{Rn}$  peaks occurring in the immediate vicinity of the highest magnitude springs on this part of the river, the Devil's group and Ginnie spring.  $^{222}\text{Rn}$  peaks associated with Blue and Rum Island springs are much less pronounced because they discharge less water to the river.

During the intermediate flow stage, the 1993 transect (Figure 26a), begins to reveal more dramatic fluctuations in the  $^{222}\text{Rn}$  plot across the entire distance of the transect. The flow stage had dropped sufficiently to observe the ground water contributions from Rum Island and Blue springs. Peak #2 on Figure 26a corresponds to the contribution from Blue spring. The down-stream shift in the  $^{222}\text{Rn}$  peak is attributed to longitudinal mixing processes in the stream. Visual field observations on this date revealed that the clear water from the spring channel entered the river on the south bank and flowed down-stream before mixing into the tea-colored river water. Peak #3 on Figure 26a records the possible presence of a ground water vent in the stream bed up-stream of Devil's Ear. This same peak was observed again during the lowest flow stage in 1992. Finally, the general rise in  $^{222}\text{Rn}$  concentrations at the end of the plot reflects the ground water contribution from the Devil's group and July springs.

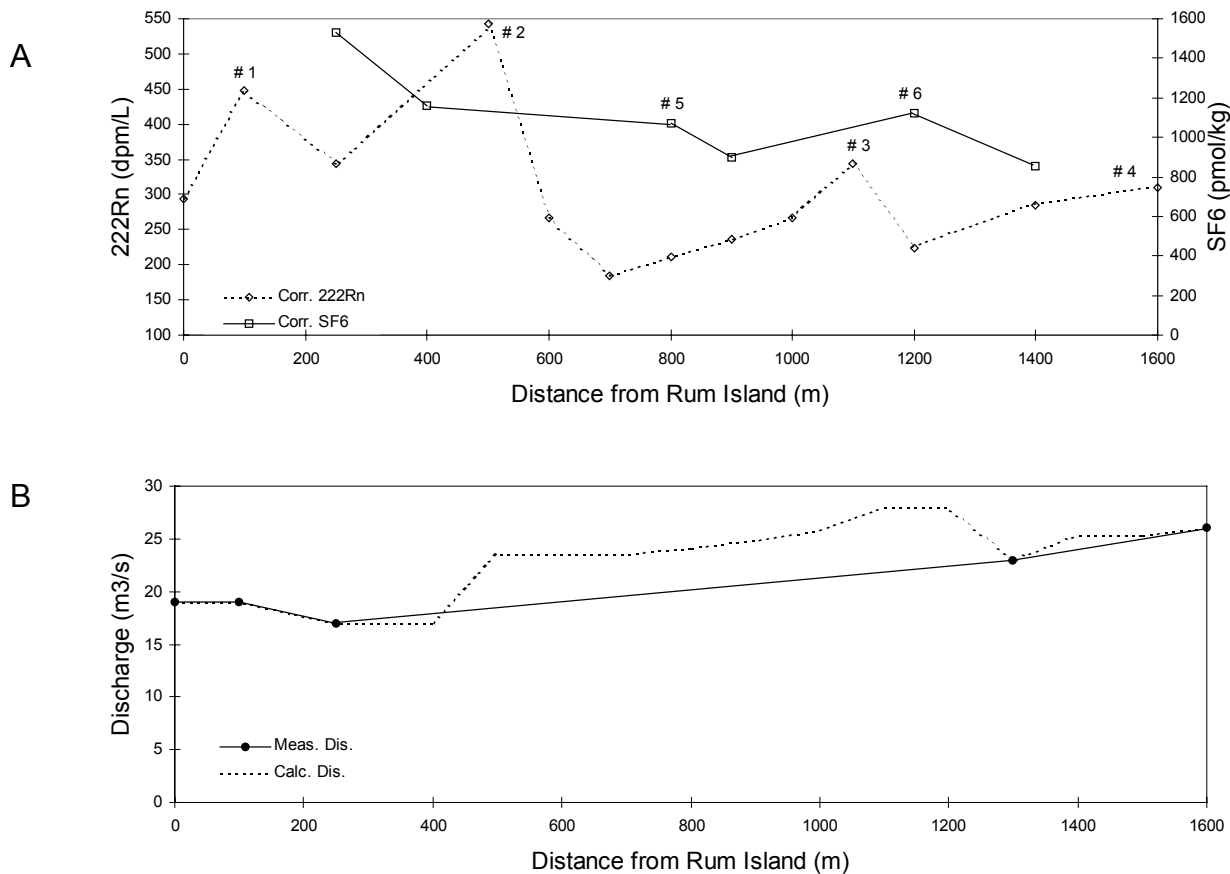


Figure 26. (a) Corrected  $^{222}\text{Rn}$  and  $\text{SF}_6$  concentrations vs. transect distance and (b) measured and calculated discharge vs. transect distance measured during the June, 1993 sampling of the Santa Fe River between Rum Island and July spring, north-central Florida. Peaks in  $^{222}\text{Rn}$  concentrations correspond to ground water influx to the river. Peaks in  $\text{SF}_6$  concentrations indicate the return of river water that had been diverted underground up-stream.

The largest fluctuations in the  $^{222}\text{Rn}$  concentrations occur during the lowest flow stage in 1992 (Figure 25a). These fluctuations reflect a smaller hydrostatic head in the river permitting more ground water influx from vents in the river channel. The ground water contributions from Rum Island and Blue springs are pronounced and the peak associated with Blue spring is again shifted down-stream of the spring run. Field observations during this transect were similar to those during the 1993 transect. Peak #2 on Figure 25a records the same spring vent or seep up-stream of Devil's Ear spring observed during the intermediate flow stage in 1993. The most pronounced fluctuations occur near the Devil's group and July springs.

Clearly, fluctuations in  $^{222}\text{Rn}$  concentrations increase as the stream discharge decreases. These fluctuations may be linked to mixing conditions in the river. During the higher flow stages, the river water and ground water inputs are better mixed. The increased mixing conditions combined with

increased hydrostatic head in the river reduce the  $^{222}\text{Rn}$  signature from the lower magnitude springs and vents. At the lower stages, the stream flow is not as well mixed. The reduced hydrostatic head permits increased ground water contribution from smaller springs or vents in the river channel and the reduced mixing between ground water and river water causes more erratic fluctuations in the  $^{222}\text{Rn}$  concentrations.

Specific stream flow components were calculated for each transect using the methods and equations described in chapter 4. For each transect, the predetermined high and low values for gas exchange were used to calculate a potential range in component discharges. Figure 27 shows the location of individual stream flow components plotted with calculated discharge along the sampled transect for each of the sampling periods.

Each bar or peak shown on Figure 27 represents the flow component added to or subtracted from the river between the point of reference on the plot and the nearest up-stream sampling point marked by a corrected tracer concentration. Refer to Tables 6, 7, and 8 for the location of the corrected tracer values.

Stream flow losses are calculated from decreases in discharge measured along the transect. For this reason, each peak represents the cumulative stream loss that occurred in the river between the point indicated on the graph and the next point of measured discharge up-stream. Corrected  $\text{SF}_6$  values were not as numerous as the  $^{222}\text{Rn}$  values therefore, the return flow quantities reflect a contribution over a greater distance on the transect.

On the plot from the 1991 sampling period, peaks #1 and #2 correspond to Rum Island and Blue springs which indicate an average, combined ground water influx of approximately  $6 \text{ m}^3/\text{s}$ . Peak group #3 corresponds to the Devil's group and July springs. The average combined ground water contribution from these springs was approximately  $11 \text{ m}^3/\text{s}$ . Finally, peak #4 accounts for a  $4 \text{ m}^3/\text{s}$  ground water contribution from Ginnie spring. The remaining three peaks are attributed to previously unrecorded springs or ground water seeps within the river channel.

The largest quantity of stream flow loss during the September, 1991 sampling period occurred between 1250 and 1600 meters on the transect. According to the measured discharge in the river and the ground water influx components, approximately  $16 \text{ m}^3/\text{s}$  of stream water was lost to the aquifer along this part of the transect which directly overlies part of the Devil's Ear cave system.



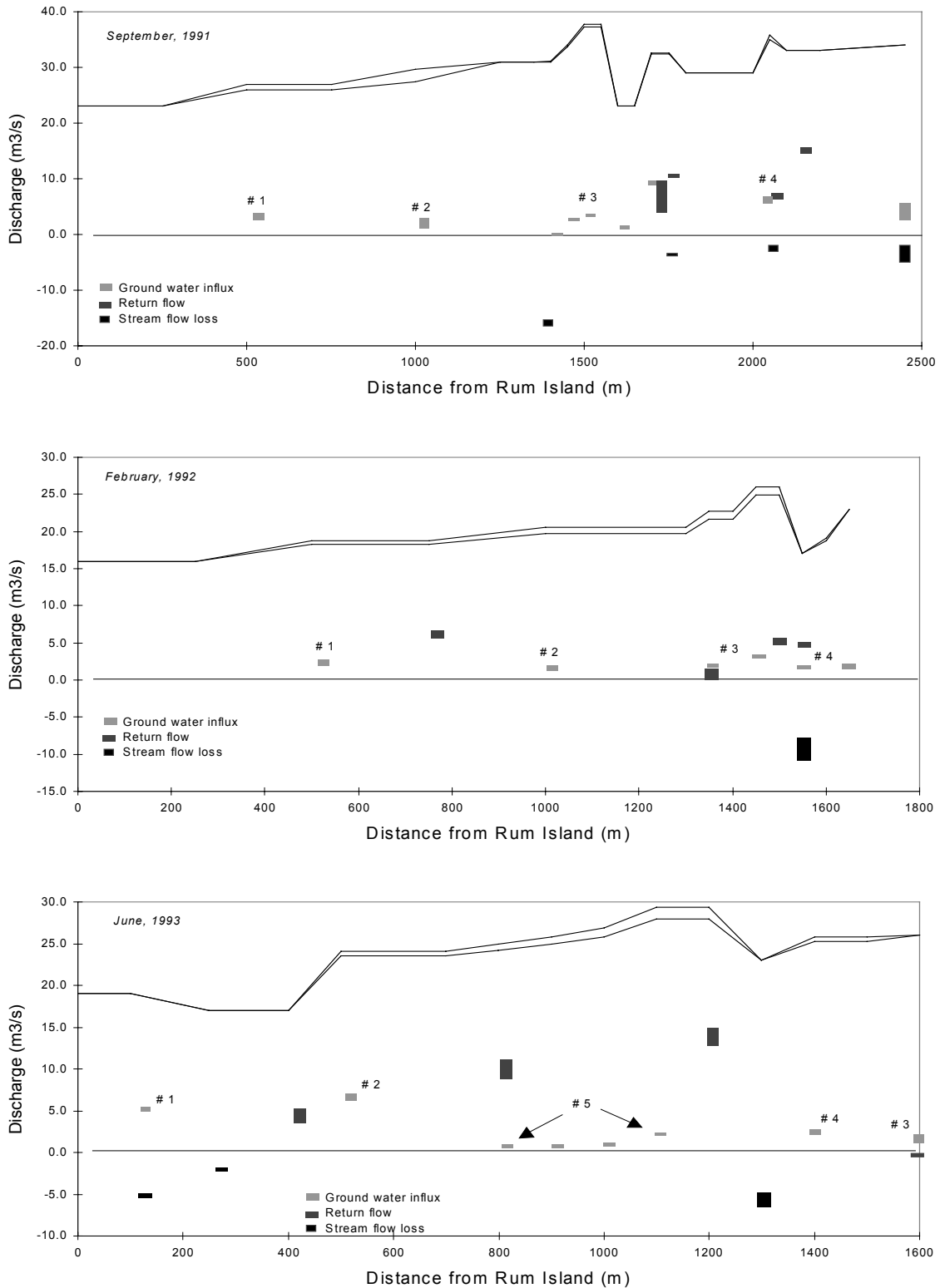


Figure 27. Variations in calculated stream discharge and flow components determined at high and low values of the gas transfer velocity for the reach of the Santa Fe River between Rum Island and Ginnie spring. Position of the vertical bars indicates flow component magnitude. Length of the vertical bars indicates variation with gas transfer velocity.

During the February, 1992 transect, peaks #1 and #2 reflect a 4 m<sup>3</sup>/s ground water contribution from Rum Island and Blue springs. The locations of these peaks on the transect corresponds to those measured in 1991. Peak group #3 corresponds to the Devil's Group and July springs. The approximate calculated ground water contribution from these springs was 4 m<sup>3</sup>/s. The remaining two peaks may indicate approximately 5 m<sup>3</sup>/s coming from previously unrecognized springs or seeps within the river channel. However, given the highly varied <sup>222</sup>Rn peaks shown in Figure 25 which were attributed to stream mixing variations and the proximity of peak #4 to Devil's Ear, it is likely that the ground water contribution indicated by peak #4 was actually generated by Devil's Ear spring. In this case, the ground water discharge from the Devil's Group and July springs would have been approximately 7 m<sup>3</sup>/s.

During the February, 1992 sampling period, discharge measurements indicated approximately 9 m<sup>3</sup>/s of stream flow loss along the transect. Due to the sparse measurement interval, this figure represents the cumulative flow loss between 0 and 1550 meters on the transect.

During the June, 1993 sampling period, peaks #1 and #2 account for the ground water contributions from Rum Island and Blue springs. The total ground water influx from these two springs was over 12 m<sup>3</sup>/s. Peak #3 and (due to the mixing variations in the stream depicted on Figure 26) peak #4 account for an approximately 4 m<sup>3</sup>/s of ground water influx from the Devil's Group and July springs. Peak group #5 indicates approximately 5 m<sup>3</sup>/s of ground water entering the river through previously undetected springs or seeps in the river channel up-stream of Devil's Ear spring.

Stream flow losses were calculated at four locations along the transect during the June, 1993 sampling period. The loss shown at the beginning of the transect was calculated from direct measurement of a decrease in discharge at the beginning of the transect. The larger loss shown at the end of the transect is the cumulative total over most of the transect up-stream of Devil's Ear spring.

Figure 28 shows the calculated range in flow component interactions caused by varying the gas transfer velocities (k) of <sup>222</sup>Rn and SF<sub>6</sub> between their highest and lowest determined values during each of the sampling periods. During the September, 1991 sampling, ground water influx to this reach of the Santa Fe River ranged from 30 to 37 m<sup>3</sup>/s; stream Flow loss ranged from 23 to 27 m<sup>3</sup>/s; and return flow ranged from 37 to 44 m<sup>3</sup>/s. During the February, 1992 sampling, ground water influx ranged from 12 to 14 m<sup>3</sup>/s; stream flow loss ranged from 8 to 11 m<sup>3</sup>/s; and return flow ranged from 16 to 19 m<sup>3</sup>/s. During the June, 1993 sampling, ground water influx ranged from 20 to 23 m<sup>3</sup>/s; stream flow loss ranged from 13 to 14 m<sup>3</sup>/s; and return flow ranged from 26 to 31 m<sup>3</sup>/s. Stream flow loss : ground water influx ratios were 0.75 in 1991, 0.710 in 1992, and 0.63 in 1993. Figure 29 shows that the magnitude of the flow components is proportional to the total discharge of the river.

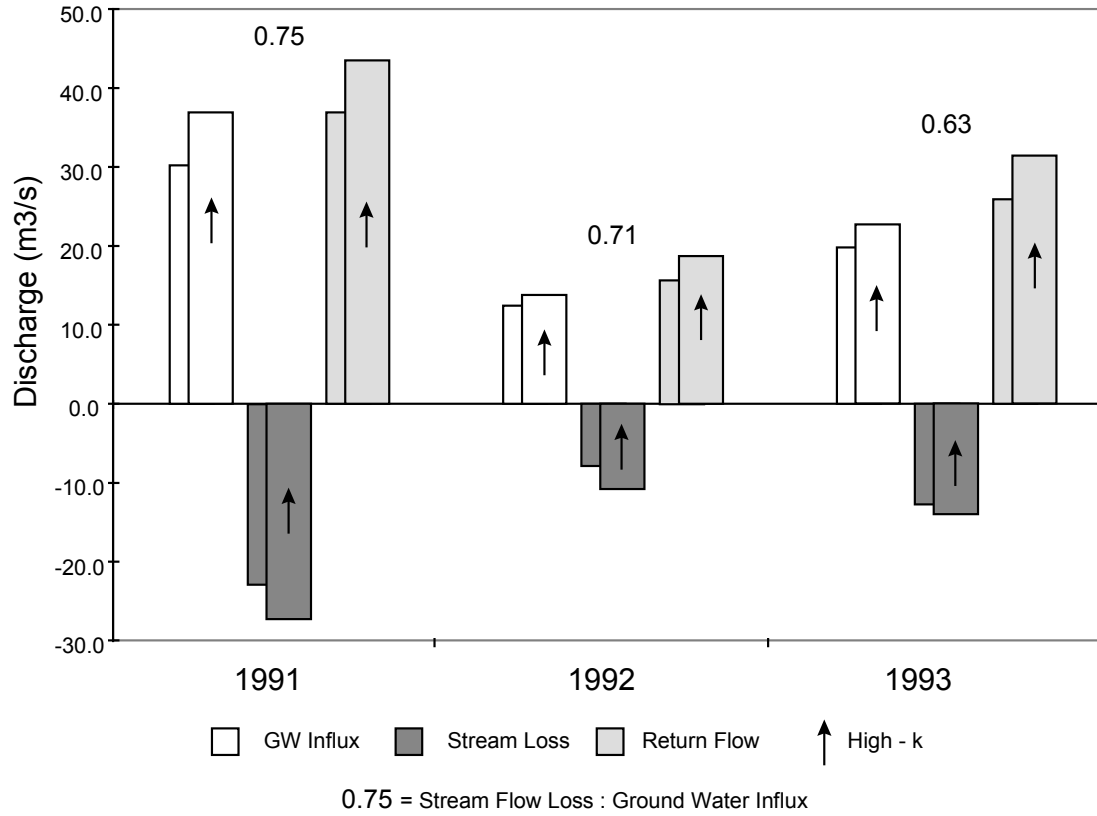


Figure 28. Variation in flow components with gas transfer velocity on the reach of the Santa Fe River between Rum Island and Ginnie spring, north-central Florida for the sampling periods between September, 1991 and June, 1993.

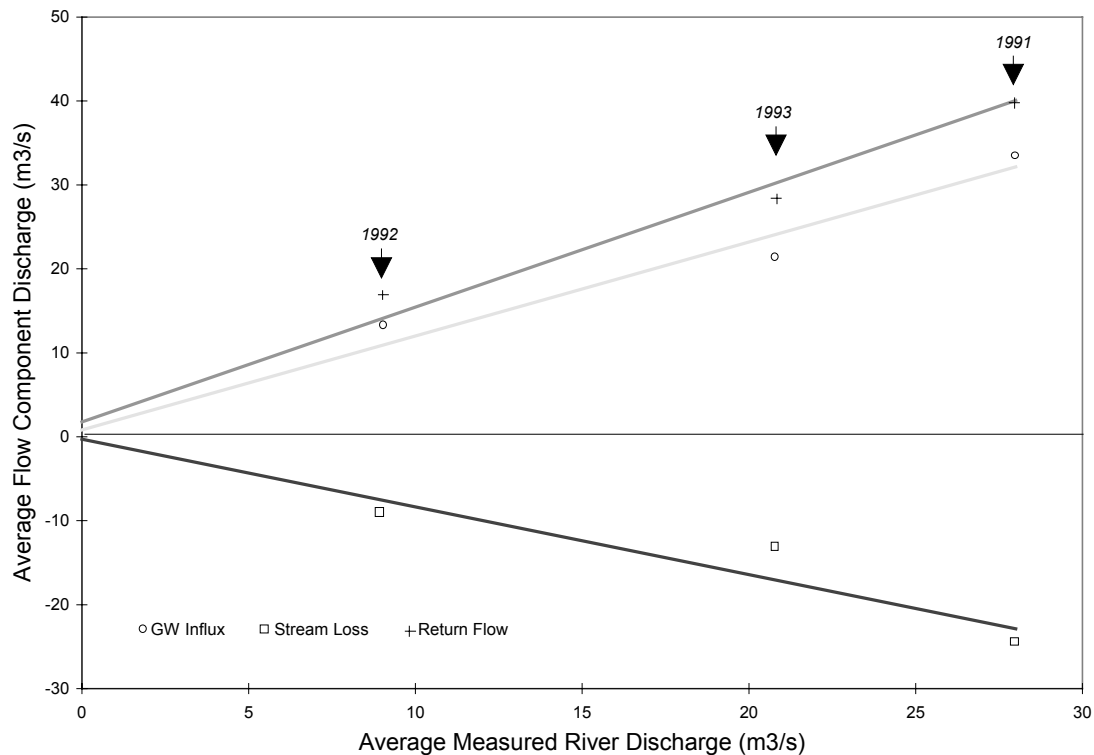


Figure 29. Variations in flow components with overall river discharge for the reach of the Santa Fe River between Rum Island and Ginnie spring, north-central Florida for the sampling periods between September, 1991 and June, 1993.

Ground water influx components attributed to the major springs along the transect were compared to available published discharge values. Rosenau and others (1977) and Wilson and Skiles (1989) have reported discharge values from Blue, Devil's group, July, and Ginnie springs. The method used to determine spring discharges listed in Rosenau and others (1977) is uncertain, however the values listed in Wilson and Skiles (1989) were determined by physical measurement of water velocity from the spring and cross-sectional area of the spring vent. Table 9 compares the calculated discharges from Blue spring, the Devil's Group of springs, July spring, and Ginnie spring to the corresponding values taken from Wilson and Skiles (1989) and Rosenau and Others (1977).

Though there is general agreement between the published and calculated values for Blue and the Devil's group of springs in 1991 and 1992, there was a large recorded difference between the calculated and published discharges for Ginnie spring in 1991 and Blue spring and the Devil's group in 1993. Since the stage of the river or the error incorporated in the calculation of discharge was not reported in the publications, it was impossible to make a clear comparison between the calculated and published spring discharge values. However, the spring discharge values calculated with the  $^{222}\text{Rn}$  method reflect definite fluctuations with the stage of the river which can not be determined based on the

few reported values in the available literature. The error associated with the  $^{222}\text{Rn}$  method is discussed in the following section.

*Table 9. Comparison of calculated and published spring discharges for select springs along the reach of the Santa Fe River between Rum Island and Ginnie spring, north-central Florida for the sampling periods between September, 1991 and June, 1993.*

Spring	Calc. Dis. 1991 (m <sup>3</sup> /s)	Calc. Dis. 1992 (m <sup>3</sup> /s)	Calc. Dis. 1993 (m <sup>3</sup> /s)	Ave. Calc. Dis. (m <sup>3</sup> /s)	Wilson & Skiles, 1989 (m <sup>3</sup> /s)	Rosenau & Others, 1977 (m <sup>3</sup> /s)	Ave. Pub. Dis. (m <sup>3</sup> /s)	% Diff.
Rum Island	3.4	2.4	5.3	3.7	*	*	*	*
Blue	2.1	1.7	6.8	3.5	*	2.0	2.0	42.9
Combined	5.5	4.1	12.1	5.6	*	*	*	*
Devil's Group	*	*	*	*	6.4	0.3 - 2.8	4.0	*
July	*	*	*	*	2.1	*	2.1	*
Combined	10.8	7.0	4.2	7.3	8.5	*	6.1	16.4
Ginnie	4.3	*	*	4.3	1.2	1.3	1.3	69.8

*note: \*indicates that either the discharge was not calculated or could not be separated from the combined total.*

### Error Calculation

The overall error associated with ground water influx and return flow values was determined by tracing the analytical error through the respective calculations. Since there was a 10% error associated with sampling and analytical techniques, a 10% margin was added to each of the  $^{222}\text{Rn}$  and  $\text{SF}_6$  values measured in the stream. Subsequently, those values were run through equation 6 to determine background values and equations 8 and 13 to calculate the magnitude of the ground water influx and return flow components respectively. From this point, the resultant component discharges were compared to the original values and a % difference was determined. The % difference was then considered to be the margin of error associated with these methods. Component discharges calculated from high and low values for the gas transfer velocity were averaged in order to approximate an error value for the overall method.

Tables 10, 11, and 12 show the error calculations for ground water influx and return flow components determined for each of the three sampling periods. The average error for each method and the standard deviation of the calculated % differences are listed at the bottom of each table.

The average error calculated for the ground water influx component was 17.6%. The range of error was tight with a standard deviation of less than 4%. These data indicate that the  $^{222}\text{Rn}$  method for the calculation of ground water influx to a stream can be considered accurate to within less than 20% of a determined value.

The values obtained for the return flow component of the stream discharge are less reliable. The average error calculated for the return flow component was 32.2%. There was a large range in the calculated error which is reflected by a standard deviation of over 24%. The largest range occurred in the 1992 transect which had an average error of over 49% and a standard deviation of over 60%.

For each year, the return flow component is the largest, however considering the nature of the experiments, return flow should not measure greater than the stream flow loss. The larger return flow components in each experiment is a manifestation of the larger error associated with the calculations. These observations as well as the error data indicate that the SF<sub>6</sub> method for calculating return flow components needs to be refined and can only be regarded as a qualitative estimation of stream/aquifer interactions in the Santa Fe River basin.

Close inspection of the data from the 1992 transect, as well as the others, shows that the largest errors are associated with computation of negative values for the respective flow components. Negative values are generated when the actual measured concentration of the gaseous tracer in the stream is lower than the calculated background concentration at that point. Since no appreciable amount of either tracer should be lost over a short distance in the river due to processes other than gas exchange, the negative values must be linked to the incorporated range of error in the method.

For the most part, the negative values obtained for both ground water influx and return flow fell within the calculated error range. The large error range that was calculated for the return flow component during the 1992 sampling period is related to the low flow stage of the river. Stream mixing variations were shown to be greater during lower flow stages. These variations cause greater degrees of lateral mixing that disturbed the normal decline of SF<sub>6</sub> concentrations due to gas exchange. Further research should be conducted to determine how to insure that the stream or part of the stream under study is well mixed with respect to SF<sub>6</sub> before sampling begins.

It is clear that the majority of the error associated with these methods occurs in the determination of the gas transfer velocity. There are many physical parameters incorporated in the calculation of  $k$  which are either difficult or impossible to accurately measure in the field. These include wind speed, water turbulence, and the stream channel roughness. Since the background calculations are based on  $k$ , the error associated with the determination of  $k$  is propagated further each time a background concentration is calculated. In view of this, the magnitude of the calculated stream flow components is more accurate when performed over a large transect distance. The drawback with using a large sampling interval is that the locations of the interactions can not be determined. But, as the sampling interval is decreased, more background calculations must be made and the magnitude of the components becomes less exact.

The SF<sub>6</sub> method as well as any other gaseous tracer method is most accurate in situations where the only mechanism for tracer loss from the stream is gas exchange across the air/water interface.

The complicated ground water/surface water interactions in the Santa Fe River make the accurate calculation of the gas transfer velocity difficult, however the SF<sub>6</sub> method presents the most viable solution especially when carried out over large sampling intervals.

*Table 10. Errors associated with ground water influx and return flow calculations for the reach of the Santa Fe River between Rum Island and Ginnie spring, north-central Florida for the September, 1991 sampling period.*

Dis. from Rum Is. (m)	Real <sup>222</sup> Rn (dpm/L)	<sup>222</sup> Rn + 10% (dpm/L)	Real G.W. Influx (m3/s)	+ 10% G.W. Influx (m3/s)	% Dif.	Real SF <sub>6</sub> (pmol/kg)	SF <sub>6</sub> + 10% (pmol/kg)	Real Return Flow (m3/s)	+ 10% Return Flow (m3/s)	% Dif.
0	227	250								
250										
500	295	325	3.4	3.9	14.1	1062	1168			
750										
1000	320	352	2.1	2.5	16.0					
1250										
1300										
1350										
1400	287	316	-0.8	-1.0	18.0					
1450	330	363	2.8	3.3	16.6					
1500	380	418	3.6	4.2	18.5					
1550	267	294								
1600	295	325	1.3	1.6	15.9					
1650										
1700	495	545	9.5	11.1	16.9	438	482	7.0	7.9	13.2
1750	430	473	-4.8	-6.3	32.2	555	611	10.7	12.3	14.7
1800	310	341	9.4	-11.8	24.9					
1850						356	392	-10.7	-13.1	23.0
2000						315	347	-1.3	-1.5	15.7
2050	405	446	6.4	7.5	17.1	418	460	7.1	8.1	13.6
2100										
2150						671	738	15.3	17.7	15.2
2200										
2450	431	474	4.3	5.2	21.0	281	309	-19.3	-24.1	24.9
			Average	error %:	19.2					17.2
			Standard deviation	of errors:	4.9					4.4

Table 11. Errors associated with ground water influx and return flow calculations for the reach of the Santa Fe River between Rum Island and July spring, north-central Florida for the February, 1992 sampling period.

Dis. from Rum Is. (m)	Real <sup>222</sup> Rn (dpm/L)	<sup>222</sup> Rn + 10% (dpm/L)	Real G.W. Influx (m3/s)	+ 10% G.W. Influx (m3/s)	% Dif.	Real SF <sub>6</sub> (pmol/kg)	SF <sub>6</sub> + 10% (pmol/kg)	Real Return Flow (m3/s)	+ 10% Return Flow (m3/s)	% Dif.	
0	405	446									
250	323	355	-2.3	-2.7	20.3	2623	2885	-44.9	-127.4	183.8	
500	391	430	2.4	2.8	16.7	1185	1304	6.2	7.3	17.0	
750	268	295	-3.6	-4.3	19.6	1534	1687				
1000	320	352	1.7	2.0	15.0						
1250											
1300	250	275	-1.6	-1.9	16.6						
1350	325	358	2.1	2.4	14.8	1144	1258	-0.1	-0.2	39.1	
1400	261	287	-1.9	-2.2	17.2						
1450	376	414	3.2	3.7	15.1						
1500	257	283	-3.9	-4.7	19.4	1253	1378	5.4	6.3	15.9	
1550	316	348	1.8	2.0	15.0	1548	1703	4.9	5.8	18.8	
1600											
1650	356	392	2.0	2.3	16.8	856	942	-7.2	-8.7	21.6	
Average					error %:	16.9					49.4
Standard deviation					of errors:	1.9					60.6



Table 12. Errors associated with ground water influx and return flow calculations for the reach of the Santa Fe River between Rum Island and July spring, north-central Florida for the June, 1993 sampling period.

Dis. from Rum Is. (m)	Real <sup>222</sup> Rn (dpm/L)	<sup>222</sup> Rn + 10% (dpm/L)	Real G.W. Influx (m3/s)	+ 10% G.W. Influx (m3/s)	% Dif.	Real SF <sub>6</sub> (pmol/kg)	SF <sub>6</sub> + 10% (pmol/kg)	Real Return Flow (m3/s)	+ 10% Return Flow (m3/s)	% Dif.
0	293	322								
100	448	493	5.3	6.1	15.6					
250	343	377	-3.4	-4.2	22.1					
400						1529	1682			
500	542	596	6.8	8.0	16.8	1159	1275	4.5	6.2	37.8
600	266	293	-13.0	-17.0	30.2					
700	185	204	-2.1	-2.4	14.9					
800	212	233	0.8	0.9	12.9					
900	236	260	0.8	0.9	13.5	1069	1176	10.2	12.3	21.5
1000	267	294	1.0	1.1	14.1	896	986	-4.2	-5.7	34.8
1100	343	377	2.3	2.7	14.9					
1200	224	246	-3.5	-4.1	17.3					
1300						1120	1232	14.0	17.0	21.0
1400	285	314	2.5	2.9	13.7					
1500						852	937	-5.6	-7.5	34.4
1600	310	341	1.7	2.0	15.1					
			Average	error %:	16.8					29.9
			Standard deviation	of errors:	4.7					7.2

### The Cave Experiments

Two sets of underwater speleological investigations were conducted in the Devil's Ear cave system in conjunction with the 1992 and 1993 river experiments. A total of 21 dives were conducted in the system that accounted for approximately 80 underwater man-hours. As many as 15 water samples were collected on each dive. The average linear penetration into the cave from the entrance at Devil's Ear spring was over 1000 meters and the average depth of each dive was over 30 meters.

The dives were conducted to take water samples from specific locations within the cave system and make morphologic observations of the cave. Table 13 shows the logs and agendas for each of the 21 research dives. The sampling locations were standardized as much as possible, however there were some discrepancies due to logistical considerations. Figure 30 is a map of the Devil's Ear cave system superimposed onto part of the USGS High Springs SW topographic quadrangle showing the sampling locations and the position of the overlying river.

The primary objective of the water sampling strategy was to measure  $^{222}\text{Rn}$  concentrations through out the cave system. Water samples from both sampling events were also measured for  $\delta^{18}\text{O}$ . Water samples collected during the 1992 transect were measured for four major cation components: Ca, Mg, Na, and K. The average measured  $^{222}\text{Rn}$  concentrations in the cave during the 1992 and 1993 transects ranged from 382 to 492 dpm/L with standard deviations of 154 and 165 dpm/L. The large variations of  $^{222}\text{Rn}$  concentrations reflect river water intrusion to the cave system.  $\delta^{18}\text{O}$  measurements in the cave correspond to the  $^{222}\text{Rn}$  data but there was very little variation in Mg, Na, and K concentrations. Table 14 shows  $^{222}\text{Rn}$ ,  $\delta^{18}\text{O}$ , and major cation concentrations measured at the sampling locations in the cave system as well as at local wells and springs during the two cave sampling experiments. Parameter averages and standard deviations are also included in Table 14.

Table 13 Dive logs and agendas for the 1992 and 1993 research dives conducted in the Devil's Ear cave system on the Santa Fe river, north-central Florida.

Dive #	Dive Date	Depth m	Linear Pen. m	Dive Time minutes	Decom. Time minutes	Description
1	16-Jan-92	30	300	50	35	Installed Flux box, Collected <sup>222</sup> Rn samples, Measured velocity.
2	21-Jan-92	30	600	50	35	Collected Rn222 samples.
3	10-Feb-92	34	900	60	60	Made observations regarding flow state.
4	14-Feb-92	34	900	75	90	Transect #1: Collected Rn222 samples, Measured water velocity. Right Line, Split Tunnel
5	15-Feb-92	34	1100	75	90	Transect #1: Collected Rn222 samples, Measured water velocity. Hinkel, River Intrusion Tunnel
6	16-Feb-92	34	1400	75	90	Transect #1: Collected Rn222 samples, Measured water velocity. Mainland, Main Line
7	11-Mar-92	30	900	70	60	SF6 Injection Experiment, Collected water samples. Mainlands, Split Tunnel, River Intrusion Tunnel
8	16-Mar-92	33	1100	60	60	Collected Limestone Samples. Hinkel, White Room, Split Tunnel
9	18-Mar-92	30	800	55	35	Collected water samples. Split Tunnel, Big Room
10	20-Mar-92	34	1100	60	60	Made detailed observations of cave.
11	21-Mar-93	34	1400	60	60	Made detailed observations of cave.
12	20-Feb-93	34	1100	70	80	Made observations regarding flow state.
13	01-Jun-93	34	1100	60	60	Made observations regarding flow state.
14	06-Jun-93	5		120		Dived from Rum Island to Devil's Ear to locate boils and sinks.
15	07-Jun-93	5		120		Dived from Rum Island to Devil's Ear to locate boils and sinks.
16	12-Jun-93	34	900	75	90	Transect #2: Collected Rn222, AA, and O18 samples. Right Line, Split Tunnel
17	13-Jun-93	34	1100	75	90	Transect #2: Collected Rn222, AA, and O18 samples. Hinkel, River Intrusion Tunnel
18	14-Jun-93	34	1400	75	90	Transect #2: Collected Rn222, AA, and O18 samples. Mainland, Main Line
19	20-Jun-93	32	1100	45	30	Collected duplicate water samples.
20	21-Jun-93	34	1400	60	60	Made detailed observations of cave.
21	22-Jun-93	34	1100	60	60	Made detailed observations of cave.
Participating Divers:			Todd R. Kincaid			
			Jarrod Jablonski		Average Bottom Time: 65 minutes	
					Average Decom. Time: 65 minutes	
Total Bottom Time:			21 hours		Average Cave Penetration: > 1000 meters	
Total Decom. Time:			17 hours		Average Depth: > 30 meters	

note: Decom. = Decompression  
Pen. = Penetration

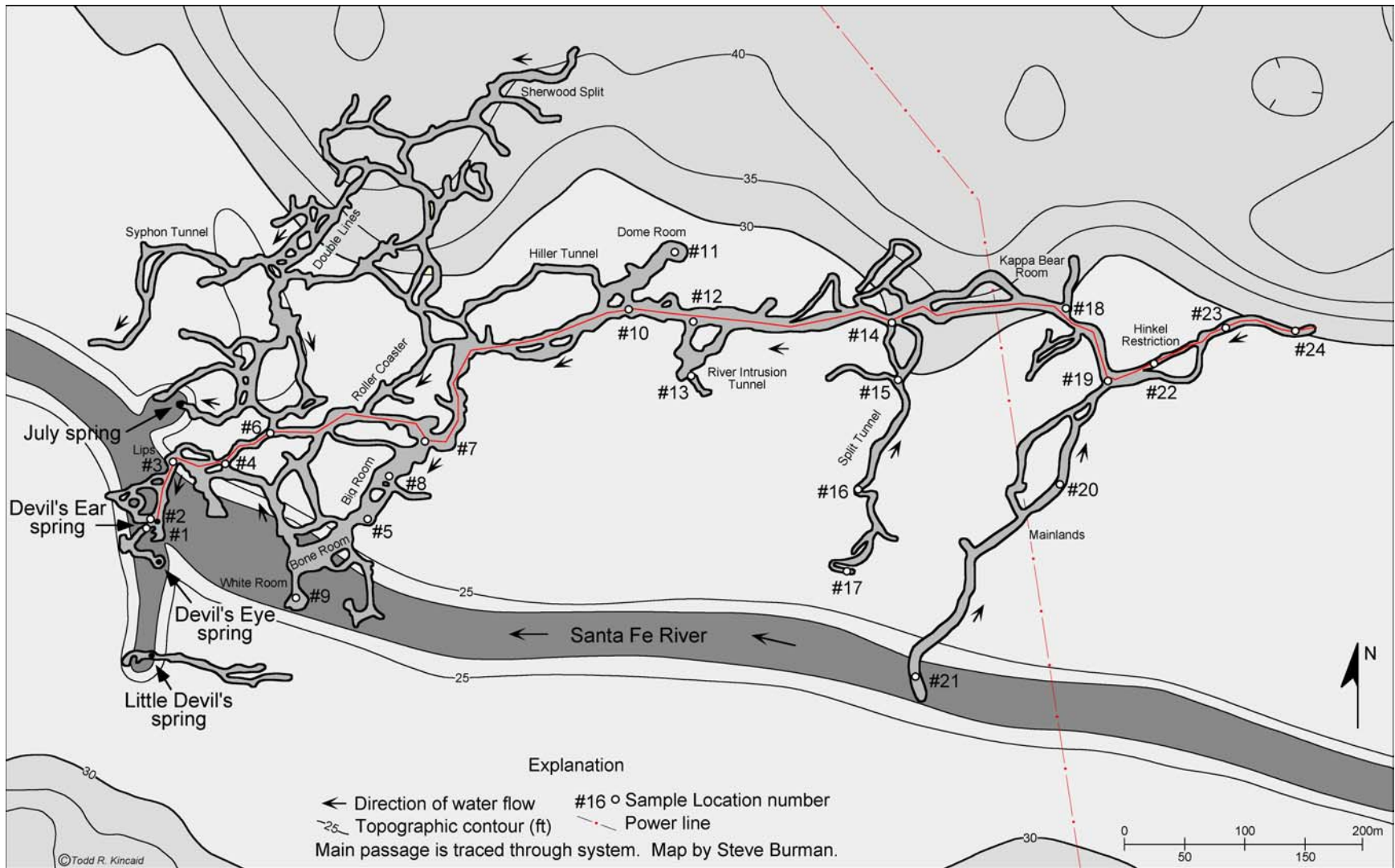


Figure 30. Map of the Devil's Ear cave system on the Santa Fe river, north-central Florida showing the sampling locations and the relative position of the overlying Santa Fe river.

Table 14.  $^{222}\text{Rn}$ ,  $\delta^{18}\text{O}$ , and major cation concentrations measured in the Devil's Ear cave system on the Santa Fe river, north-central Florida and local wells and springs for the February, 1992 and June, 1993 cave experiments.

Location	Ref. #	MLD m	OLD m	1992 Radon dpm/L	1992 % GW	1993 Radon dpm/L	1993 % GW	1992 $\delta^{18}\text{O}$	1993 $\delta^{18}\text{O}$	Ca mg/L	Mg mg/L	Na mg/L	K mg/L
Basin	1	0	0	337	43	460	54	-3.48	-3.56	33.9	7.2	3.6	0.6
Depot	2	20	0	319	41	*	*	*	*	*	*	*	*
Lips	3	80	0	340	44	478	56	-3.57	*	34.6	7.0	2.9	0.5
Right Line Junction	4	170	0	*	*	545	64	*	-3.52	*	*	*	*
Right Line B. Stat.	5	170	120	*	*	403	47	*	-3.64	*	*	*	*
Hill 400 Junction	6	240	0	408	52	*	*	*	*	*	*	*	*
Big Room Junction	7	340	0	386	49	349	41	*	-3.62	*	*	*	*
Big Room	8	340	60	179	23	*	*	-3.48	*	33.5	6.5	3.0	0.4
White Room	9	170	150	738	95	*	*	*	*	*	*	*	*
Dome Room Junct.	10	430	0	352	45	506	60	*	-3.66	*	*	*	*
Dome Room	11	430	-60	402	52	*	*	*	*	*	*	*	*
River Int. Junction	12	520	0	340	44	385	45	-3.33	-3.62	31.9	6.6	3.6	0.5
River Int. at Res.	13	520	60	316	41	344	40	*	-3.48	*	*	*	*
Split Tunnel Junct.	14	670	0	358	46	375	44	-3.38	-3.64	44.7	6.7	4.4	0.5
Split Tunnel T	15	670	90	336	43	*	*	-3.52	-3.75	45.2	6.6	3.2	0.5
Split Tunnel Fiss.	16	670	240	*	*	326	38	-1.95	-3.52	30.7	6.6	3.1	0.4
Split Tunnel End	17	670	300	*	*	*	*	-3.52	*	30.5	6.4	2.5	0.6
Kappa Bear Room	18	880	0	628	81	411	48	*	-3.59	*	*	*	*
Mainland Junct.	19	940	0	315	40	342	40	-3.49	-3.62	33.0	6.8	3.4	0.6
Mainland B. Room	20	940	150	302	39	224	26	*	-3.68	*	*	*	*
Mainland End	21	940	370	148	19	*	*	*	*	*	*	*	*
Hinkel Res.	22	1010	0	723	93	743	87	-3.53	-3.66	34.0	7.1	5.7	0.8
1st Room Hinkel	23	1130	0	*	*	729	86	*	*	*	*	*	*
2nd Room Hinkel	24	1220	0	*	*	818	96	*	*	*	*	*	*
Cave Avg. Value				384.8		492.2		-3.33	-3.61	35.2	6.8	3.5	0.5
Cave Std. Dev.				154.3		165.2		0.46	0.07	5.0	0.3	0.9	0.1
<u>Add. Locations</u>													
July spring	25			765	98	656	77	*	-3.66	49.1	7.1	3.1	0.6
Rum Island Spg.				780		*		*	-3.70	51.7	7.1	3.3	0.5
Little Devils Spg.	26			793		850		*	*	*	*	*	*
Ginnie spring				765		870		*	*	*	*	*	*
Ginnie Well				800		830		*	*	*	*	*	*
Ground water Well				780		850		*	-3.97	46.6	2.8	2.9	1.1
Sinkhole				12		*		*	*	37.8	1.9	1.9	2.9
Flux Box	26			39		35		*	*	*	*	*	*
Total Avg. Value				448.5		543.9		-3.33	-3.64	38.4	6.2	3.3	0.8
Total Std. Dev.				242.0		226.3		0.46	0.11	7.2	1.6	0.9	0.6

notes: a. \* indicates sample lost or not taken  
b. MLD = "Main Line Distance" distance in cave up-stream of basin in main tunnel  
c. OFD = "Off Line Distance" distance in side tunnels from main tunnel, (-) indicates north

### *<sup>222</sup>Rn and % River Water Measurements*

Ground water percentages were calculated with equation 9 from the <sup>222</sup>Rn concentrations measured in the water samples collected from the cave system. Figure 31 shows the <sup>222</sup>Rn concentrations and the corresponding ground water percentages for transects A to A' and B to A' during both the February, 1992 and June, 1993 cave experiments. River water percentage values indicate the approximate river water component of the conduit flow at a particular point in the cave.

During both experiments, a dramatic decrease in the <sup>222</sup>Rn concentration occurred between the Hinkel Restriction and the discharge point at Devil's Ear spring. During the February, 1992 experiment, the ground water component of conduit flow was reduced from over 85% up-stream of the Hinkel Restriction to less than 45% at the basin. The <sup>222</sup>Rn measurements indicate that rapid recharge from the overlying Santa Fe River accounted for as much as 57% of the discharge at the Devil's Ear spring during the February, 1992 experiment and 46% during the June, 1993 experiment. Note that there was more river water intrusion to the cave system during the period of lower river flow (February, 1992).

According to the <sup>222</sup>Rn data, the conduits up-stream of the Hinkel Restriction were the major source of pure ground water along transect A-A' in the cave system. During both experiments, over 80% of the conduit flow measured beyond the Hinkel was determined to be pure ground water. The Dome Room junction (location #10), the Hill 400 junction (between location #'s 7 and 4), and the Kappa Bear Room (location #18) also contribute pure ground water to the cave system. These junctions connect northern passages to the main tunnel and were marked by abrupt increases in <sup>222</sup>Rn concentrations. Reductions in <sup>222</sup>Rn concentrations correspond to a reduced ground water flow component and were measured at three conduit junctions during the two experiments: Mainland, Split Tunnel, and River Intrusion junctions. All three are intersections between the main passage and smaller conduits that deliver water to the main conduit from the south side of the cave system. During the June, 1993 experiment, the Big Room junction was also marked by a significant decrease in <sup>222</sup>Rn concentration indicating further river water intrusion. Figure 30 shows that all of these conduits trend south toward the river. The Split Tunnel and the Big Room are directly beneath the Santa Fe river. Visual observations in the cave indicate that water clarity in these tunnels is greatly reduced containing tea-colored as opposed to the crystal clear water found up-stream of the Hinkel Restriction. During the June, 1993 experiment, dark water was observed to be seeping into the main passage from fractures near the floor of the main conduit between the Right Line Junction and the River Intrusion Junction.

Figure 31b shows transect B-A' from the back of the Mainland region out and to the end of the main conduit past the Hinkel Restriction. This region is an extensive network of large and small passages that trend south toward the Santa Fe river. Cave-divers commonly encounter less than two

meters of visibility in this region attesting to the reduced water clarity conditions caused by an influx of dark, tea-colored water.

$^{222}\text{Rn}$  concentrations measured in the back of the Mainland region indicate that 80% of the water during the February, 1992 experiment was recently intruded river water which dropped to 70% during the June, 1993 experiment. During both experiments, the ground water flow component increased toward the main passage to approximately 40% at the Mainland junction and rose to approximately 90% up-stream of the Hinkel Restriction. The extensive Mainland region was the largest contributor of river water to the cave system during both experiments.

Figure 32 shows ground water percentage contour maps for the February 1992 and June 1993 cave experiments. The contour lines show the sources and distribution of pure ground water and intruded river water throughout this section of the aquifer. Darker areas correspond to sections of the cave containing progressively greater amounts of intruded river water.

Both maps show that surface water influx to the cave system originates from the passages on the south side of the system which trend toward and in some cases directly underlie the Santa Fe River. The sections of the cave system contributing the most river water to the cave system are the: Mainlands region, Split Tunnel, River Intrusion Tunnel, and the Big Room (sections A, B, C, and D on Figure 32).

The contour maps indicate that the northern conduits are the major contributors of pure ground water to the cave system. The data also correlates with tracing experiments carried out by Kincaid and others (1992), which demonstrated that the recharge area for Devil's Ear and July springs lies on the north side of the river. The three major sources of pure ground water influx to the cave system are the conduits up-stream of the Hinkel Restriction, the conduits north of July spring, and the White Room (sections E, F, and G on figure 32).

Both the Hinkel Restriction and July spring lie on the north side of the cave system while the White Room is on the south side. Estimates of ground water flow based on conduit diameter and water velocity indicate that the conduits up-stream of the Hinkel Restriction are the largest contributors of pure ground water to the cave system and that these conduits represent a major drainage feature of the northern ground water recharge area. Much of the water in from section D on Figure 32 discharges at July spring and thus has little effect on the ground water flow component of the discharge at Devil's Ear spring. The White Room has been suggested by Wilson and Skiles (1988) to be physically connected to the Little Devil's Cave System where the source of the ground water is the recharge area on the south side of the Santa Fe River. Ground water entering the cave system from the White Room mixes with the water in the Big Room region where the ground water flow component is reduced.

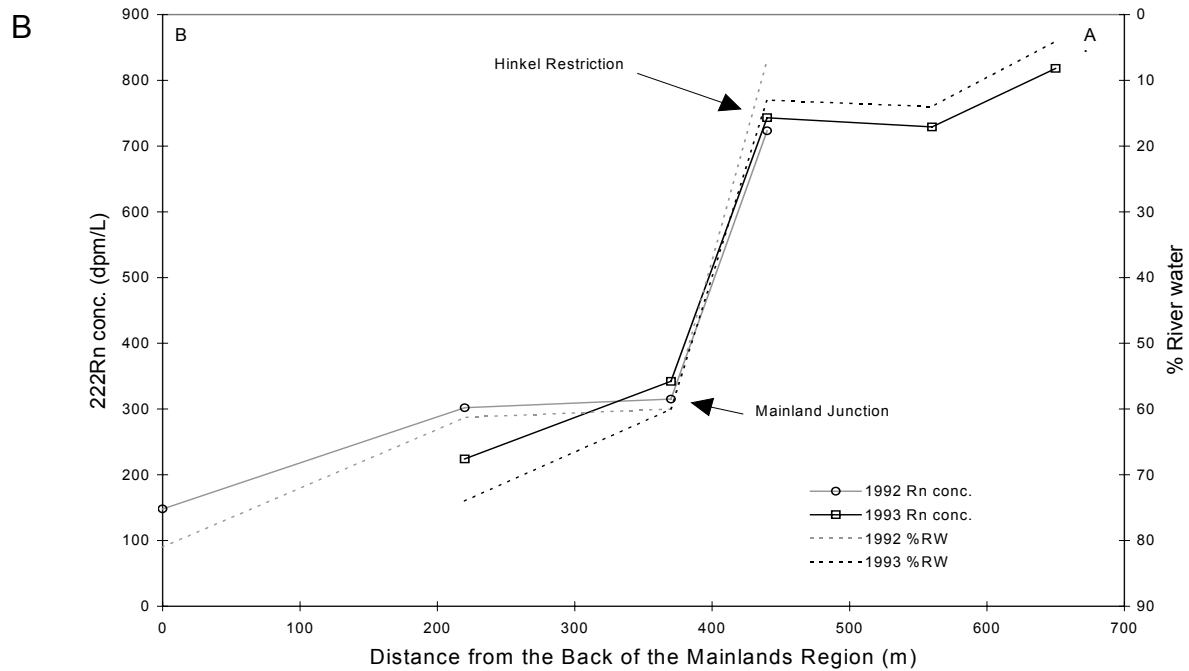
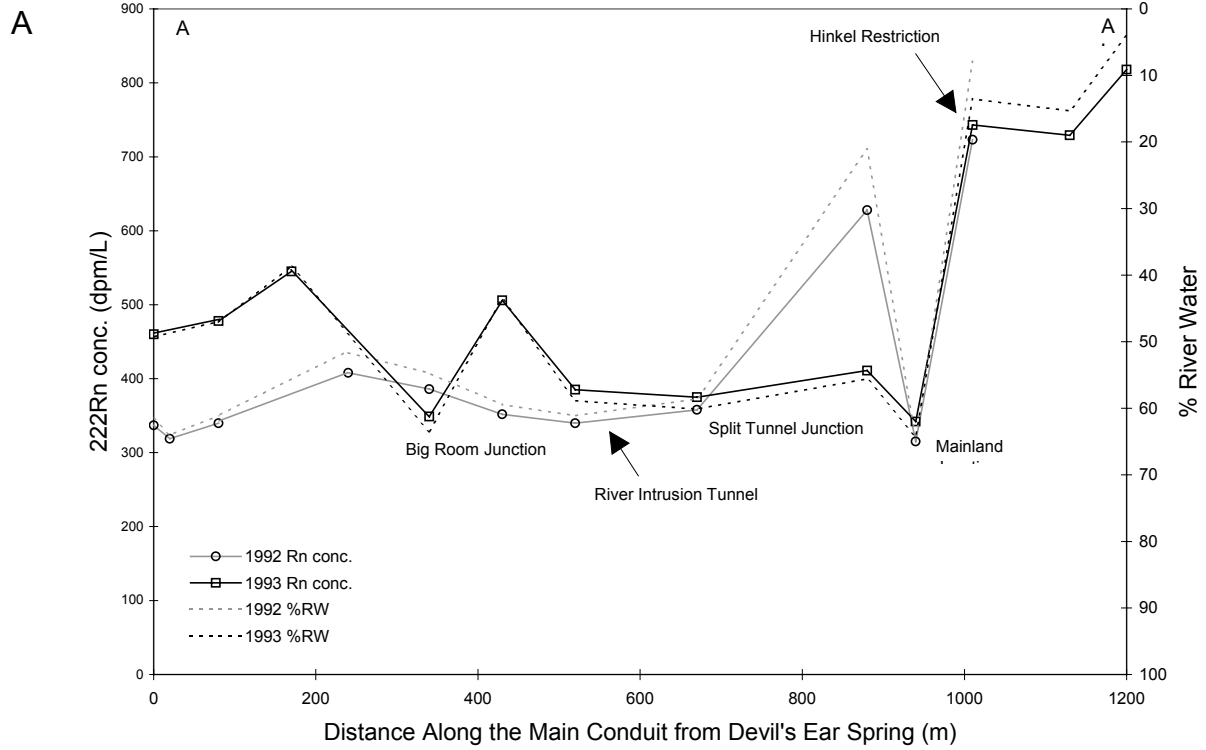


Figure 31.  $^{222}\text{Rn}$  concentrations and the corresponding percentage of river water in the conduit flow measured across transects (A) A-A' and (B) B-A' through the Devil's Ear cave system on the Santa Fe river, north-central Florida.



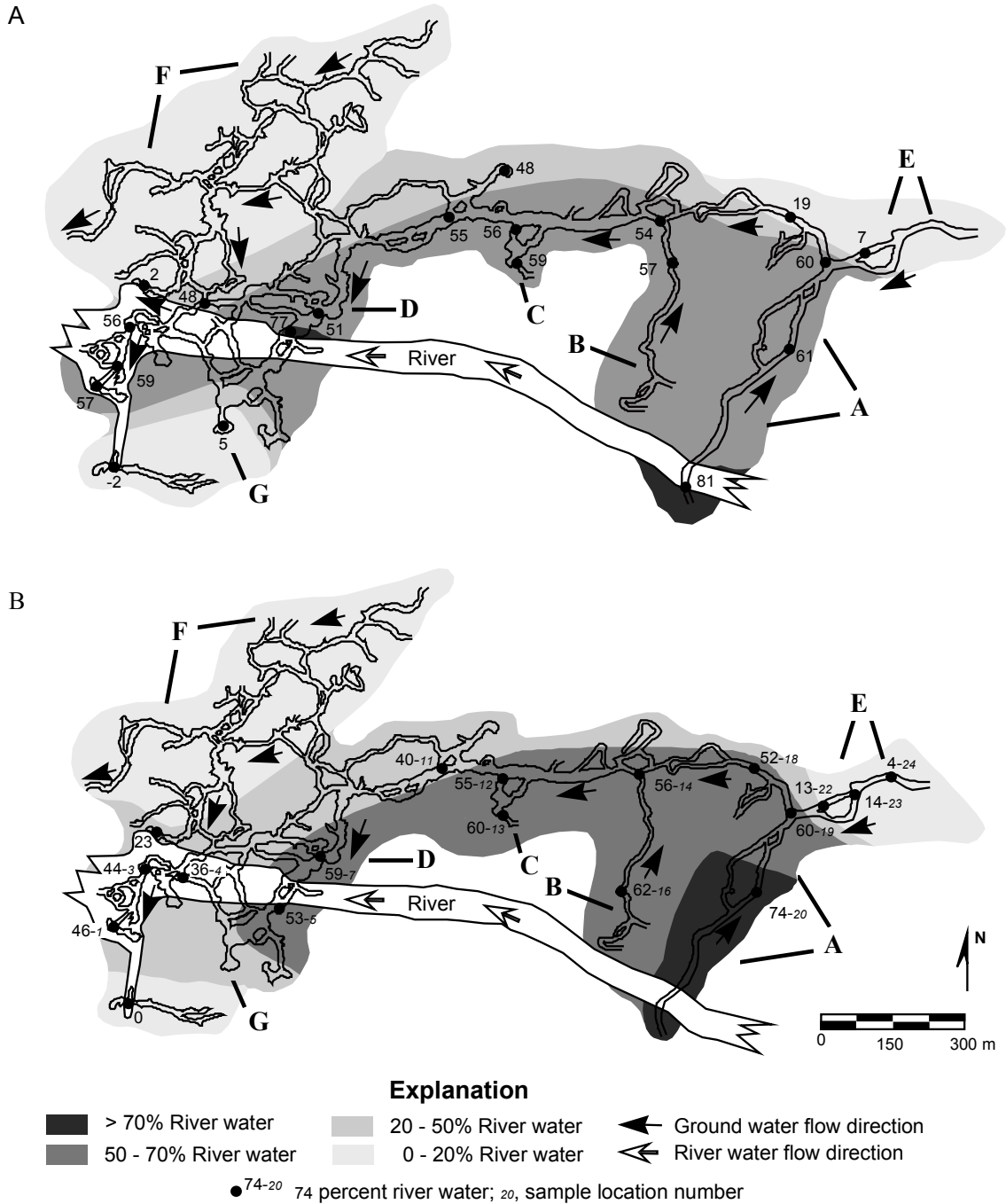


Figure 32. Contour maps showing the distribution of intruded river water in the Devil's Ear cave system on the Santa Fe river, north-central Florida during the (A) February, 1992 and (B) June, 1993 cave sampling experiments. Darker regions are the areas of greatest river water intrusion to the aquifer.

### $\delta^{18}\text{O}$ and Major Cations

Water samples collected during the February 1992 cave experiment from 11 locations within the cave system were measured for  $\delta^{18}\text{O}$  and four major cation concentrations: Ca, Mg, Na, and K. Figure 32a is a combined plot showing  $\delta^{18}\text{O}$ , Ca, Mg, and Na+K values measured during the 1992 experiment. The most prominent feature on the plot is the  $\delta^{18}\text{O}$  peak that was measured at the fissure in the Split Tunnel. The fissure is a vertical joint in the limestone that trends straight up from the top the tunnel at 30 meters to a depth of approximately 10 meters where it continues but becomes impassable. The water sample was taken from the top of passable part of this fissure. The more positive  $\delta^{18}\text{O}$  value suggests that river water is intruding to the cave system through this fissure. Tannin water and extremely weathered limestone with heavy goethite surface encrustation were visually observed in the Split Tunnel. These observations correlate with the  $\delta^{18}\text{O}$  data and indicate a direct hydrologic connection with more aggressive and  $\delta^{18}\text{O}$  enriched river water.

No significant variations were observed in the dissolved concentrations of Mg or Na+K. Although variations in dissolved Ca concentrations were observed in the cave, these were difficult to interpret alone. The average recorded Ca concentration in the cave system was 35.2 mg/L with a standard deviation of only 5.0. The narrow range of recorded values agrees with both reported values in the Santa Fe River at 39 mg/L (Hunn and Slack, 1983) and reported values in the upper Floridan aquifer in this region at 40 - 50 mg/L (Spangler and Silverman, 1982).

Figure 33b shows the 1993 plot of  $\delta^{18}\text{O}$  values measured in the cave and at July spring, Rum Island spring, and the ground water well. The average  $\delta^{18}\text{O}$  value measured in the cave was  $-3.61\text{‰}$ . There was not much variation in the cave samples; the standard deviation was only  $0.07\text{‰}$ . However, the observed variations correlate well with the 1992  $\delta^{18}\text{O}$  data, the  $^{222}\text{Rn}$  data, and visual observations in the cave. The most positive values were recorded in the Split Tunnel at the fissure and the River Intrusion Tunnel. These values correlate to an influx of more  $^{18}\text{O}$  enriched river water. The most negative value was recorded in the ground water well which correlates to the more enriched  $^{16}\text{O}$  values expected in ground water.

The  $\delta^{18}\text{O}$  values measured in the cave support the  $^{222}\text{Rn}$  data and indicate the active intrusion of surface water to the cave system. Enriched  $\delta^{18}\text{O}$  values were measured in the Split Tunnel at the fissure in both experiments confirming that this was a zone of surface water intrusion. In the 1993 experiment, a relatively enriched  $\delta^{18}\text{O}$  value,  $(-3.48\text{‰})$  was also recorded in the River Intrusion Tunnel. Both of these tunnels had very little water flow and the samples were collected from dark, tannin water suggesting that the  $\delta^{18}\text{O}$  signature was more pronounced in low flow areas where the water was not quickly mixed.

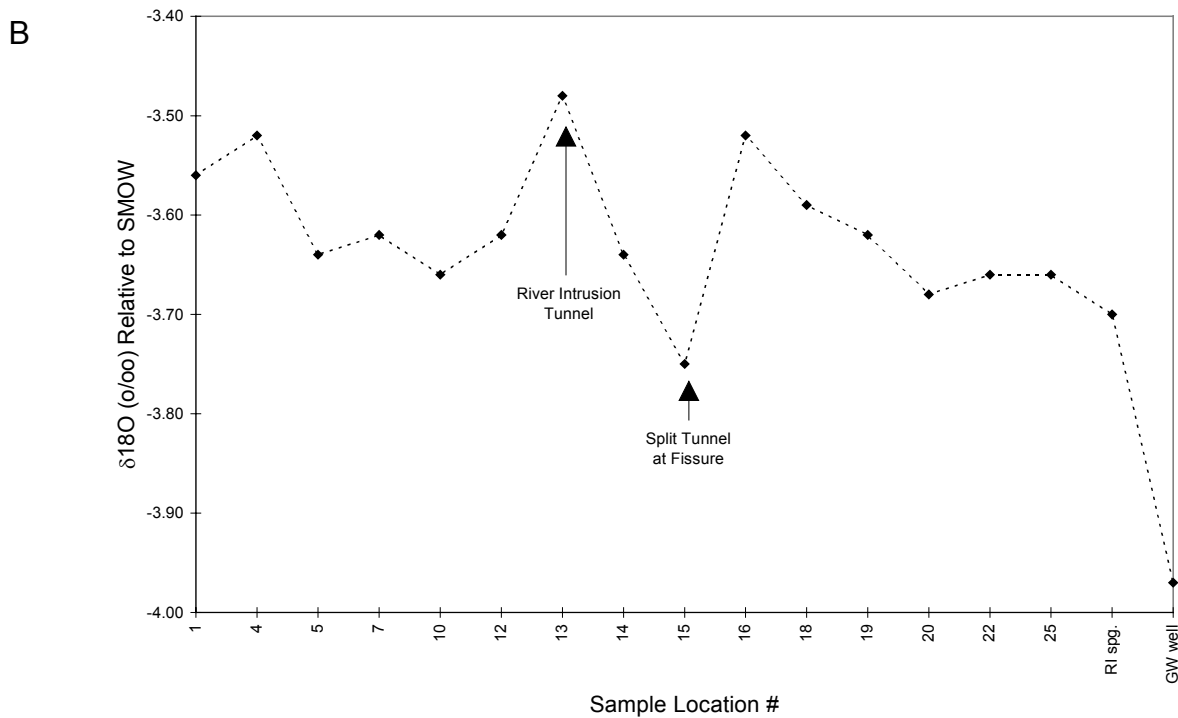
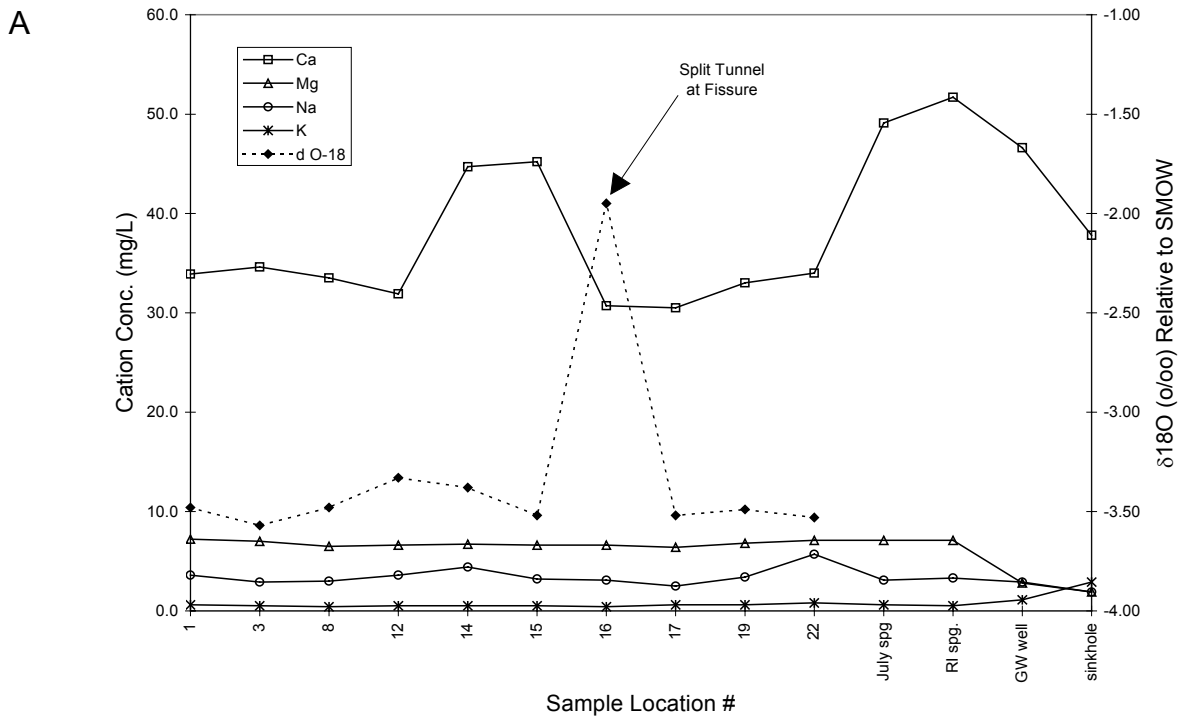


Figure 33.  $\delta^{18}\text{O}$  values and major cation concentrations measured in the Devil's Ear cave system on the Santa Fe river, north-central Florida during the (A) February, 1992 and (B) June, 1993 cave experiments. More negative  $\delta^{18}\text{O}$  values correspond to purer ground water.

## **CHAPTER 6**

### **DISCUSSION**

#### *Groundwater - Surface Water Exchange*

The fact that the cave system experienced more river intrusion during a period of lower recorded river stage indicates that groundwater - surface water exchange is not a simple direct function of the stage of the Santa Fe River. Rainfall and groundwater level data collected from the field area and the Northern Highlands by the Suwannee River and St. Johns River Water Management Districts during this investigation provide the clues necessary to explain this complication. Rainfall data collected from Gainesville located in the Northern Highlands physiographic province and O'leno State Park located in the High Springs Gap physiographic province show that there was significantly more rainfall in the highlands than in the lowlands during the February 1992 sampling period when the greatest amount of intruded river water was measured in the cave system. On the contrary, there was more rainfall in the lowlands than in the highlands during the June 1993 sampling period when the least amount of intruded river water was recorded. Refer back to Figure 8 which shows the location of the Devil's Ear cave system and the Santa Fe River in relation to the highland and lowland physiographic provinces.

Groundwater levels were measured in a Department of Transportation (DOT) well located approximately 2 km west of the field area. Those data show that the water level in the Floridan aquifer was higher during the June 1993 sampling period when there was more rainfall over the lowlands and less river water intrusion to the cave system. Figure 34 compares water levels in the Floridan aquifer with regional precipitation data collected from the highland and lowland regions surrounding the Devil's Ear cave system during the February, 1992 and the June, 1993 sampling periods.

The hydraulic data and the results of this investigation reveal that the groundwater - surface water exchange process is dictated by a net head difference between the aquifer and the river. Figure 35 is a conceptual model of the mechanisms controlling groundwater circulation between the Devil's Ear cave system and the Santa Fe River. Though the entire geologic section beneath the river including the cave system is part of the Floridan aquifer, for the purpose of this discussion, the river-aquifer system is divided into three parts: the Santa Fe river, the conduits in the aquifer, and the saturated Ocala Limestone in between.

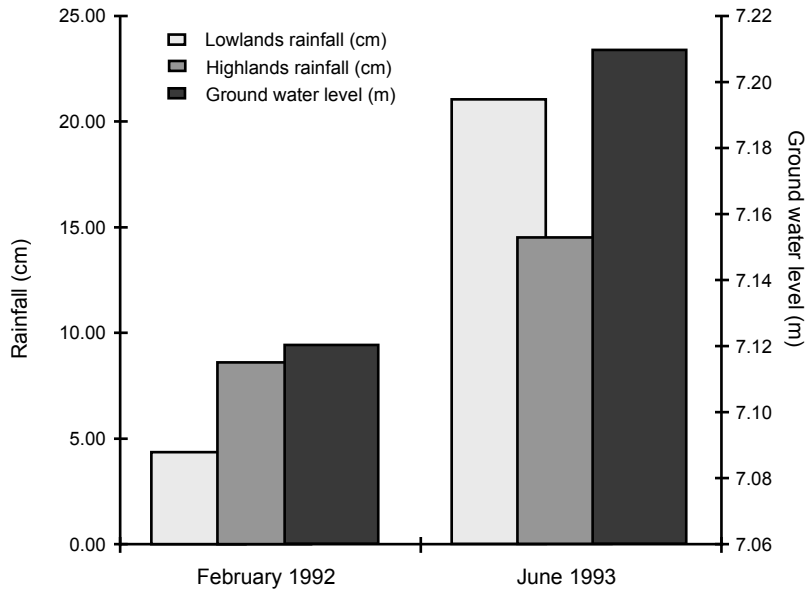
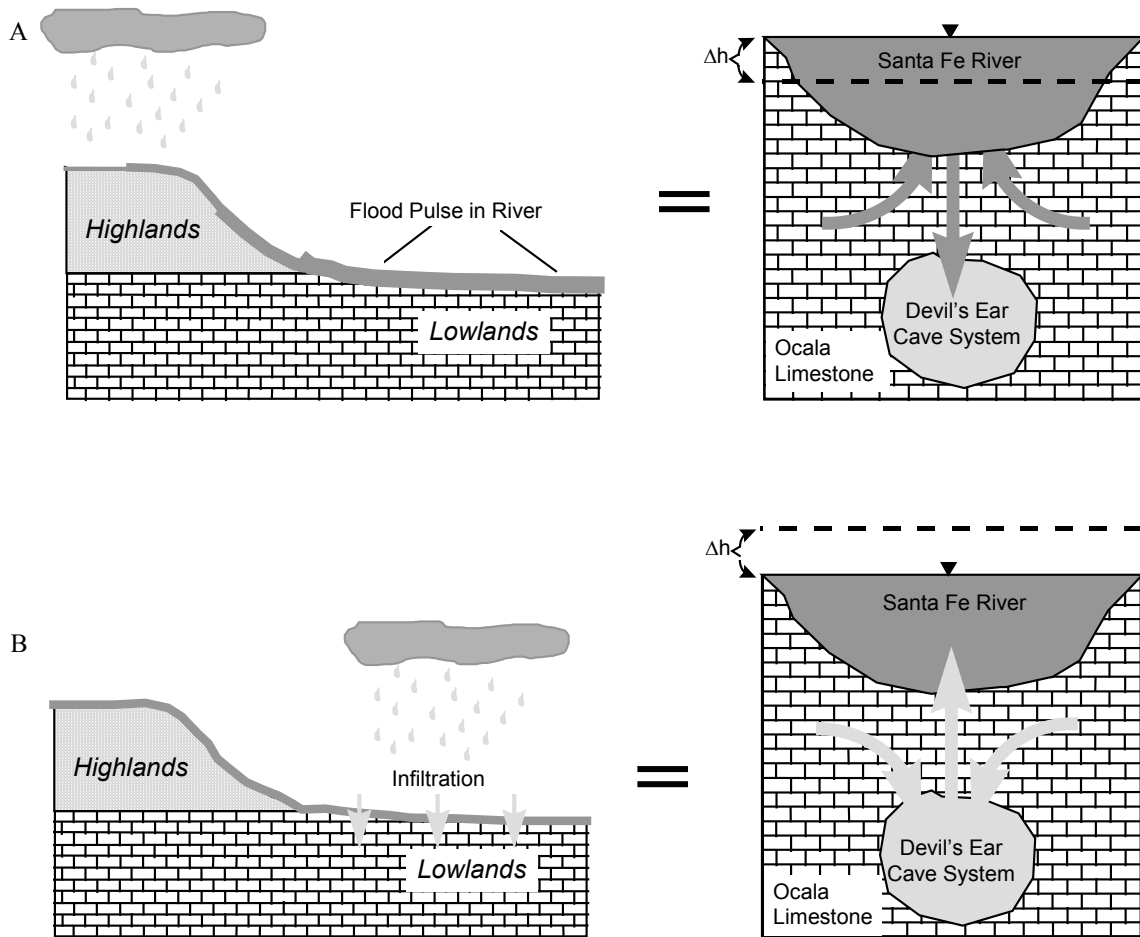
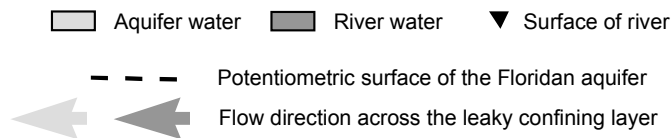


Figure 34. Comparison of water levels in the Floridan aquifer near the Devil's Ear cave system and rainfall in the Northern Highlands and lowland physiographic provinces, north-central Florida. Notice that there was more rainfall in the highlands than in the lowlands during the February, 1992 sampling period when there was more river water intrusion to the Devil's Ear cave system but the flow stage of the Santa Fe River was at its lowest point. Data are from the Suwannee River and St. Johns River water management districts.



#### Explanation



**Figure 35.** Groundwater - surface water exchange between the Santa Fe River and the extremely permeable conduits in the Floridan aquifer across a 30 m thick section of Ocala Limestone which is a leaky confining layer. (A) The stage of the river is above the potentiometric surface of the aquifer forcing downward leakage from the river to the aquifer. (B) The potentiometric surface of the aquifer is above the stage of the river forcing upward leakage from the aquifer to the river.

The 30-m thick section of saturated Ocala Limestone above the cave system is a leaky confining layer separating the extremely permeable conduits from the overlying river. The confining layer allows a hydraulic gradient to develop between the river and the cave and contains water in storage that is displaced when either a downward or upward hydraulic gradient develops. The rate at which water moves through this layer is dependent on the magnitude and duration of the hydraulic gradient.

The river receives water from both runoff in the highlands and spring discharge in the lowlands. Therefore, head in the river is dependent on both the quantity of aquifer discharge to the river and the quantity of surface runoff received by the river and its tributaries. In contrast, head in the cave is primarily dependent only on the quantity of recharge. Thus, surface runoff, which is greater in regions where the aquifer is confined, is the independent variable that causes the head difference. The magnitude and direction of the hydraulic gradient between the river and the cave is, therefore, a direct function of the distribution of major regional precipitation events.

When precipitation is concentrated on the Northern Highlands where the Santa Fe River is not in hydraulic connection with the Floridan aquifer, the water accumulates in the river as overland flow and the flood pulse moves downstream onto the unconfined part of the aquifer. The subsequent increase in river stage produces a downward hydraulic gradient causing large amounts of river water to invade the cave through the leaky confining layer (Figure 35a). Observations of water clarity reductions in the cave, by the author as well as other cave-divers, after large flood events originating in the highlands of the upper Santa Fe River reveal that river water intrusion to the aquifer takes place in as little as one day.

Figure 34 shows that more rainfall fell over the highlands than in the lowlands during the February, 1992 experiment. Corresponding to the model presented in Figure 35a, there was more recorded river water intrusion to the aquifer and a greater ratio of stream flow loss : groundwater influx in the river. Though the overall stage of the river was less than during the June, 1993 experiment, most of the river's hydrostatic head resulted from surface runoff flowing down-stream off the Northern Highlands and onto the lowlands where the Floridan aquifer is unconfined and is partly recharged by the Santa Fe river.

Conversely, when precipitation is concentrated on the lowland regions where the Floridan aquifer is unconfined, recharge to the aquifer results from direct infiltration with no resulting flood wave in the river. The hydraulic head in the cave rises above that of the river where a rising river stage is caused only by increased spring discharge. The resulting upward hydraulic gradient causes flow from the cave to the river (Figure 35b). The water in the cave will clear as the tannin surface water from the Santa Fe River is flushed up and out through the confining layer.

Figure 34 shows that there more rainfall fell in the lowlands than in the highlands during the June, 1993 sampling period. Increased rainfall onto the limestone plain above the unconfined Floridan aquifer raised the groundwater levels above those recorded during the February, 1992 experiment. An increased potentiometric surface in the aquifer reduced the downward hydraulic gradient between the river and the aquifer which was evidenced by reduced river water intrusion to the aquifer and a reduced stream flow loss : groundwater influx ratio in the river.

### Return Flow

Return Flow describes water reentering the river channel that has been diverted underground flowing beneath the stream bed but having little interaction with the underlying aquifer. The concept of return flow is not new to this investigation. Huntoon, (1992a;b) describes epikarst in China as having formed by aggressive, acidic water causing increased dissolution in the upper zone of limestone units exposed along the base of river channels. The epikarstic limestone provides an avenue for water to flow along the rock sediment contact beneath the actual river bottom. In another investigation conducted by Kennedy and others (1984), deliberate chemical tracers injected into a mountain stream in Santa Clara County, California verified the existence of "under-flow" which was described as river flow that was diverted under the stream channel resurfacing down-stream.

In this investigation, the anomalous peaks in SF<sub>6</sub> concentrations down-stream of the injection point demonstrate that water was diverted underground and returned to the river channel near the point marked by the peak. SF<sub>6</sub> is not lost to the atmosphere while dissolved in the water flowing underground. The return flow marked by higher than expected SF<sub>6</sub> concentrations is quickly diluted once it reenters the river channel. The SF<sub>6</sub> concentration drops dramatically and then resumes a normal decline due to gas exchange across the river surface.

Qualitatively, the SF<sub>6</sub> data confirms the existence of the return flow component. Quantification using the SF<sub>6</sub> concentrations is admittedly much more tenuous. Using equations 10 - 13 presented in chapter 4, the magnitude of the return flow component ranged from 15 - 40 m<sup>3</sup>/s over the entire length of the transect during the three sampling periods. The error range calculated in chapter 5 ranged from plus or minus 17 - 49 percent. Sources of error in the calculations were: (1) sampling and analytical techniques, (2) discharge measurement, (3) calculation of the gas exchange coefficient, (4) locating the point of stream flow loss, and (5) dilution to SF<sub>6</sub> concentrations in the river caused by groundwater influx. Future investigations should focus on smaller rivers with little or known groundwater influx to constrain the error and refine the quantification technique.



## **CHAPTER 7**

### **SUMMARY AND CONCLUSIONS**

This investigation was designed to study the interactions between groundwater and surface water in the western Santa Fe River which dissects the unconfined Floridan aquifer. The investigation focused on the reach of the river between Rum Island and Ginnie spring and addressed the exchange of water between the Santa Fe River and the underlying Devil's Ear cave system.

Three hypotheses about the groundwater - surface water interactions were tested. Hypothesis #1 contended that a significant part of the water circulating through the Devil's Ear cave system is surface water from the overlying Santa Fe river. Hypothesis #2 contended that a major part of the discharge from Devil's Ear spring is resurgent surface water originating from the Santa Fe river. Hypothesis #3 contended that in the western Santa Fe River basin, the river both gains water from and loses water to the underlying Floridan aquifer.

Three experiments were carried out at different flow stages in which SF<sub>6</sub> and <sup>222</sup>Rn were used to quantify groundwater influx and stream flow loss. In addition, two experiments were conducted within the Devil's Ear cave system to measure river water intrusion to the Floridan aquifer. Timing of the two experiments corresponded to high and low flow stages of the Santa Fe river. <sup>222</sup>Rn and δ<sup>18</sup>O were used to quantify and map the distribution of intruded river water in the cave system. Finally, a conceptual model was generated to describe the mechanisms controlling the exchange process.

Between Rum Island and Ginnie spring, groundwater influx to the Santa Fe River increased with as the stage of the river rose during the three sampling periods demonstrating a hydraulic connection between the river and the aquifer. Groundwater influx ranged from 12 to 32 m<sup>3</sup>/s between low and high flow stages. Since the groundwater influx was consistently greater than stream flow loss the Santa Fe River is a gaining stream as is depicted by standard potentiometric surface maps. However, significant stream flow loss was measured during this investigation that can not be detected on those maps. The magnitude of the stream flow loss ranged from 10 m<sup>3</sup>/s during the low stage to 25 m<sup>3</sup>/s during the high stage.

The conduits trending south toward the Santa Fe River contributed the most intruded river water to the Devil's Ear cave system. Three specific regions of the cave system were responsible for the most river water intrusion to the overall system discharge: the Mainland region, Split Tunnel, and River Intrusion Tunnel. Intruded river water accounted for between 46 and 57 percent of the discharge from devil's ear spring during the high flow and low flow stages of the Santa Fe river. There was more river water intrusion to the cave system during the low flow stage of the river. Thus, the amount of river water intrusion to the aquifer is not merely dependent on the stage of the overlying river.

The northern conduits particularly those in the Hinkel Restriction area and upstream of July spring were the largest contributors of pure groundwater to the system. Thus, the primary recharge area for Devil's Ear, Devil's Eye, and July springs is the region north of the Santa Fe river. Pure groundwater was also measured in the White Room indicating that there is some hydraulic connection to the Little Devil's cave system and the recharge area on the south side of the Santa Fe river.

The distribution of regional precipitation is the primary mechanism responsible for the exchange of water between the Santa Fe River and the underlying Floridan aquifer. When rainfall is concentrated over the Northern Highlands where the Floridan aquifer is confined by the Hawthorn Formation, surface runoff moves down-stream as a flood pulse in the river. The subsequent rise in stage causes a downward hydraulic gradient between the river and the infinitely permeable conduits in the aquifer. When rainfall is concentrated over the lowlands where the Floridan aquifer is unconfined, direct infiltration raises the potentiometric surface of the aquifer and generates an upward hydraulic gradient between the aquifer and the river. The magnitude of the hydraulic gradient determines the quantity of groundwater influx to the river or river water intrusion to the aquifer.

The findings of this study demonstrate the vulnerability of the unconfined sections of the Floridan aquifer to rapid contamination from surface streams. The  $^{222}\text{Rn}$  and  $\delta^{18}\text{O}$  data and water clarity observations presented in chapter 5 clearly demonstrate the occurrence of rapid river water intrusion to the unconfined Floridan aquifer. The two component mixing model used in this investigation revealed that as much as 57 percent of the discharge at Devil's Ear spring can be river water that has recently intruded into the Devil's Ear cave system. Observations of water clarity reductions in the cave system during and after flood events that originated in the Northern Highlands physiographic province reveal that wholesale contamination of the major karstic conduits underlying the Santa Fe River can occur in as little as one day.

Given the prevalence of karst in Florida, the hydrologic character of the part of the western Santa Fe River basin investigated in this study can be considered typical of other regions in Florida where rivers or streams dissect the unconfined Floridan aquifer. Currently, environmental regulations in Florida segregate groundwater from surface water in these regions and permit high nitrate sewage from dairies, and fertilizers and pesticides from agricultural lands to be discharged to rivers and streams. However, the results of this investigation demonstrate that there can be no clear distinction between ground and surface waters in these regions. Instead, water is actively exchanged between the aquifer and rivers and streams at scales that are imperceptible to standard hydraulic analyses. Contaminants that enter the river will be carried into the aquifer by the exchange process and potentially degrade water quality.

## REFERENCES

- Andrews, W.J., 1992. Reconnaissance of Water Quality at Nine Dairy Farms in North Florida, 1990 - 1991: *Water Resources Investigations Report 92-4058*, U.S. Geological Survey.
- Biddlecomb, A.H., 1993. Hydrogeology and Karst Development of the Robinson Sinks Area, Alachua County, Florida. Master's Thesis, University of Florida.
- Briel, L., 1976, An Investigation of the  $^{234}\text{U}/^{238}\text{U}$  Disequilibrium in the Natural Waters of the Santa Fe River Basin of North-Central Florida. Ph.D. Dissertation, Florida State University.
- Broecker, W.S. and Peng, T., 1982. Tracers in the Sea. Lamont-Doherty Geological Observatory, Columbia University, Palisades, New York.
- Burman, S. Map of the Devil's Ear Cave System,. Ginnie Springs, High Springs, Florida, Unpublished Map.
- Chen, C.S., 1965. The Regional Lithostratigraphic Analysis of Paleocene and Eocene Rocks of Florida. Geological Bulletin No. 45, Florida Geological Survey.
- Ellins, K.K., 1992, Stable Isotopic Study of the Groundwater of the Martha Brae River Basin, Jamaica: *Water Resources Research*, Vol. 28, No. 6, pp. 1597-1604.
- Ellins, K.K.; Kincaid, T.R.; Hisert, R.A.; Johnson, N.A.; Davison, C.A.; and Wanninkhof, R.H., 1991, Using  $^{222}\text{Rn}$  and  $\text{SF}_6$  to Determine Groundwater Gains and Stream Flow Losses in the Santa Fe River: *Hydrogeology of the Western Santa Fe River Basin*, Field Trip Guidebook No. 32., Southeastern Geological Society.
- Ellins, K.K.; Roman-Mas, A.; and Lee, R., 1990. Using  $^{222}\text{Rn}$  to Examine Groundwater/Surface Discharge Interaction in the Rio Grande De Manati, Puerto Rico: *Journal of Hydrology*, Vol.115, pp. 319-341.
- Ellins, K.K., Simpson, H.J., and Mathieu, G., 1989. A Study of Surface Discharge Fluctuations in the Martha Brae River in Jamaica Using  $^{222}\text{Rn}$  (abstract), EOS Transactions, American Geophysical Union, Vol. 70, No. 15, pp. 334.
- Elsinger, R.J. and Moore, W.S., 1983. Gas Exchange in the Pee Dee River Based on  $^{222}\text{Rn}$  Evasion. Geophysical Research Letters, Vol. 10, No. 6, pp. 443-446.
- Fernald, E.A. and Patton, D.J., 1984, *Water Resources Atlas of Florida*, Library of Congress Catalog No. 84-081758, Institute of Science and Public Affairs, Tallahassee, Florida.
- Gonfiantini, R. and Simonot, M., 1987. Isotopic Investigation of Groundwater in the Cul-De-Sac Plain, Republic of Haiti. International Symposium on the Use of Isotope Techniques in Water Resources Development, International Atomic Energy Agency in co-operation with UNESCO. Vienna, Austria.
- Handbook of Chemistry and Physics, 72<sup>nd</sup> Edition, 1992. CRC Press.
- Hisert, R.A. and Ellins, K.K., 1991. Determination of the Underground Flow Path of the Santa Fe River Using  $\text{SF}_6$ . Hydrogeology of the Western Sata Fe River Basin, Field Trip Guidebook No. 32. Southeastern Geological Society.
- Hisert, R.A., Ellins, K.K., Johnson, N.A., Kincaid, T.R., and Davison, C.A., 1991. Estimating Stream Mixing Characteristics Using Radon-222 and Sulfur Hexafluoride in the Karstic Environment of the Santa Fe River, Florida. (abstract) Geological Society of America Abstracts pp. 345.

- Hisert, R.A., 1994, *A Multiple Tracer Approach to Determine the Ground Water and Surface Water Relationships in the Western Santa Fe River, Columbia County, Florida*: Unpublished Ph.D. Dissertation, Department of Geology, University of Florida, Gainesville, FL 32601.
- Hunn, J.D. and Slack, L.J., 1983, Water Resources of the Santa Fe River Basin, Florida, *Water-Resources Investigations Report 83-4075*, U.S. Geological Survey.
- Huntoon, P.W., 1992a. Exploration and Development of Ground Water from the Stone Forest Karst Aquifers of South China. *Ground Water*, Vol. 30, No. 3, pp. 324-330.
- Huntoon, P.W., 1992b. Hydrogeologic Characteristics and Deforestation of the Stone Forest Karst Aquifers of South China. *Ground Water*, Vol. 30, No. 2, pp. 167-176.
- Kaufmann, R.F. and Bliss, J.D., 1978, Radium-226 in Ground Water of West Central Florida, *Water Resources Bulletin*, Vol. 14, No. 6.
- Kennedy, V.C., Jackman, A.P., Zand, S.M., Zellweger, G.W., and Avanzino, R.J., 1985. Transport and Concentration Controls for Chloride, Strontium, Potassium, and Lead in Uvas Creek, a Small Cobble-bed Stream in Santa Clara County, California. *Journal of Hydrology*, Vol. 75, pp. 67-110.
- Key, R.M., 1981, *Examination of Abyssal Sea Floor and Near-Bottom Water Mixing Processes Using Radium-226 and Radon-222*, Unpublished Ph.D. Dissertation, Texas A&M University.
- Kincaid, T.R., Denizman, C., and Ellins, K.K., 1992, Using SF<sub>6</sub> to Establish the General Recharge Area for Three Springs in the Santa Fe River, Florida, Annual Meeting of the Geological Society of America, Cincinnati, Ohio. Abstracts with Programs p. A300.
- Ledwell, J.R., 1982. Gas Exchange Across the Air/Water Interface. Ph.D. Dissertation, Harvard University, Cambridge, Massachusetts.
- Meadows, P.E., 1991. Potentiometric Surface of the Upper Floridan Aquifer in the Suwannee River Water Management District, Florida. Open-File Report 90-582, U.S. Geological Survey.
- Meyer, F.W., 1962. Reconnaissance of the Geology and Ground-Water Resources of Columbia County, Florida. Report of Investigations No. 30, Florida Geological Survey.
- Miller, J.A., 1986. Hydrogeologic Framework of the Floridan Aquifer System in Florida and Parts of Georgia, Alabama, and South Carolina. Professional Paper 1403-B, U.S. Geological Survey.
- National Council on Radiation Protection and Measurements. Evaluation of Occupational and Environmental Exposures to Radon and Radon Daughters in the United States. NCRP Report No. 78.
- Otton, J.K., 1992. The Geology of Radon. Open-file Report 0-326-248, U.S. Geological Survey.
- Puri, H.S., 1957. Stratigraphy and Zonation of the Ocala Group. Geological Bulletin No. 38, Florida Geological Survey.
- Puri, H.S., Yon, J.W. Jr., and Oglesby, W.R., 1967. Geology of Dixie and Gilchrist Counties, Florida. Geological Bulletin No. 49, Florida Geological Survey.
- Rama and Moore, W.S., 1984. Mechanism of Transport of U-Th Series Radioisotopes from Solids into Ground Water. *Geochemica et Cosmochimica Acta* Vol. 48, pp. 395-399.
- Roessler, C.E., Smith, Z.A., Bolch, W.E., and Prince, R.J., 1979. Uranium and Radium-226 in Florida Phosphate Materials. *Health Physics*, Vol. 37, pp. 269-277.
- Rogers, A.S., 1958, *Physical Behavior and Geologic Control of Radon in Mountain Streams*, Geological Bulletin No. 1052-E, U.S. Geological Survey.
- Rosenau, J.C., Faulkner, G.L., Hendry, C.W. Jr., and Hull, R.W., 1977, Springs of Florida, Bulletin No. 31, U.S. Geological Survey.
- Rupert, F.R., 1988. The Geology and Geomorphology of Gilchrist County, Florida. Open-File Report 18, Florida Geological Survey.

- Scott, T.M., 1988. The Geology and Geomorphology of the Hawthorn Group (Miocene) of Florida. Bulletin 59, Florida Geological Survey.
- Scott, T.M., 1991, The Geology of the Santa Fe River Basin, Central-northern Peninsular Florida, *Hydrogeology of the Western Santa Fe River Basin*, Field Trip Guidebook No. 32, Southeastern Geological Society.
- Shaw, R.D., and Prepas, E.E., 1990, Groundwater-Lake Interactions: I. Accuracy of Seepage Meter Estimates of Lake Seepage, *Journal of Hydrology*, Vol. 119, pp. 105-120.
- Simpson, H.J., Herczeg, A.L., Anderson, R.F., Trier, R.M., Mathieu, G.G., and Deck, B.L., 1985. Mobility of Radionuclides in High Chloride Environments, A Case Study of Waters Within and Near the Delaware Basin, Southeastern New Mexico. Division of Radiation Programs and Earth Sciences, Office of Nuclear Regulatory Research, U.S. Nuclear Regulatory Commission, Washington, D.C. 20555, NRC FIN B7057.
- Spangler, D.P., 1981, Florida's water Resources with Particular Emphasis On Ground water, Proceedings of the First Annual Symposium on Florida Hydrogeology, Northwest Florida Water Management District, Havana, Florida.
- St. Johns River Water Management District, Palatka, Florida, Unpublished Rainfall and Ground Water Level Data.
- Suwannee River Water Management District, Live Oak, Florida, Unpublished Rainfall and Ground Water Level Data.
- Wanninkhof, R.H., 1986. Gas Exchange Across the Air-Water Interface Determined with Man Made and Natural Tracers. Ph.D. Dissertation, Columbia University.
- White, W.A., 1970, *The Geomorphology of the Florida Peninsula*, Geological Bulletin No. 51, Florida Geological Survey.
- White, W.B., 1988. Geomorphology and Hydrology of Karst Terrains. Oxford University Press, New York.
- Williams, K.E.; Nicol, D.; and Randazzo, A.F., 1977, *The Geology of the Western Part of Alachua County, Florida*, Report of Investigations No. 85, Florida Geological Survey.
- Wilson, W.L. and Skiles, W.C., 1989. Partial Reclassification of First-Magnitude Springs in Florida. The Proceedings of the 3<sup>rd</sup> Multidisciplinary Conference on Sinkholes and the Environmental Impacts of Karst. St. Petersburg, Florida.
- Wilson, W.L. and Skiles, W.C., 1988. Aquifer Characterization by Quantitative Dye Tracing at Ginnie Spring, Northern Florida, *The Proceedings of the Second Conference on Environmental Problems in Karst Terranes and Their Solutions*, The Association of Groundwater Scientists and Engineers, Nashville, Tennessee.
- Winsberg, M.D., 1990. Florida Weather. University of Central Florida Press.

## **BIOGRAPHICAL SKETCH**

(UPDATED 2006)

Todd Richard Kincaid was born in Hollywood, Florida on July 21, 1968 and raised by his mother Charlotte L. Poindexter. As a child, he moved with his family from Florida to Arizona for 2 years and then to Kentucky for 4 years eventually returning to Orlando, Florida where he attended school from grades 6 through 12 and graduated from Winter Park High School in 1986.

After high school, he attended the U.S. Air force Academy in Colorado Springs, Colorado for one year. In August 1987, he entered the University of Florida where he received a Bachelor of Science in geology in May 1991. He financed part of his undergraduate career by working as a scuba instructor for the University of Florida Academic Diving Program and in Naples, Maine and St. Croix, U.S.V.I.

In August 1991, Todd entered graduate school at the University of Florida to pursue a Master of Science in Hydrogeology under Dr. Katherine Ellins. His research focused on ground water and surface water interactions between the Floridan aquifer and the western Santa Fe River. While in graduate school at the University of Florida, he worked as an environmental consultant for GeoSolutions Inc. in Gainesville, Florida. He also held several teaching assistantships including one for field geology and a research assistantship. He graduated from the University of Florida with a Master of Science in hydrogeology in April, 1994.

In August, 1994, Todd began a Ph.D. program at the University of Wyoming in karst hydrology under Dr. Peter Huntoon and Dr. Neil Humphrey. His research addressed the fractal scale dependence of karstic permeability. His work focused on comparing the morphologic and hydrologic characteristics of underwater cave systems in the Woodville Karst Plain of North Florida and the Taurus Mountain Aquifer on Southern Turkey through 3-D modeling of the cave systems. He received his Ph.D. from the University of Wyoming in June, 1999.

After completing his Ph.D., Todd co-founded a hydrogeological consulting firm in 1999 (Hazlett-Kincaid, Inc.) dedicated to modeling groundwater flow in complex geological environments for water resources protection and development. He is currently the Vice-President of Hazlett-Kincaid, Inc. and actively involved in karst hydrogeology. He is also the Science Director for Global Underwater Explorers, a non-profit organization dedicated to protecting underwater environments through education, research, and exploration, and a member of the Steering Committee for the Hydrogeology Consortium, a non-profit group organized to improve groundwater resource protection in Florida through fostering cross-discipline public outreach.

Todd attributes his professional interests to a love for water and for travel that both began at an early age. He began scuba diving at age eleven and has been a cave diver for nearly 20 years. His travels have allowed him to live and dive in many places across the U.S. and around the world and he uses those experiences to frame a broad perspective on the importance of and approaches to water resource protection. Todd currently lives in Reno, NV where, aside from diving and hydrogeology, he enjoys hiking, climbing, kayaking, and traveling with his wife Kristie Connolly.